UNIVERSIDADE ESTADUAL PAULISTA – UNESP
CÂMPUS DE JABOTICABAL

SOIL GREENHOUSE GAS EMISSIONS AND THEIR RELATIONS TO SOIL ATTRIBUTES IN A SUGARCANE AREA

Elton da Silva Bicalho
Engenheiro Agrônomo

2016

UNIVERSIDADE ESTADUAL PAULISTA – UNESP
CÂMPUS DE JABOTICABAL

SOIL GREENHOUSE GAS EMISSIONS AND THEIR RELATIONS TO SOIL ATTRIBUTES IN A SUGARCANE AREA

Elton da Silva Bicalho
Orientador: Prof. Dr. Newton La Scala Júnior
Coorientador: Prof. Dr. Alan Rodrigo Panosso

Tese apresentada à Faculdade de Ciências Agrárias e Veterinárias – Unesp, Câmpus de Jaboticabal, como parte das exigências para a obtenção do título de Doutor em Agronomia (Produção Vegetal)

2016

B583s Bicalho, Elton da Silva
Soil greenhouse gas emissions and their relations to soil attributes in a sugarcane area / Elton da Silva Bicalho. – – Jaboticabal, 2016
x, 80 p. : il. ; 29 cm

Tese (doutorado) - Universidade Estadual Paulista, Faculdade de Ciências Agrárias e Veterinárias, 2016
Orientador: Newton La Scala Júnior
Coorientador: Alan Rodrigo Panosso
Banca examinadora: Carlos Eduardo Pellegrino Cerri, Janaina Braga do Carmo, Gener Tadeu Pereira, Teresa Cristina Tarlé Pissarra
Bibliografia

1. Dióxido de carbono. 2. Metano. 3. Óxido nitroso. 4. Produção potencial. 5. Respiração do solo. 6. Transporte gasoso. I. Título. II. Jaboticabal-Faculdade de Ciências Agrárias e Veterinárias.

CDU 631.42:633.61

Ficha catalográfica elaborada pela Seção Técnica de Aquisição e Tratamento da Informação – Serviço Técnico de Biblioteca e Documentação – UNESP, Câmpus de Jaboticabal.

unesp
UNIVERSIDADE ESTADUAL PAULISTA
Câmpus de Jaboticabal
unesp Jaboticabal

CERTIFICADO DE APROVAÇÃO

TÍTULO DA TESE: SOIL GREENHOUSE GAS EMISSIONS AND THEIR RELATIONS TO SOIL ATTRIBUTES IN A SUGARCANE AREA

AUTOR: ELTON DA SILVA BICALHO
ORIENTADOR: NEWTON LA SCALA JUNIOR
COORIENTADOR: ALAN RODRIGO PANOSSO

Aprovado como parte das exigências para obtenção do Título de Doutor em AGRONOMIA (PRODUÇÃO VEGETAL), pela Comissão Examinadora:

Prof. Dr. ALAN RODRIGO PANOSSO
Departamento de Matemática / FEIS / UNESP - Ilha Solteira/SP

Prof. Dr. CARLOS EDUARDO PELLEGRINO CERRI
Departamento de Ciência do Solo / ESALQ - USP - Piracicaba/SP

Profa. Dra. JANAINA BRAGA DO CARMO
Departamento de Engenharia Florestal / UFSCAR / Câmpus Sorocaba - Sorocaba/SP

Prof. Dr. GENER TADEU PEREIRA
Departamento de Ciências Exatas / Faculdade de Ciencias Agrarias e Veterinarias de Jaboticabal

Profa. Dra. TERESA CRISTINA TARLE PISSARRA
Departamento de Engenharia Rural / Faculdade de Ciencias Agrarias e Veterinarias de Jaboticabal

Jaboticabal, 04 de fevereiro de 2016

CURRICULAR ACTIVITIES OF THE AUTHOR

Elton da Silva Bicalho was born in São Paulo, SP, Brazil on June 21, 1985. He earned his Bachelor of Science Degree in Agronomy in February, 2010 from the Faculty of Agrarian and Veterinary Sciences, Jaboticabal campus of the São Paulo State University (FCAV–UNESP). At that time, he was awarded for attaining the highest grade point average of the 2009 graduating class with the Faculty of Agrarian and Veterinary Sciences Award (Jaboticabal, SP, Brazil), and for best student of the 2009 graduating class with the Engineering Institute Award (São Paulo, SP, Brazil). During his bachelor's degree, he was grantee of the National Council for Scientific and Technological Development (CNPq) during the period between August, 2007 and August, 2009. In February, 2012, he earned his Master in Agronomy (Crop Production) from the FCAV–UNESP, and was grantee of the CNPq. In March, 2012, he joined to the Graduate Program in Agronomy (Crop Production) at the FCAV–UNESP, with a collaborative period from March, 2014 to February, 2015 in the University of Minnesota, Department of Soil, Water and Climate, St Paul, MN, USA, and was grantee of the São Paulo Research Foundation (FAPESP).

“In the living of life, things get mixed up. Life is like that: first it blows hot, then, cold; it tightens, then loosens; it soothes, then disquiets. What life demands of us is courage.”

“The Devil to Pay in the Backlands”
by João Guimarães Rosa

To my mom

ACKNOWLEDGEMENTS

I am grateful to my advisors Newton La Scala Júnior, Alan Rodrigo Panosso and Kurt A. Spokas, who helped me a lot and made easier the processes of learning and writing this doctoral dissertation.

I am really grateful to my great friends Daniel De Bortoli Teixeira and Mara Regina Moitinho; without the help of them all, this work would not have been possible.

I am grateful to Adriana, Norival, Shirley and Zezé, from the Department of Exact Sciences of the Faculty of Agrarian and Veterinary Sciences, Jaboticabal campus of the São Paulo State University (FCAV–UNESP), for being available for any help.

I am grateful to the Graduate Program in Agronomy (Crop Production) of the Faculty of Agrarian and Veterinary Sciences, Jaboticabal campus of the São Paulo State University (FCAV–UNESP).

I am grateful to the Department of Soil, Water, and Climate of the University of Minnesota for the support and facilities for conducting all the laboratory experiments, to the United States Department of Agriculture, Agricultural Research Service (USDA–ARS), and especially to Martin G. DuSaire for all the help.

I am grateful to the Coordination for the Improvement of Higher Education Personnel (CAPES) and to the São Paulo Research Foundation (FAPESP) for the financial support (processes number 2013/00360–7 and 2013/24926–0).

And I am also grateful to the São Martinho Mill for providing the area and facilities to this work.

SUMMARY

Page

EMISSÃO DE GASES DE EFEITO ESTUFA E SUA RELAÇÃO COM ATRIBUTOS DO SOLO EM ÁREA DE CANA-DE-AÇÚCAR

RESUMO – A produção dos principais gases de efeito estufa (GEE: CO_2, CH_4 e N_2O) é influenciada por práticas agrícolas que causam alterações nos atributos físicos, químicos e biológicos do solo, afetando diretamente sua emissão para a atmosfera. O objetivo deste estudo foi investigar a emissão de CO_2 do solo (F_{CO_2}) em condições de campo e a produção potencial de CO_2, CH_4 e N_2O do solo (P_{CO_2}, P_{CH_4} e P_{N_2O}, respectivamente) em condições de laboratório, além de suas relações com os atributos do solo em uma área de cana-de-açúcar colhida mecanicamente. A área experimental constituiu-se de um gradeado simétrico radialmente de 50 × 50 m contendo 133 pontos espaçados em distâncias mínimas de 0,5 m no centro da malha amostral. Foram conduzidas oito avaliações para F_{CO_2}, temperatura e umidade do solo durante um período de 19 dias. Os atributos físicos e químicos do solo foram determinados por meio de amostragem na profundidade de 0–10 cm. A quantificação de P_{CO_2}, P_{CH_4} e P_{N_2O} consistiu de incubação em laboratório e determinação da concentração dos gases por meio de cromatografia gasosa. F_{CO_2} apresentou um valor de emissão média de 1,19 µmol CO_2 m^{-2} s^{-1}, enquanto a produção de GEE em laboratório foi de 2,34 µg C–CO_2 g^{-1} d^{-1} e 0,20 ng N–N_2O g^{-1} d^{-1} respectivamente para P_{CO_2} e P_{N_2O}. Não foi observada produção ou oxidação significativa de CH_4. A análise de fatores mostrou a formação de dois processos independentes que explicaram quase 72% da variância total observada nos dados. O primeiro processo foi relacionado ao transporte de F_{CO_2} em campo e sua relação com atributos físicos do solo, tais como microporos, macroporos, relação C/N, umidade e densidade, mostrando a dependência entre F_{CO_2} e a porosidade do solo. O segundo processo foi relacionado à produção potencial de CO_2 e N_2O do solo em condições de laboratório e sua relação com atributos químicos do solo, tais como soma de bases, pH e fósforo disponível, os quais afetam a atividade microbiana e contribuem para a produção de GEE. Embora apresentados como independentes, esses processos estão relacionados e ocorrem simultaneamente no solo, fornecendo informações sobre sua variabilidade e mostrando se as emissões em campo são devidas aos processos de transporte de gás ou aos níveis de carbono no solo e sua qualidade. Além disso, a dependência espacial de F_{CO_2} está relacionada à porosidade do solo, assim como a dependência espacial de P_{CO_2} e P_{N_2O} está relacionada aos atributos químicos do solo. Adicionalmente, foi observada anisotropia principalmente em condições de campo, principalmente para os atributos relacionados à porosidade do solo, já que o solo pulverizado utilizado no laboratório perde sua estrutura e, consequentemente, o efeito do manejo encontrado em condições de campo.

Palavras-chave: dióxido de carbono, metano, óxido nitroso, produção potencial, respiração do solo, transporte gasoso

SOIL GREENHOUSE GAS EMISSIONS AND THEIR RELATIONS TO SOIL ATTRIBUTES IN A SUGARCANE AREA

ABSTRACT – The production of the main soil greenhouse gases (GHG: CO_2, CH_4 and N_2O) is influenced by agricultural practices that causes changes in soil physical, chemical and biological attributes, directly affecting their emission to the atmosphere. The aim of this study was to investigate the infield soil CO_2 emissions (F_{CO_2}) and the soil CO_2, CH_4 and N_2O production potentials (P_{CO_2}, P_{CH_4} and P_{N_2O}, respectively) in laboratory conditions, and their relationship to soil attributes in a mechanically harvested sugarcane area. The experimental area consisted of a 50 × 50-m radially symmetrical grid containing 133 points spaced at minimum distances of 0.5 m in the center of the sample grid. It was carried out eight evaluations of F_{CO_2}, soil temperature and soil moisture over a period of 19 days. Soil physical and chemical attributes were determined by sampling at a depth of 0–10 cm. The quantification of P_{CO_2}, P_{CH_4} and P_{N_2O} consisted of laboratory incubation and determination of gas concentration by gas chromatography. F_{CO_2} presented an infield average emission value of 1.19 μmol CO_2 m^{-2} s^{-1}, while GHG production in laboratory was 2.34 μg C–CO_2 g^{-1} d^{-1} and 0.20 ng N–N_2O g^{-1} d^{-1} for P_{CO_2} and P_{N_2O}, respectively. No significant production or oxidation was observed for CH_4. The factor analysis showed the formation of two independent processes that explained almost 72% of the total variance observed in the data. The first process was related to the transport of F_{CO_2} and its relation to soil physical attributes, such as microporosity, macroporosity, the C/N ratio, soil moisture and soil bulk density, showing the dependence between F_{CO_2} and soil porosity. The second process was related to the soil CO_2 and N_2O production potentials in laboratory conditions and their relation to soil chemical attributes, such as sum of bases, pH and available phosphorus, which affects the microbial activity and contributes to the GHG production. Although presented as independent, these processes are coupled and occur simultaneously in the soil, in addition to provide information about their variability, showing if the infield emissions are due to the gas transport processes or to soil carbon levels and their quality. Furthermore, the spatial dependence of F_{CO_2} is related to soil porosity, as well as the spatial dependence of P_{CO_2} and P_{N_2O} is related to soil chemical attributes. In addition, anisotropy occurred mainly under infield conditions, mostly for the attributes related to soil porosity since disturbed soils used under laboratory conditions lose their structure and hence the effect of the management found under infield conditions.

Keywords: carbon dioxide, methane, nitrous oxide, production potentials, soil respiration, gas transport

1 INTRODUCTION

Anthropogenic emissions of carbon dioxide (CO_2), methane (CH_4) and nitrous oxide (N_2O) have increased since the preindustrial era. These greenhouse gases (GHG) are mainly related to the burning of fossil fuels, land use and land use change, especially in agriculture, being mostly responsible for climate change (SCHNEIDER et al., 2001). The concentration of CO_2 in the atmosphere increased from 278 ppm in 1750 to 390.5 ppm in 2011; during the same period, there was an increase in the atmospheric concentration of CH_4, increasing from 722 ppb to 1,803 ppb; it was also observed in the concentration of N_2O, which increased from 271 ppb in 1750 to 324.2 ppb in 2011 (CIAIS et al., 2013).

In Brazil, in 2005, the total CO_2 emissions were estimated to be 1,638 Tg, especially in the sector of land use change and forestry, which accounted for 77% of these emissions (BRASIL, 2010). It should be noted that this total includes the emissions related to lime use in soils, which accounted for 7.5 Tg of CO_2. The CH_4 emissions were estimated to be 18.1 Tg, primarily attributed to the agricultural sector, which accounted for 70% of the total CH_4 emission (BRASIL, 2010). Similarly, N_2O emissions were estimated to be 546 Gg, with the agricultural sector accounting for 87% of the total N_2O emission (BRASIL, 2010).

Agricultural activities, such as soil tillage, influence GHG emission from soil to the atmosphere (LA SCALA; BOLONHEZI; PEREIRA, 2006; CORRADI et al., 2013; MOITINHO et al., 2013; SILVA-OLAYA et al., 2013; TEIXEIRA et al., 2013a; IAMAGUTI et al., 2015) since agricultural management practices in the production systems result in significant physical changes in the soil, altering the gains and losses of soil organic matter (EPRON et al., 2004; SARTORI et al., 2006; LAL, 2009). In agricultural areas, such variations occur mainly in the 0–30-cm soil layer, and are mostly due to mechanized soil disturbances and induced changes in quantity and quality of organic matter (JENKINSON et al., 1992; CHAN, 2001). In tropical soils, the set of all those variations could represent up to 50% of the initial carbon stock in the first 20 cm of the soil (FELLER; BEARE, 1997).

Similarly, soil porosity is also influenced by agricultural activities, directly affecting the transport of GHG in the soil (XU; QI, 2001; JASSAL et al., 2004; EPRON et al., 2006; BALL, 2013). In this case, gas exchange between soil and the atmosphere is regulated by the oxygen entry into the soil and the escape of GHG, which is directly related to the number and interconnectivity of pores in the soil, which could also limit soil oxygenation and thus microbial activity (FANG et al., 1998; BALL, 2013). In the same way, in a study conducted in Australia, in a sugarcane area under burning management and nitrogen fertilization, it was observed elevated rates of soil N_2O emissions for five months, which were related to increased soil porosity, frequent soil wetting and high content of soil organic carbon (DENMEAD et al., 2010).

Sugarcane is produced commercially worldwide and it is an important source of biomass used for the production of the ethanol, which is an alternative to fossil fuels. Brazil has a sugarcane crop area of approximately 9 million hectares and it is expected to produce in the 2015/2016 cropping season approximately 663 million tons of this culture (CONAB, 2015). The large amounts of crop residues left on the soil surface after harvest in mechanically harvested sugarcane areas have tremendous impact on the production processes and on the biogeochemical cycling of carbon and nitrogen, affecting soil organic matter dynamics and consequently GHG emissions (CERRI et al., 2013). In addition to influencing the carbon and nitrogen cycles, the environmental conditions and soil management practices adopted during the sugarcane crop cultivation may result in changes in soil physical, chemical and biological attributes, directly affecting microbial activity and thus the production of CO_2, CH_4 and N_2O and their exchanges between soil and the atmosphere (BLAIR, 2000; SARTORI et al., 2006; CERRI et al., 2007, 2013; DENMEAD et al., 2010; ALLAIRE et al., 2012; BALL, 2013; SIGNOR; CERRI, 2013; SIGNOR; PISSIONI; CERRI, 2014; TAVARES et al., 2015).

Considering that the sugarcane production could play an important role in soil GHG emissions because soil management may interfere with the fluxes of carbon and nitrogen between terrestrial ecosystems and the atmosphere, the aim of this study was to investigate the infield soil CO_2 emissions and the soil CO_2, CH_4 and N_2O production potentials in laboratory conditions, and their relationship to soil attributes in a mechanically harvested sugarcane area.

2 LITERATURE REVIEW

2.1 Soil greenhouse gases emission

The increased concentration of GHG in the atmosphere is the main cause of the global warming. In this scenario, it is worth noting that the conversion of forests and native grasslands areas to agricultural or pasture areas decreases the content of organic matter in tropical and subtropical soils due to the short and long-term consequences of disturbances caused by soil tillage associated to low levels of organic material addition (SARTORI et al., 2006). The process of soil carbon loss to the atmosphere is called soil CO_2 emission, or soil respiration, and it is the result of the microbial activity (chemical oxidation) and roots respiration. This process is considered the second largest source of CO_2 emission to the atmosphere, second only to the oceans (LAL, 2001; FOLLETT, 2001).

It is estimated that the carbon stock in Brazil soils at a depth of 0–30 cm is approximately 36.4 ± 3.4 Pg C, and changes in land use and agricultural practices account for more than two thirds of the total GHG emitted by soils (BERNOUX et al., 2002). Therefore, the importance of agriculture in this scenario is related not only to the process of soil carbon loss, but also to its significant potential for atmospheric carbon mitigation (FOLLETT, 2001) since agricultural soils can act as a source or a sink of atmospheric carbon depending on their use and management (USSIRI; LAL, 2009).

Soil GHG emission and its transport to the atmosphere is influenced by soil attributes, which present major effects when influenced by climate and cropping (BALL, 2013). This emission is also directly related to biological activity, such as roots respiration and decomposition of organic matter by microbial activity, which is influenced by soil temperature and soil moisture (AMUNDSON; DAVIDSON, 1990; LAL; FAUSEY; ECKERT, 1995; OHASHI; GYOKUSEN, 2007; DOMINY; HAYNES; ANTWERPEN, 2002; EPRON et al., 2006; CONCILIO et al., 2009; RYU et al., 2009). Although the GHG production and emission processes are mainly biological, soil physical attributes influence soil biology due to their effect on the physical environment (GREGORICH et al., 2006; BALL, 2013).

Different factors related to the physical, chemical and biological processes influence soil GHG emission, such as organic matter content (DOMINY; HAYNES; ANTWERPEN, 2002; KEMMITT et al., 2008; LAL, 2009), microbial activity (LLOYD; TAYLOR, 1994; FANG et al., 1998; EPRON et al., 2006; RYU et al., 2009), phosphorus content (DUAH-YENTUMI; RONN; CHRISTENSEN, 1998), soil pH (FUENTES et al., 2006), soil physical attributes, such as soil bulk density and soil porosity, which are responsible for soil oxygenation and transport of the gases from soil to the atmosphere (XU; QI, 2001; SCHWENDENMANN et al., 2003; EPRON et al., 2006), in addition to the factors that alter soil organic matter content, such as soil management and soil biomass addition (LAL, 2009).

Soil tillage practices destroy soil aggregates that offer physical protection to the organic matter against the action of microorganisms, increasing its decomposition and mineralization rates, especially in conventional management system, which presents a greater potential for GHG emissions when compared to less invasive soil management practices, such as the no-tillage system (SIX; ELLIOTT; PAUSTIAN, 1999). Management of certain agricultural crops, particularly sugarcane, can play an important role in the balance of soil GHG emissions to the atmosphere. In sugarcane areas under mechanically harvesting system, crop residues are left on the soil surface, favoring a greater accumulation of organic matter and reducing the emissions of GHG when compared to the burned sugarcane system (RAZAFIMBELO et al., 2006; CERRI et al., 2007; LUCA et al., 2008). In this context, when evaluating soil CO_2 emissions in both management systems, Panosso et al. (2009) observed, over 70 days of study, emissions 39% higher in the burned sugarcane system when compared to the mechanically harvesting system. This fact is attributed to the acceleration of the mineralization process of soil organic matter due to the burning of crop residues.

Climatic conditions and cultural practices adopted in the management of sugarcane, in addition to influencing the carbon cycle, also influence the nitrogen cycle and hence the N_2O and CH_4 exchanges between soil and the atmosphere. In a study conducted in Australia, in a sugarcane area under residue burning and nitrogen fertilization, it was observed a soil CH_4 emission of 19.9 kg CH_4 ha^{-1} (DENMEAD et al., 2010), which corresponds from 0.5% to 5.0% of the CH_4 emission in wetlands (BARTLETT et al., 1988) and areas under rice cultivation (WASSMAN; LANTIN; NEUE, 2000). In the same study, soil N_2O emissions were estimated to be 72.1 kg N_2O ha^{-1} with elevated rates for five months, which were related to high soil porosity, frequent soil wetting and high content of soil organic carbon (DENMEAD et al., 2010). In fact, the most important factors related to soil N_2O emissions are related to water-filled pore space, soil temperature and topsoil mineral N content (CONEN; DOBBIE; SMITH, 2000), in addition to soil type, soil tillage, nitrate fertilizer, residue incorporation and compaction (ARAH et al., 1991; BALL, 2013).

2.2 Spatial variability of soil greenhouse gases and soil attributes

Several environmental factors and soil management practices can result in changes in soil physical, chemical and biological attributes, influencing the production and emission of CO_2, CH_4 and N_2O in the soil (DASSELAAR et al., 1998; SARTORI et al., 2006; CERRI et al., 2007; DENMEAD et al., 2010). As an alternative to evaluate the complexity of the relationship among these factors, geostatistical analysis allows us to derive the spatial and temporal variability patterns of different soil attributes, including soil GHG emission, and develop a spatial variability model dependent on the scale and direction of sampling (BURROUGH, 1981; PALMER, 1988).

Therefore, most soil attributes present spatial variability; it means that the values assumed by certain attributes in a specific position in the study area vary according to the direction and separation distance between the neighboring samples. Under these conditions, the observations cannot be considered as independent and, therefore, the analyses based only on classical statistics show to be inadequate and a more detailed statistical processing is required. Several studies have investigated the spatial variability of soil physical (GONÇALVES; FOLEGATTI; MATA, 2001; WANG et al., 2002; CORÁ et al., 2004; SOUZA et al., 2004; HERBST et al., 2009; ALLAIRE et al., 2012; BERNARDI et al., 2014), chemical (TRANGMAR; YOST; UEHARA, 1986; CORÁ et al., 2004; SOUZA et al., 2004; BARBIERI; MARQUES JÚNIOR; PEREIRA, 2008; ALLAIRE et al., 2012; BERNARDI et al., 2014) and biological attributes (FRANKLIN; MILLS, 2003; HERBST et al., 2009), and some of them have studied the spatial variability of soil GHG emissions relating it to soil attributes (DASSELAAR et al., 1998; LA SCALA et al., 2000a; LA SCALA et al., 2003; HERBST et al., 2009; PANOSSO et al., 2009; BRITO et al., 2010; TEIXEIRA et al., 2011; ALLAIRE et al., 2012; BICALHO et al., 2014).

According to Brito et al. (2009), the spatial variability characterization of soil CO_2 emission can provide relevant information to better understand the dynamics of CO_2 in the soil-atmosphere system. In addition, soil attributes involved in the production and transport processes of CO_2 also show a high spatial variability, making complex to understand the variation of CO_2. On the other hand, Herbst et al. (2009) pointed out that the aspects related to the temporal variability of soil CO_2 emission are simple to be assessed when compared to the aspects related to its spatial variability since there are few information about the extension of spatial dependence of heterotrophic respiration and the variations within a certain area or experimental plot.

2.3 Anisotropy of soil greenhouse gases and soil attributes

Soil attributes, in addition to present spatial dependence, could also present anisotropy. In other words, soil attributes could present different spatial variability patterns in different directions. The anisotropy occurs because the spatial distribution of soil attributes is the result of a complex interaction of soil formation processes that act with varying intensity in different directions and spatial scales (TRANGMAR; YOST; UEHARA, 1986). Thus, management practices in agricultural areas may result in anisotropy, affecting attributes such as carbon, soil porosity and soil water content, which are directly related to soil respiration (LA SCALA et al., 2009).

In this context, fractal geometry provides new concepts for the mathematical description of heterogeneous measures, as in the case of soil attributes. According to Burrough (1981), the fractal dimension can be used as a useful indication of the autocorrelation complexity on various scales of natural phenomena, offering the possibility of measuring and integrating information related to soil physical, chemical and biological phenomena (PERFECT; KAY, 1995). The characterization of fractal dimension applied to the derivation of non-continuous spatial and temporal phenomena (MANDELBROT, 1977) could be used in spatial variability studies, especially in studying phenomena that are scale dependent (PERFECT; KAY, 1995; EGHBALL et al., 1999).

Fractal dimension is a great factor for characterizing the anisotropy of soil attributes since this parameter has been shown to be sensitive to the actions of external elements such as landscape, rain precipitation, vegetation cover, management practices and soil tillage (EGHBALL et al., 1999; VIDAL VÁZQUEZ; MIRANDA; PAZ GONZÁLEZ, 2005; LA SCALA et al., 2009; USOWICZ; LIPIEC, 2009; VIDAL VÁZQUEZ et al., 2010). These factors consequently affect other soil attributes related to soil GHG production and its transport in the soil, such as soil carbon content, soil porosity, soil moisture and oxygen content (LA SCALA et al., 2009; PANOSSO et al., 2012).

Quantifying soil complexity is a very important task to better understand the impacts of management on the spatial and temporal variability in its attributes. Although it is expected that the fractal models lead to a more accurate description of soil than the methods of classical geometry, the fractal parameters should not be taken as definitive for describing the heterogeneity of the soil system, but as a more accurate tool that can help to get insights into the sources and consequences of the observed complexity (PACHEPSKY; CRAWFORD, 2004).

3 MATERIAL AND METHODS

3.1 Location and description of the study area

The study was conducted in a production area with a 38-year history of sugarcane (*Saccharum* spp.) crop cultivation located at Santa Cândida farm in Pradópolis, São Paulo State, Brazil (21° 20’ S and 48° 08’ W; average altitude: 515 m) (Figure 1). The regional climate is classified as $B_2rB'_4a'$ (THORNTHWAITE, 1948), indicating a mesothermal region with rainy summers and dry winters. The mean annual precipitation registered was 1,517 mm, concentrated from October to March (81.1%), and less frequent precipitations and in lower intensity from April to September (18.9%); the mean annual temperature registered was 22.5 °C.

Figure 1. General view of the study area located in Pradópolis, São Paulo, Brazil.

The soil of the experimental area is classified as a high-clay Oxisol (Eutrustox, USDA Soil Taxonomy), and the slope was determined to be 3–4%. The sugarcane plantation was established in 2004, and the variety cultivated was CTC 14, which was in the eighth ratoon stage when our experiment was installed in the area. The area had been mechanically harvested for the last 15 years prior to the study, and after each harvest approximately 12 t ha^{-1} yr^{-1} of crop residues remained on the soil surface. In this area, on August 23 and 24, 2012, a 50 × 50-m radially symmetrical grid was installed containing 133 points spaced at minimum distances of 0.5 m in the center of the sample grid (Figures 2 and 3) to quantify the infield soil CO_2 emission along with sampled soil for GHG production potentials and soil attributes.

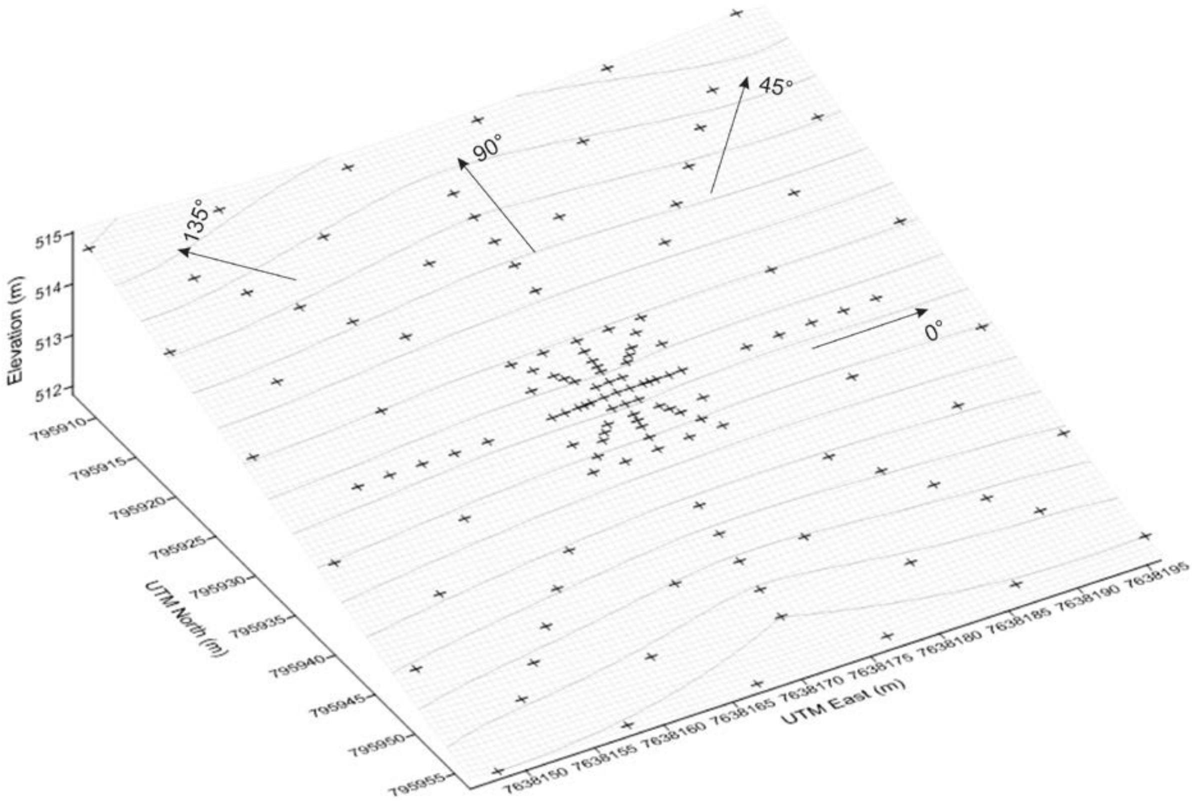

Figure 2. Representation of the sampling grid with 133 points (+) that was used to quantify the infield soil CO_2 emission, soil CO_2, CH_4 and N_2O production potentials, and soil attributes in the experimental area.

Figure 3. Construction of the sampling grid in the experimental area located at Santa Cândida farm, Pradópolis, São Paulo State, Brazil.

3.2 Infield soil CO_2 emission, soil temperature and soil moisture

Infield measurements of soil CO_2 emission (F_{CO_2}), soil temperature (T_s) and soil moisture (M_s) at all the grid points were recorded on August 27, 29 and 31, and on September 3, 5, 7, 11 and 14, 2012. On all days, the measurements were recorded in the morning from 8:00 to 9:30 h using two portable LI-8100 automated soil CO_2 flux systems (LI-COR, Lincoln, NE, USA) (Figure 4); the devices were tested and calibrated with each other before the beginning of the experiment. The LI-8100 system uses optical absorption spectroscopy in the infrared spectrum (IRGA–Infrared Gas Analyzer) to monitor changes in the CO_2 concentration inside a closed chamber. The chamber was coupled to the soil PVC collars that had been installed 24 h prior to the beginning of the measurements at all 133 sample points in order to reduce the disturbance caused during the insertion of the PVC collars in the soil (LA SCALA et al., 2000a; PANOSSO et al., 2009; BRITO et al., 2010; BICALHO et al., 2014).

Figure 4. Portable LI-8100 system (on the left) used to measure the in situ soil CO_2 emission and soil temperature, and TDR system (on the right) used to measure the soil moisture in the experimental area.

A portable sensor from the LI-8100 system was used to measure T_s by using a 20-cm probe (thermistor based) that was inserted 10 cm into the soil near the soil PVC collars (Figure 4). The measurements of M_s (in % of volume) were carried out using a Time Domain Reflectometry (TDR) system (Hydrosense TM, Campbell Scientific Inc., Logan, UT, USA), which consists of two 12-cm probes that are inserted into the soil, also near the soil PVC collars (Figure 4).

3.3 Soil sampling and analysis of soil chemical and physical attributes

Soil samples from a depth of 0–10 cm were obtained from all 133 grid points on September 24 and 25, 2012, after all the F_{CO_2}, T_s and M_s measurements had been recorded (Figure 5). Those samples were dried and sieved through a 2-mm mesh prior to further analyses that included soil organic matter (SOM) content, estimated by the soil organic carbon, which was determined by the wet oxidation method (modified Walkley–Black method), and the available phosphorus (P), K, Ca, Mg, and H + Al content (RAIJ et al., 2001), which allowed for the calculation of the sum of bases (Bases) and cation exchange capacity (CEC).

Figure 5. Extraction of soil samples from a depth of 0–10 cm from all 133 grid points in the experimental area.

The total content of soil nitrogen was obtained using a dry combustion technique in the presence of oxygen at 1440 °C. The soil carbon stock (C_{stock}) was calculated according to Veldkamp (1994) using the following equation:

$$C_{stock} = \frac{OC \times D_s \times E}{10}, \quad (1)$$

where C_{stock} is the soil carbon stock (Mg ha^{-1}), OC is the organic carbon content (g kg^{-1} = SOM/1.724), D_s is the soil bulk density (kg dm^{-3}) and E is the depth of soil layer (10 cm).

The particle size distribution of sand, silt and clay was determined by the pipette method after soil dispersion by using 1 molar solution of sodium hydroxide and sand sieving (DONAGEMA et al., 2011). The soil bulk density (D_s) was determined using the volumetric ring method, which consists of non-deformed samples collected by a sampler adapted to cylinders with an average internal volume of 50 cm^3 (DONAGEMA et al., 2011). The total pore volume (TPV, in % of volume), macropores (Macro) and micropores (Micro) was determined using the tension table method in which undisturbed soil samples were saturated and then drained to a potential equal to −0.006 MPa using a porous plate (DONAGEMA et al., 2011). The air-filled pore space (AFPS, in % of volume) fraction was calculated as the difference between the TPV and M_s.

3.4 Production potentials of soil greenhouse gas

The quantification of soil CO_2, CH_4 and N_2O production potentials (P_{CO_2}, P_{CH_4} and P_{N_2O}, respectively) was carried out using the 133 dry soil samples collected in the experimental area, which were sub-sampled from the soil chemical characterization. Additionally, soil microbial biomass (SMB) was also determined on the soils by adapting the methods of substrate induced respiration (glucose addition) by Anderson and Domsch (1978).

The method used for the evaluation consisted of a 50–60-day laboratory incubation with controlled temperature and soil water content adjusted to field capacity, and determination of rate changes in the headspace gas concentration by gas chromatography (SPOKAS; REICOSKY, 2009; SPOKAS, 2013). In the process of incubation, triplicates of 5 g of soil were taken from each of the 133 soil samples and placed in 125 mL vials. Then, 1.5 mL of deionized water was added in each vial, which was sealed with butyl rubber septa and pre-incubated at 25 °C for 6 days (Figure 6). Following this period, the vials were opened and vented for 20 minutes and re-sealed. The first gas sampling occurred 1–2 days after this procedure. Laboratory tests were conducted to establish the timing of this pre-incubation period, which was needed to allow for the development of equilibrium steady state GHG production conditions (CABRERA, 1993; FIERER; SCHIMEL, 2003).

Periodic headspace gas samples over the 50–60 days were analyzed to assess the production rate of the GHG. The headspace of the incubation was analyzed by taking 5 mL with syringes and injected into vials previously helium-flushed (Figure 7). The gas samples were injected into three different analytical columns contained in a single chromatograph (Figure 8). The first column (1000 µL) is a Porapak Q (0.32 mm × 1.8 m) with a minimum of 30 mL min^{-1} helium flow rate, which is connected to an electron capture detector (ECD) for analyzing N_2O. The second column (500 µL) is a Porapak N (0.32 mm × 1.8 m) with the same helium flow rate of the first column and connected to an analyzed flame ionization detector (FID) for CH_4 analysis. The third column (1.0 mL) is a CTR–1 column with a 45 mL min^{-1} helium flow rate and connected to a thermal conductivity detector (TCD) used to measure CO_2, O_2, and N_2. The gas chromatograph was calibrated by injecting 5 mL of known calibration gases into separate vials, which were used as standards.

Figure 6. Process of incubation in which triplicates consisting of soil and deionized water were placed in vials and sealed with butyl rubber septa.

Figure 7. Process of flushing helium into vials used to analyze the headspace gas samples in the gas chromatograph.

Figure 8. Gas chromatograph with three different analytical columns used to assess the production rate of soil greenhouse gases.

3.5 Analysis of results

Initially, the variability of the data was analyzed by using descriptive statistics (mean, standard error of mean, minimum, maximum and coefficient of variation) and linear correlation analysis, and then by using the multivariate exploratory analyses of principal components and factor analysis. For the extraction of factors, we used the principal component analysis (PCA), calculated from the correlation matrix between the variables (JEFFERS, 1978). The PCA analyzes the interdependence between the variables and condenses the information that is contained in the set of original variables into a set of smaller dimension compound of new latent variables, preserving a relevant amount of the original information. The new variables are the eigenvectors (principal components), generated by linear combinations of the original variables and constructed from the eigenvalues of the covariance matrix (HAIR JUNIOR et al., 2005). The correlation between the characteristics (variables) and the principal components is obtained by the following expression:

$$r_{xj}(pc_h) = \frac{a_{jh}\sqrt{\lambda_h}}{s_j}, \tag{2}$$

where a_{jh} is the coefficient of the j variable in the h-th principal component, λ_h is the h-th characteristic root (eigenvalue) of the covariance matrix, and s_j is the standard deviation of the j variable.

From the PCA, the data were submitted to the factor analysis, which is also a multivariate exploratory technique that allows observing the relationship between a set of variables. The first factor can be considered as the best summary of the linear relation shown in the data. The second factor is defined as the second best linear combination of variables and subject to the constraint of being orthogonal to the first factor; in order to be orthogonal to the first factor, it must be determined from the remaining variance after the first factor has been extracted. Thus, the second factor can be defined as the linear combination of variables that explains most of the residual variance after the effect of the first factor has been removed from the data. To redistribute the variance, we used the Quartimax normalized rotation in the factorial matrix whose ultimate effect provides a simple factorial pattern and theoretically more significant since the rotation is performed exactly to redistribute the variance from the first factors to the last ones.

We considered the first two factors, whose eigenvalues were higher than the unit and determined from the graph of the latent roots in relation to the number of factors in their order of extraction, being the shape of the resulting curve used to assess the cutoff point (KAISER, 1958). The coefficients of the linear functions, which define the factor loadings, were used in interpreting its meaning considering the signal and the relative size of the loadings as an indication of the weight to be assigned to each variable. Only the loadings with high values were considered for the interpretation, i.e., usually those higher than or equal to 0.50 in absolute value. After standardization of the variables (zero mean and unit variance), the analysis was carried out using the software Statistica 7.0 (StatSoft Inc., Tulsa, OK, USA).

In order to assess the spatial variability of soil greenhouse gases and soil attributes, the data were submitted to geostatistical analysis. The geostatistical analysis is based on the theory of regionalized variables, which is defined as a numerical function with a spatial distribution that varies from one location to another, with apparent continuity and complex variation (MATHERON, 1963). A regionalized variable is a random variable that takes on different values according to their position in space, being considered the realization of a set of random variables called random function and symbolized by $Z(x_i)$. This theory assumes that each variable $z(x_i)$ is modeled as a random variable $Z(x_i)$, which is expressed by the sum of three components: a structural component associated with a constant average value or a constant trend, a random component spatially correlated, and a random noise or residual error (BURROUGH, 1986).

The measured value $z(x_i)$ of certain random variable is a realization of the stochastic process $Z(x_i)$, where x_i is a fixed position. Each observation is described by its value and position information expressed by a coordinate system. The closest geographically observations tend to have similar values, which can be assessed by measures of association. Thus, the geostatistical analysis determines the degree of spatial dependence, or spatial autocorrelation, between observations based on the direction and distance between them.

The probabilistic interpretation of a regionalized variable as realization of a stochastic process $Z(x_i)$ only makes sense if it is possible to infer the distribution function or law of probability $Z(x_i)$ (JOURNEL; HUIJBREGTS, 1978). One of the limitations of the data analysis with spatial dependence is related to the impossibility of an experiment be repeated indefinitely and perform inference from a single realization. Thus, to estimate values at non-sampled locations it should be introduced restrictions of statistical stationarity, which allows that an experiment can be repeated even if the samples are collected at different points because they belong to the same population and have the same statistical moments.

The stochastic process $Z(x_i)$ is defined as stationary if all statistical moments are invariant to any point x_i. In other words:

$$E\,[(Z(x_i)] = m\,, \tag{3}$$

where $Z(X_i)$ is the random function and m is the mean of the variable values, which does not depend on the separation distance h. If we choose two different points in the area separated by the vector h, the mean value of the difference $[Z(x_i) - Z(x_i + h)]$ is:

$$E\,[(Z(x_i) - Z(x_i + h)] = 0 \tag{4}$$

Thus, we have the first-order stationarity, also known as average stationarity. However, for geostatistical analysis, it is also needed a second-order stationarity, which implies that for each pair of a random variable the covariance function $Cov(h)$ exists and is dependent on the distance h (VAUCLIN et al., 1983).

$$Cov(h) = E\,[Z(x_i)\,Z(x_i + h)] - m^2 \tag{5}$$

The second-order stationarity is not an easy condition to be satisfied since it implies the existence of a finite variance of the measured values, which is difficult to verify. Therefore, a simple alternative called intrinsic hypothesis can be assumed, which requires that for every vector h the variance of the increment $[Z(x_i) - Z(x_i + h)]$ be finite and independent of the position in the study area (TRANGMAR; YOST; UEHARA, 1986). Thus, we have the following function:

$$Var\,[Z(x_i) - Z(x_i + h)] = E\,[Z(x_i) - Z(x_i + h)]^2 = 2\gamma(h) \tag{6}$$

By definition, the Equation (6) represents the variogram:

$$2\gamma(h) = E\,[Z(x_i) - Z(x_i + h)]^2 \tag{7}$$

However, the semivariogram $\gamma(h)$ is more commonly used than the variogram, and when the intrinsic hypothesis is fulfilled, it can be estimated by the following equation (BURROUGH; MCDONNELL, 1998):

$$\hat{\gamma}(h) = \frac{1}{2N(h)} \sum_{i=1}^{N(h)} \left[Z(x_i) - Z(x_i + h)\right]^2 , \tag{8}$$

where $\hat{\gamma}(h)$ is the estimation of the semivariance at separation distance h, N is the number of pairs separated by distance h, $Z(x_i)$ is the value of the variable Z at the point x_i, and $Z(x_i + h)$ is the value of the variable Z at the point $x_i + h$. The graph of $\hat{\gamma}(h)$ as a function of h is called experimental semivariogram, which exhibits a purely random or systematic behavior and it is described by theoretical mathematical models.

In this study, we tested isotropic and anisotropic semivariograms considering the spherical, exponential and Gaussian models, as the Equations (9), (10) and (11), respectively. The best model was selected from the cross-validation process.

$$\begin{cases} \hat{\gamma}(h) = C_0 + C_1\left[\frac{3}{2}\left(\frac{h}{a}\right) - \frac{1}{2}\left(\frac{h}{a}\right)^3\right]; \text{ if } 0 < h < a \\ \hat{\gamma}(h) = C_0 + C_1; \text{ se } h \geq a \end{cases} \tag{9}$$

$$\hat{\gamma}(h) = C_0 + C_1\left[1 - \exp\left(-3\frac{h}{a}\right)\right]; \text{ if } 0 < h < d \tag{10}$$

$$\hat{\gamma}(h) = C_0 + C_1\left[1 - \exp\left(-3\left(\frac{h}{a}\right)^2\right)\right]; \text{ if } 0 < h < d \tag{11}$$

where d is the maximum distance of the semivariogram and C_0, C_1, $C_0 + C_1$ and a are the parameters of the semivariogram; C_0 is called nugget effect and represents the semivariance found at the intercept with the Y axis, C_1 is the contribution, i.e., the difference between the sill ($C_0 + C_1$) and the nugget effect (C_0), and characterizes the spatial dependence of a continuous stochastic processes, $C_0 + C_1$ is called sill and represents the semivariance value in which the semivariogram curve stabilizes, and a is the distance over which the samples are spatially correlated.

The estimation of soil greenhouse gases and other soil attributes at non-sampled places in the study area was carried out by using the ordinary kriging technique considering the adjusted models to the experimental semivariograms, calculated as the following equation:

$$\hat{z}(x_0) = \sum_{i=1}^{N} \lambda_i \, z(x_i) \tag{12}$$

where $\hat{z}(x_0)$ is the estimated value of the variable at the point 0, N is the number of values used in the prediction, λ_i is the weighting associated with each value, and $z(x_i)$ is the observed value at the point i. Both experimental semivariograms and ordinary kriging was calculated by using the software GS+ 9.0 (Gamma Design Software, LLC, Plainwell, MI, USA).

An anisotropic characterization of the spatial variability patterns was carried out considering both isotropic and anisotropic geostatistical models; in order to determine the variables that presented anisotropy, it was considered the cross-validation and the anisotropy factor. In addition, another method was used in order to determine whether the anisotropy exists or not to the study variables in the experimental area. This method uses fractal dimension (D_F) to represent the spatial dependence of the studied variables. The semivariogram method was used for the calculation of D_F (MIRANDA, 2000; VIDAL VÁZQUEZ; MIRANDA; PAZ GONZÁLEZ, 2005). This method uses the semivariance estimated to different distances, in accordance to the Equation (8), and D_F is calculated from the regression slope in a log–log graph of semivariance against distance (MARK; ARONSON, 1984).

The spatial structure of fractal surfaces can be described by means of a power law, as shown in the following relation:

$$\left| z(x) - z(x+h) \right| \propto h^{H}, \tag{13}$$

where z is the value of the attribute at x location, h is the separation distance and H is the fractal codimension or Hölder exponent (HUANG; BRADFORD, 1992). Comparing Equations (8) and (13), we can derive the following expression to denote a fractal characteristic at a given scale:

$$\hat{\gamma}(h) \propto h^{2H} \tag{14}$$

or, expressed in another way:

$$\log[\hat{\gamma}(h)] \propto 2H \log[h] \tag{15}$$

According to Equation (15), the slope of the experimental variogram on the log–log scale is equal to $2H$. The H exponent can then be obtained by means of a linear regression taken in this log–log graph by the following equation (PERFECT; KAY, 1995):

$$H = \lim_{h \to 0} \frac{\log[\hat{\gamma}(h)]}{2\log[h]} \tag{16}$$

If $0 < H \leq 1$, the fractal codimension is defined as follows:

$$H = d - D_F , \tag{17}$$

where D_F is the fractal dimension and d is the Euclidian dimension of the system in which the fractal distribution has been described. For lines, surfaces and volumes, d is equal to 1, 2 and 3, respectively.

The presence of this linear relationship indicates that the fractal model is appropriate to simulate the spatial dependence in the studied scale (PACHEPSKY; CRAWFORD, 2004). When $H = 0$, the value of D_F is equal to 3, which represents the lack of a spatial variability structure, as there would be no relationship between the way the attribute varies in space and the distance between points. In this case, there is no fractal dimension, and the methodology does not apply. However, when $0 < H < 3$, the fractal dimension has values that characterize the presence of the spatial variability structure and the dependence of the attribute studied with h (PALMER, 1988). Thus, for the distribution of a given attribute in the soil, its D_F is given by:

$$D_F = 3 - \frac{\log[\hat{\gamma}(h)]}{2\log[h]} \tag{18}$$

However, since the log–log of semivariance against distance is equal to the angle of the linear regression, we have that:

$$D_F = 3 - \frac{1}{2} b , \tag{19}$$

where b is the angular coefficient of the linear regression.

The D_F calculation was performed using methodology developed by Miranda (2000). It was calculated considering different combinations of separation distances and lag intervals. In this case, the separation distance varied from 5 to 60 m with a

5-m interval, and the lag interval considered for each separation distance varied from 0.5 to 12 m with a 0.5-m interval. Also, for the calculation of D_F, it was considered only semivariograms that had at least 5 points in the semivariance curve and, for each point in the curve, a minimum of 30 pair of points. The directions considered were 0°, 45°, 90° and 135°; 0° represents the direction parallel to the sugarcane row, 90° represents the slope of the study area, and 45° and 135° corresponds to the direction of the sugarcane ratoon elimination during the field reform (Figure 2). Afterwards, fractograms, which show the D_F values for different distances and scales, were constructed and used in the anisotropic analysis of spatial dependence between soil greenhouse gases and other soil attributes.

4 RESULTS AND DISCUSSION

4.1 Descriptive statistics

The infield F_{CO_2} presented a mean value of 1.19 µmol CO_2 m^{-2} s^{-1}, with a minimum of 0.50 µmol CO_2 m^{-2} s^{-1}, a maximum of 2.29 µmol CO_2 m^{-2} s^{-1} and a CV of 31.68% (Table 1). These rates are similar to those observed in experiments conducted previously in the same geographic region with sugarcane crops (BRITO et al., 2010; PANOSSO et al., 2011, 2012; CORRADI et al., 2013; BICALHO et al., 2014; TAVARES et al., 2015). The variations in F_{CO_2} observed in those studies, even carried out in areas of the same region, are related to changes in soil attributes for each area, such as soil temperature, soil moisture, soil organic matter, microbial activity, pH, the C/N ratio, phosphorus content, soil bulk density and soil porosity (DUAH-YENTUMI; RONN; CHRISTENSEN, 1998; FUENTES et al., 2006; KEMMITT et al., 2008; CONCILIO et al., 2009; NGAO et al., 2012; OYONARTE et al., 2012; BALL, 2013; TEIXEIRA et al., 2013a; KARHU et al., 2014; MOITINHO et al., 2015). These controlling factors are directly dependent on the environmental conditions and the management of the agricultural area, and small variations in each of them may lead to considerable variations in F_{CO_2}.

The rates of GHG production/consumption were calculated from the linear increase or decrease (slope) in the headspace concentration change with time using data obtained by sampling during the incubation period. P_{CO_2} varied from 0.93 to 4.25 µg C–CO_2 g^{-1} d^{-1}, with a mean of 2.34 µg C–CO_2 g^{-1} d^{-1} and a CV of 34.45% (Table 1). The variations in P_{CO_2} observed in this study are mainly due to soil chemical and biological attributes since the study was conducted under laboratory conditions and using disturbed soil samples. In this case, soil attributes such as pH, SOM, C/N, P, Bases and CEC could influence SMB and thus the production of CO_2 in the soil. The gas transport process, which is related to soil porosity, would not have a greater influence on the production potential process of this GHG.

The values of P_{N_2O} presented a minimum of −0.19 ng N–N_2O g^{-1} d^{-1}, which means a consumption of N_2O during the incubation period, and a maximum of 0.57 ng N–N_2O g^{-1} d^{-1}, with a mean of 0.20 ng N–N_2O g^{-1} d^{-1} and a CV of 68.31% (Table 1).

These values are relatively low when compared to other studies conducted under in-field conditions in sugarcane areas (SIGNOR; PISSIONI; CERRI, 2014; VARGAS et al., 2014). There are three key factors for N_2O emission in the soil: water-filled pore space, temperature and topsoil mineral N content (CONEN; DOBBIE; SMITH, 2000). These three key factors, especially when coupled to not optimal conditions of anaerobiosis for the denitrification process could explain the low production of N_2O in this study.

Table 1. Descriptive statistics of soil CO_2 emission, soil CO_2 and N_2O production potentials, soil microbial biomass, soil temperature, soil moisture, and other soil physical and chemical attributes in the 0–0.10-m soil layer.

Variable	Mean	SE	Min	Max	CV (%)
F_{CO_2} (µmol CO_2 m^{-2} s^{-1})*	1.19	0.03	0.50	2.29	31.68
P_{CO_2} (µg C–CO_2 g^{-1} d^{-1})	2.34	0.07	0.93	4.25	34.45
P_{N_2O} (ng N–N_2O g^{-1} d^{-1})	0.20	0.01	−0.19	0.57	68.31
SMB (mg microbial C g^{-1} h^{-1})	511.20	13.90	191.30	937.10	31.17
T_s (°C)*	20.57	0.03	19.61	21.37	1.86
M_s (%)*	9.25	0.07	7.50	11.50	9.31
D_s (g cm^{-3})	1.45	0.01	1.17	1.71	7.89
AFPS (%)	40.58	0.35	31.56	51.13	9.86
TPV (%)	49.83	0.37	41.06	59.99	8.56
Macro (%)	19.61	0.58	4.04	37.06	33.80
Micro (%)	30.36	0.23	23.03	35.18	8.50
Sand (g kg^{-1})	424.87	0.88	401.40	449.33	2.29
Silt (g kg^{-1})	99.66	1.65	55.47	144.50	19.06
Clay (g kg^{-1})	475.47	1.81	424.36	524.48	4.4
pH	5.43	0.03	4.73	6.13	6.16
SOM (g dm^{-3})	28.29	0.31	20.13	36.50	12.38
C_{stock} (Mg ha^{-1})	8.26	0.10	5.59	11.19	13.69
C/N	7.36	0.12	4.44	10.57	17.58
P (mg dm^{-3})	23.21	0.61	13.07	44.72	28.79
Bases (mmol$_c$ dm^{-3})	47.96	1.06	22.30	79.28	24.93
CEC (mmol$_c$ dm^{-3})	82.66	0.91	56.63	107.89	12.53

N = 133; *general mean of all studied days; SE–standard error of mean; Min–minimum; Max–maximum; CV–coefficient of variation; F_{CO_2}–soil CO_2 emission; P_{CO_2}–soil CO_2 production potential; P_{N_2O}–soil N_2O production potential; SMB–soil microbial biomass; T_s–soil temperature; M_s–soil moisture; D_s–soil bulk density; AFPS–air-filled pore space; TPV–total pore volume; Macro–macroporosity; Micro–microporosity; Sand–sand content; Silt–silt content; Clay–clay content; SOM–soil organic matter; C_{stock}–carbon stock; C/N–carbon to nitrogen ratio; P–available phosphorus; Bases–sum of bases; CEC–cation exchange capacity.

There was no production or consumption of CH_4. This fact may be related to a lack of optimal conditions for the performance of the methanogenic bacteria. The essential soil chemical and mineralogical properties for the occurrence of the redox condition involves mainly O, N, Fe, Mn, S, and C (PONNAMPERUMA, 1972). In this process, Fe and Mn are reduced and the methanogenic bacteria, in anaerobic conditions, begin to use C as an electron acceptor, resulting in the production of CH_4 (PETERS; CONRAD, 1996; BODEGOM; STAMS, 1999). Under infield conditions, Signor, Pissioni and Cerri (2014) observed an increase in soil CH_4 emissions as a function of the increasing amount of sugarcane crop residues left on the soil surface. In this case, the production of CH_4 in the soil occurs in microsites where there is no oxygen, as in anaerobic zones at the center of the soil aggregates.

The values of T_s and M_s presented small changes during the 19 days of infield measurements. T_s varied from 19.61 °C to 21.37 °C, with a mean to the period of 20.57 °C, and M_s varied from 7.50% to 11.50% (v/v), presenting a mean of 9.25% (v/v) (Table 1). The main factors that control the temporal variations of F_{CO_2} are T_s and M_s (TEDESCHI et al., 2006; KOSUGI et al., 2007; OHASHI; GYOKUSEN, 2007; CONCILIO et al., 2009); in our study, the small changes in these main factors could be related to the presence of crop residues on the soil surface, reflecting in the infield F_{CO_2} variations over the studied days. Maintaining crop residues on the soil surface creates a physical barrier that preserves M_s, providing a thermal insulation (USSIRI; LAL, 2009). It also reduces the daily maximum temperatures and raises the minimum temperatures compared to soils without vegetation cover (TOMINAGA et al., 2002).

In addition, studies conducted in sugarcane areas showed that F_{CO_2} increases with an increase in the amount of crop residues on the soil surface (CARMO et al., 2013; SIGNOR; PISSIONI; CERRI, 2014). This fact can be attributed to the positive relationship between the amount of CO_2 emitted by the soil and SOM, which is related to the addition of crop residues on the soil surface (OLIVEIRA et al., 2013; SIGNOR; PISSIONI; CERRI, 2014; VARGAS et al., 2014). On the other hand, short-term period studies also conducted in sugarcane areas showed that the crop residues on the soil surface may contribute to a significant reduction in soil CO_2 emissions (LA SCALA; BOLONHEZI; PEREIRA, 2006; PANOSSO et al., 2011; CORRADI et al., 2013; SILVA-OLAYA et al., 2013).

4.2 Linear correlation analysis

The linear correlation analysis was significant (P<0.05) for F_{CO_2} and some soil physical attributes related to soil porosity (Table 2). The soil attributes D_s (r = −0.57) and Micro (r = −0.42) showed a negative linear correlation with F_{CO_2}, whereas M_s (r = 0.52), AFPS (r = 0.45), TPV (r = 0.53) and Macro (r = 0.56) presented a positive linear correlation with F_{CO_2}. In a sugarcane-cultivated soil under mechanized harvesting located close to our study site, it was found only significant linear correlations for the soil physical attributes D_s (r = −0.32), AFPS (r = 0.18), Macro (r = 0.21), and Micro (r = −0.18); for the other soil physical and chemical attributes, the linear correlation coefficients were not significant (BICALHO et al., 2014). Correlations between F_{CO_2} and these variables have been cited frequently by several studies, demonstrating the importance of soil physical attributes for microbial activity and the gas exchange in the soil-atmosphere system, although frequently those correlations are weak (LA SCALA et al., 2000a; XU; QI, 2001; EPRON et al., 2006; OHASHI; GYOKUSEN, 2007; PANOSSO et al., 2009, 2011; HERBST et al., 2010; TEIXEIRA et al., 2013b; BICALHO et al., 2014; MOITINHO et al., 2015).

F_{CO_2} was not linearly correlated to T_s (Table 2), possibly due to low variations throughout the experiment, as measured by the CV values (Table 1). Similarly to our results, a study conducted in the same region has shown non-significant correlation between F_{CO_2} and T_s (LA SCALA; PANOSSO; PEREIRA, 2003). However, in a study conducted in a forest area in French Guiana, Epron et al. (2006) observed a positive correlation between F_{CO_2} and T_s, which is probably due to an increase in the soil microbial activity with the increase of T_s (LLOYD; TAYLOR, 1994; EPRON et al., 1999; BURTON; PREGITZER, 2003; EPRON et al., 2006; RYU et al., 2009) since forest soils may have a greater variation and diversity of microorganisms in the soil when compared to soils under a monoculture cultivation, as the sugarcane crop. On the other hand, M_s presented a positive linear correlation with F_{CO_2} (r = 0.52) (Table 2), demonstrating the importance of this attribute as a controlling factor of F_{CO_2}, mostly its temporal variation. Similarly, Vargas et al. (2014) observed that in soil cultivated with sugarcane the emissions of CO_2 increased linearly with an increase in M_s, with greater emissions when crop residues were on the soil surface.

Table 2. Pearson correlation coefficients between soil CO_2 emission, soil CO_2 and N_2O production potentials and soil microbial biomass with soil temperature, soil moisture and other soil physical and chemical attributes.

Variable	F_{CO_2}	P_{CO_2}	P_{N_2O}	SMB
F_{CO_2}	–	−0.22*	−0.26*	0.08
P_{CO_2}	−0.22*	–	0.35*	0.38*
P_{N_2O}	−0.26*	0.35*	–	0.26*
SMB	0.08	0.38*	0.26*	–
T_s	−0.10	0.12	−0.08	−0.03
M_s	0.52*	−0.23*	−0.36*	−0.01
D_s	−0.57*	0.14	0.11	−0.15
AFPS	0.45*	−0.10	−0.03	0.21*
TPV	0.53*	−0.14	−0.11	0.19*
Macro	0.56*	−0.16	−0.15	0.11
Micro	−0.42*	0.24*	0.29*	0.07
Sand	−0.10	0.03	0.00	−0.15
Silt	−0.02	0.23*	0.15	0.31*
Clay	0.07	−0.26*	−0.21*	−0.18*
pH	−0.08	0.41*	0.21*	0.62*
SOM	0.05	0.22*	0.07	0.19*
C_{stock}	−0.28*	0.22*	0.08	0.04
C/N	0.08	0.16	0.09	0.07
P	0.12	0.24*	0.12	0.41*
Bases	−0.03	0.52*	0.29*	0.57*
CEC	−0.15	0.45*	0.30*	0.35*

*Significant Pearson correlation coefficient values (P<0.05); F_{CO_2}–soil CO_2 emission; P_{CO_2}–soil CO_2 production potential; P_{N_2O}–soil N_2O production potential; SMB–soil microbial biomass; T_s–soil temperature; M_s–soil moisture; D_s–soil bulk density; AFPS–air-filled pore space; TPV–total pore volume; Macro–macroporosity; Micro–microporosity; Sand–sand content; Silt–silt content; Clay–clay content; SOM–soil organic matter; C_{stock}–carbon stock; C/N–carbon to nitrogen ratio; P–available phosphorus; Bases–sum of bases; CEC–cation exchange capacity.

P_{CO_2} showed significant and positive linear correlation coefficient with SOM (r = 0.22) and C_{stock} (r = 0.22) (Table 2), which are important factors related to the soil production and emission of CO_2. In fact, SOM is the main source of CO_2 production in the soil and it is promoted by the microbial activity (STOTZKY; NORMAN, 1961; BALL; SCOTT; PARKER, 1999; VARGAS; SCHOLLES, 2000; DOMINY; HAYNES; ANTWERPEN, 2002; KEMMITT et al., 2008; OLIVEIRA et al., 2013; VARGAS et al., 2014; TAVARES et al., 2015). On the other hand, F_{CO_2} was negatively correlated

(P<0.05) with C_{stock} (−0.28) (Table 2) in contrast to other studies which usually have found a positive relationship between the carbon stock and soil CO_2 emission (COSTA et al., 2008; LUCA et al., 2008; PANOSSO et al., 2011).

In addition, the clay content was significantly correlated with P_{CO_2} (r = −0.26), P_{N_2O} (r = −0.21) and SMB (r = −0.18) (Table 2). This and the fact that F_{CO_2} was negatively correlated with C_{stock} may be related to the existing complex relationship between clay minerals and the soil microbial activity that directly influences the production of GHG in the soil and its emission to the atmosphere. In this case, the clay could act as a protection to the organic carbon against the action of microorganisms, preventing the mineralization of SOM (LA SCALA et al., 2000b; DOMINY; HAYNES; ANTWERPEN, 2002; FUENTES et al., 2006; GRAHAM; HAYNES, 2006; SIX et al., 2006; CANELLAS et al., 2010) as well as reducing the O_2 used in the aerobic microbial decomposition processes (TSAI; BARAIBAR; ROMANI, 1992; ROBERTSON; THORBURN, 2001; TOMINAGA et al., 2002), which could explain the negative relationship found in our study.

Additionally, P_{CO_2}, P_{N_2O} and SMB showed significant correlation coefficients (P<0.05) with the most soil chemical attributes and, in general, a moderate correlation with them. It is known that the improvement of soil chemical conditions contributes to the increase of microbial activity and hence for the GHG production. In the same way, soil pH not only affects SMB, but also affects the composition of its population in the soil, providing a good environment for the activity of certain classes of microorganisms, increasing the SMB and, consequently, the rates of GHG production (FUENTES et al., 2006). Similarly, the available phosphorus content is also considered a limiting factor for microbial activity since it is an essential element in its metabolism (DUAH-YENTUMI; RONN; CHRISTENSEN, 1998).

In addition, the presence of crop residues on the soil surface in sugarcane areas under mechanically harvest management can contribute to the increase of SOM, altering the chemical properties and improving soil fertility (VARGAS; SCHOLLES, 2000; CANELLAS et al., 2003; OLIVEIRA et al., 2013; VARGAS et al., 2014); it also contributes with 56% to 82% of CEC in soils under tropical conditions, retaining cations and preventing leaching losses (RAIJ, 1981). Thus, the soil pH and nutrients content, combined with the available carbon in the soil under study, may have had an important role to create the ideal conditions for the microbial activity and the production of GHG. This fact could be evidenced by the positive and significant linear correlation between SMB and P_{CO_2} (r = 0.38) and P_{N_2O} (r = 0.26) (Table 2).

4.3 Factor analysis

The relationship of interdependence between soil greenhouse gases and soil attributes is shown in Figure 9. It was possible to identify two processes (factors) occurring in the soil, explaining almost 72% of the total variance observed in the original data. These results are consistent with the criteria established by Sneath and Sokal (1973), wherein the number of factors used in the interpretation must be such that explain at least 70% of the total variance. The Factor 1 represents almost 50% of the total variance observed, and considering the order of relevance of the factor loadings, it retained the attributes Micro (−0.81), Macro (0.74), C/N (−0.70), F_{CO_2} (0.63), M_s (0.63) and D_s (−0.62). The factor loadings represent the correlation of each variable with the factor; the higher their absolute values, the higher it is their relevance in interpreting the factor matrix (HAIR JUNIOR et al., 2005). In addition, taking into account the values and signs of the factor loadings, it was observed that F_{CO_2}, Macro and M_s are directly associated, and that the attributes D_s, Micro and C/N have a contrary association with F_{CO_2}.

The direct association between F_{CO_2} (0.63), Macro (0.74) and M_s (0.63) (Figure 9) found in our study could be related to the fact that these soil physical attributes control oxygen exchange in the soil, influencing the microbial activity and hence F_{CO_2}. It is known that the gas exchange between soil and the atmosphere is dependent on soil texture, structure and water content (BALL; SIMTH, 1991; KANG et al., 2000). Also, the respiration of macro and microorganisms, as well as roots respiration, are optimized in soils that have a higher amount of medium and large pores (macro), which allows for a better aeration in the soil (CAPECHE et al., 2004). On the other hand, the direct association of D_s (−0.62) and Micro (−0.81), which is contrary to Macro (0.74) and M_s (0.63) (Figure 9), could lead to lower soil CO_2 emissions since high values of D_s could limit the oxygen in the soil due to the decrease number of pores and the corresponding limitation of the microbial activity. Such association is characteristic of mechanically harvested sugarcane areas due to the non-tilled soil structure, which leads to soil compaction in the 0−20-cm layer due to the higher tractor traffic on the area (TOMINAGA et al., 2002; SOUZA et al., 2005; OLIVEIRA et al., 2010), especially when it is performed in clayey soils (SILVEIRA; STONE, 2003), as in the study area (Table 1).

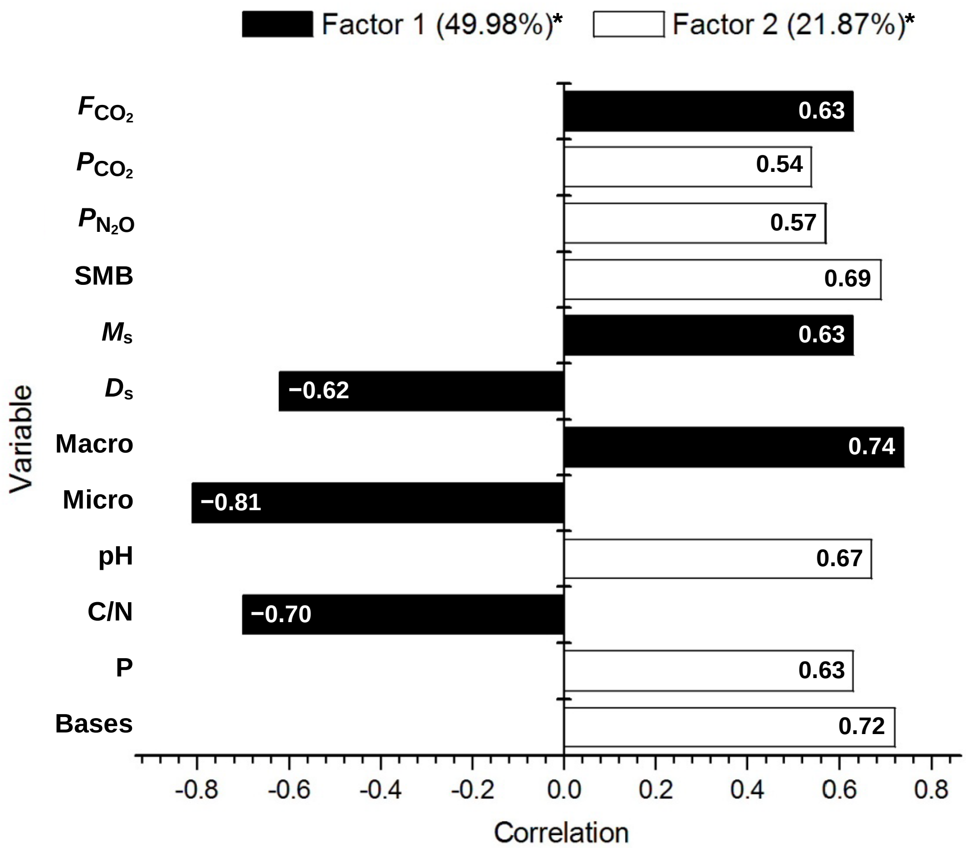

Figure 9. Factor analysis showing the correlation coefficients between the variables and the factors. *Value refers to the percentage of variation of the original set of data retained by the factor. Values within the bars are the loadings considered in the interpretation of the factor (higher than or equal to 0.5); F_{CO_2}–soil CO_2 emission; P_{CO_2}–soil CO_2 production potential; P_{N_2O}–soil N_2O production potential; SMB–soil microbial biomass; M_s–soil moisture; D_s–soil bulk density; Macro–macroporosity; Micro–microporosity; C/N–carbon to nitrogen ratio; P–available phosphorus; Bases–sum of bases.

The variables F_{CO_2} (0.63) and C/N (−0.70) were inversely associated in the Factor 1 (Figure 9). The soil C/N ratio is an important soil attribute related to the quality of soil carbon, influencing soil CO_2 emission (ALLAIRE et al., 2012; NGAO et al., 2012). Thus, the higher the C/N ratio in the soil is, the greater the difficulty for microorganisms to decay the soil organic matter, which could lead to lower values of F_{CO_2}. This fact may explain that inverse association between F_{CO_2} and the C/N ratio observed in our study. As a matter of fact, other studies have found a negative relationship between F_{CO_2} and the C/N ratio and also that a low C/N ratio in the soil increases microbial activity (KHOMIK; ARAIN; MCCAUGHEY, 2006; VESTERDAL et al., 2008; ALLAIRE et al., 2012; NGAO et al., 2012). Therefore, the Factor 1 is related to the process associated to the transport of CO_2 in the soil since some soil physical attributes related to soil structure were retained in this factor, supporting the dependence between F_{CO_2} and soil porosity.

The Factor 2 represents almost 22% of the variance of the original data, and considering the order of relevance of the factor loadings, it retained the attributes Bases (0.72), SMB (0.69), pH (0.67), P (0.63), P_{N_2O} (0.57) and P_{CO_2} (0.54) (Figure 9), which are related to the process associated to the production potentials of GHG in the soil; in other words, the laboratory derived production rates that were measured in the laboratory and some chemical attributes. Furthermore, the factor loadings of these attributes showed the same sign, indicating that they are directly associated in the Factor 2, suggesting that the improvement of soil chemical conditions contributes to the increase of microbial activity and hence for the GHG production.

In addition, it is widely reported in the literature that sugarcane crop residues left on the soil surface after harvest increase SOM, which is directly related to the time of adoption of the mechanical harvest system in sugarcane areas, being the increase of soil organic matter generally observed in the upper layers of soil (RAZAFIMBELO et al., 2006; LUCA et al., 2008; GALDOS; CERRI; CERRI, 2009; CANELLAS et al., 2010; THORBURN et al., 2012). It also alters soil chemical attributes and improves soil fertility (VARGAS; SCHOLLES, 2000; CANELLAS et al., 2003; OLIVEIRA et al., 2013; VARGAS et al., 2014). Thus, the soil pH and nutrients content, combined with the available carbon in the soil under study, may have had an important role to create the ideal conditions for the microbial activity and the production of the greenhouse gases under laboratory conditions since P_{CO_2}, P_{N_2O} and SMB are directly associated in the Factor 2.

The Factors 1 and 2 are orthogonal to each other and thus independent. It means that the attributes related to the transport of CO_2 (F_{CO_2}, D_s, Macro, Micro, C/N and M_s) (Factor 1) are not correlated to the soil greenhouse gas production potentials process quantified under laboratory conditions (P_{CO_2}, P_{N_2O}, SMB, pH, P and Bases) (Factor 2). When the characterization of CO_2 in the laboratory is considered, with the use of disturbed soil samples, it provided a means of assessing the CO_2 production potentials under ideal conditions, not considering the differences in the CO_2 emissions due to the gas transport processes, such as those related to soil porosity. However, although considered as independent by the factor analysis, these processes are coupled and occur simultaneously in soils. Therefore, soil greenhouse gases emissions are dependent on the gas production processes in the soil and its transport to the atmosphere.

4.4 Spatial variability structure of soil greenhouse gases and soil attributes

The characterization of the spatial variability structure of soil GHG and soil attributes was determined by adjusting isotropic models to the experimental semivariograms. It was observed that the adjusted semivariogram models were spherical for all the study variables (Table 3 and Figures 10 and 11). Other studies have adjusted spherical models to the experimental semivariograms for F_{CO_2} (DASSELAAR et al., 1998; LA SCALA et al., 2000a; CARDELLINI et al., 2003; KONDA et al., 2008; BRITO et al., 2010; HERBST et al., 2010; TEIXEIRA et al., 2011), T_s (AL-KAYSSI, 2002; PANOSSO et al., 2009) and M_s (PANOSSO et al., 2009). On the other hand, exponential models have been found for F_{CO_2} (TEDESCHI et al., 2006; OHASHI; GYOKUSEN, 2007) or even a lack of spatial variability (nugget effect) (PANOSSO et al., 2009), showing that in general considerable variations can be found for a single variable subject to different situations, such as soil type, crop management system, season, rain precipitation event and experimental plot size.

Also, most models presented high values of coefficient of determination, which is related to the mathematical models that describe the variability in different ways and for the existing characteristcs in the spatial patterns. In this case, spherical models describe variables with high spatial continuity, or less erratics, at closer distances (ISAAKS; SRIVASTAVA, 1989). In fact, our study was conducted in a small grid of 50 × 50 m in which the arrangement of the sampling points, placed densely at the center of the grid and showing minimum distances of 0.5 m (Figure 2), may have promoted the assessment of the variables in small-scale, being possible to capture the values of semivariance over small distances for most of the variables. This fact may have contributed to the ranges of the isotropic semivariograms have presented relatively small values for almost all variables (Table 3), which could explain the spherical models found.

Table 3. Models and estimated parameters adjusted to experimental isotropic semivariograms obtained for soil CO_2 emission, soil CO_2 and N_2O production potentials, soil microbial biomass, soil temperature, soil moisture and other soil physical and chemical attributes.

Variable	Model	C_0	C_0+C_1	A	SSR	R^2	DSD	a	b
F_{CO_2}	Sph	0.079	0.127	15.3	2.53E−04	0.91	0.62	0.35	0.73
P_{CO_2}	Sph	0.052	0.107	10.3	4.95E−04	0.67	0.49	0.28	0.88
P_{N_2O}	Sph	0.008	0.024	16.9	1.13E−05	0.94	0.34	0.09	0.64
SMB	Sph	0.073	0.119	12.0	8.42E−04	0.60	0.61	35.33	0.95
T_s	Sph	0.100	0.169	20.2	1.73E−03	0.76	0.59	−2.09	1.10
M_s	Sph	0.376	0.741	14.6	2.23E−02	0.80	0.51	2.54	0.72
D_s	Sph	0.008	0.011	18.6	1.01E−06	0.86	0.71	0.41	0.71
AFPS	Sph	8.131	15.211	4.9	9.67E+00	0.74	0.53	−0.84	1.03
TPV	Sph	8.468	15.850	4.0	6.12E+00	0.83	0.53	2.63	0.95
Macro	Sph	21.499	36.595	18.9	1.12E+01	0.93	0.59	7.70	0.61
Micro	Sph	3.244	6.127	20.2	1.01E+00	0.86	0.53	10.43	0.66
Sand	Sph	24.300	78.861	23.7	1.68E+02	0.95	0.31	−0.14	0.99
Silt	Sph	174.585	359.200	5.1	3.52E+03	0.63	0.49	5.90	0.95
Clay	Sph	205.416	390.100	5.7	1.54E+03	0.83	0.53	26.46	0.94
Ph	Sph	0.064	0.104	5.2	3.57E−04	0.68	0.62	−0.17	1.04
SOM	Sph	5.230	16.110	18.3	2.77E+01	0.80	0.32	7.84	0.73
C_{stock}	Sph	0.420	1.319	14.7	1.88E−02	0.96	0.32	2.33	0.72
C/N	Sph	0.015	0.034	15.1	1.72E−05	0.94	0.45	3.38	0.55
P	Sph	0.052	0.156	15.1	1.30E−03	0.79	0.33	2.23	0.93
Bases	Sph	0.034	0.056	9.7	1.30E−05	0.95	0.61	−6.17	1.14
CEC	Sph	46.792	113.694	10.2	4.48E+02	0.83	0.41	1.57	0.98

F_{CO_2}–soil CO_2 emission; P_{CO_2}–soil CO_2 production potential; P_{N_2O}–soil N_2O production potential; SMB–soil microbial biomass; T_s–soil temperature; M_s–soil moisture; D_s–soil bulk density; AFPS–air-filled pore space; TPV–total pore volume; Macro–macroporosity; Micro–microporosity; Sand–sand content; Silt–silt content; Clay–clay content; SOM–soil organic matter; C_{stock}–carbon stock; C/N–carbon to nitrogen ratio; P–available phosphorus; Bases–sum of bases; CEC–cation exchange capacity; Sph–spherical; C_0–nugget effect; C_0+C_1–total variance or sill; A–range (m); SSR–sum-square residue; DSD–degree of spatial dependence; a–intercept coefficient (cross-validation); b–slope coefficient (cross-validation).

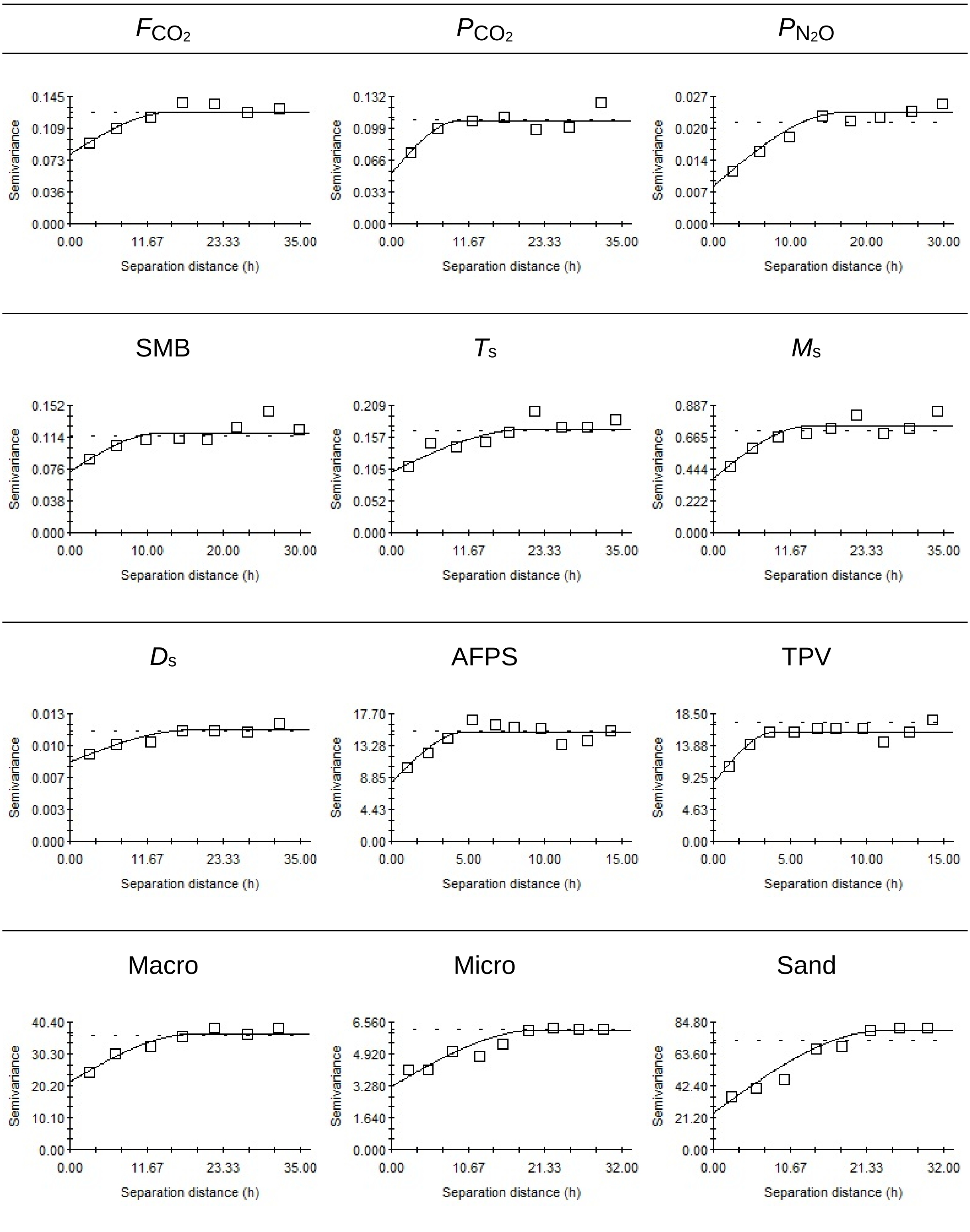

Figure 10. Adjusted isotropic semivariograms for the soil greenhouse gases and other soil attributes. F_{CO_2}–soil CO_2 emission; P_{CO_2}–soil CO_2 production potential; P_{N_2O}–soil N_2O production potential; SMB–soil microbial biomass; T_s–soil temperature; M_s–soil moisture; D_s–soil bulk density; AFPS–air-filled pore space; TPV–total pore volume; Macro–macroporosity; Micro–microporosity; Sand–sand content.

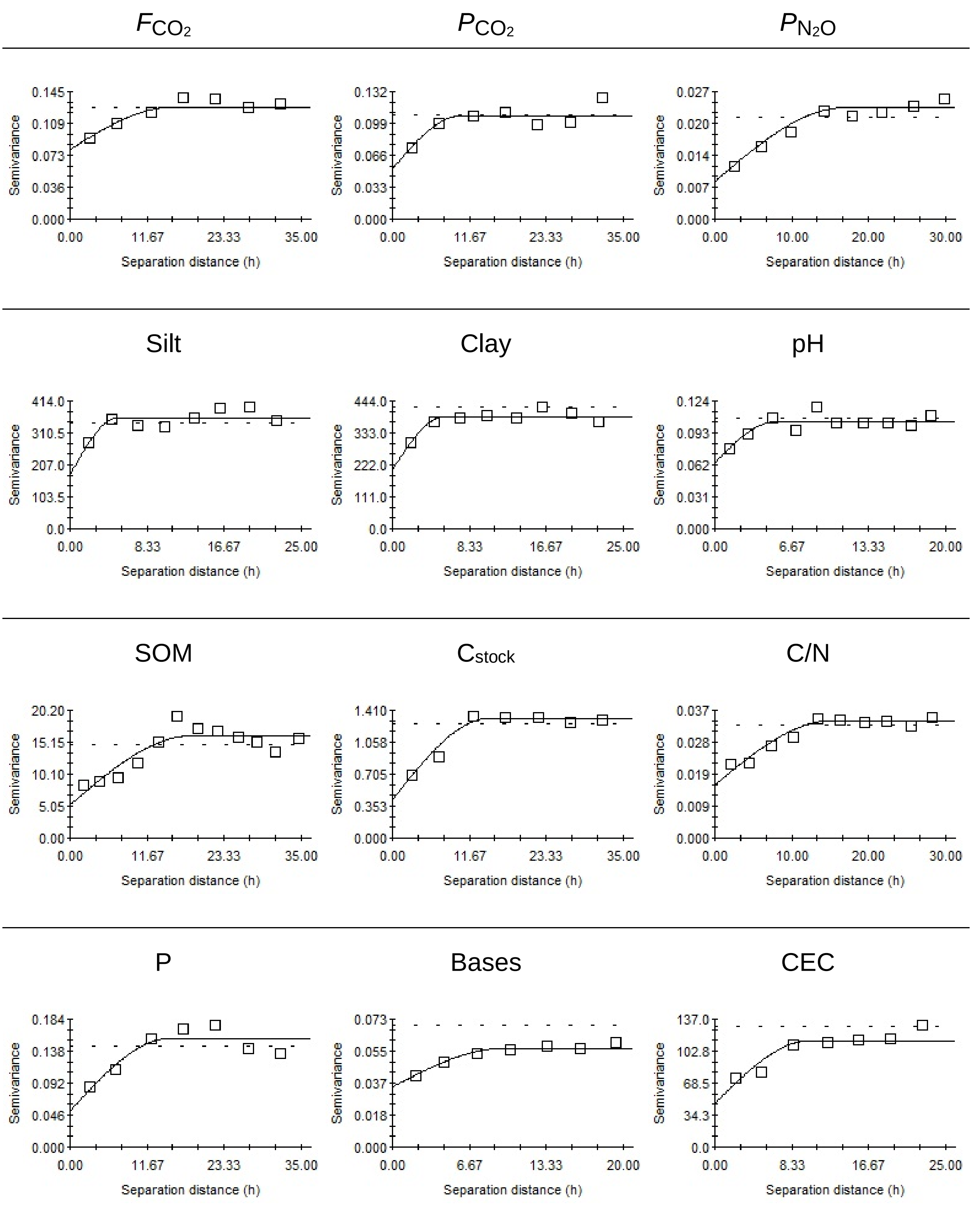

Figure 11. Adjusted isotropic semivariograms for the soil greenhouse gases and other soil attributes. F_{CO_2}–soil CO_2 emission; P_{CO_2}–soil CO_2 production potential; P_{N_2O}–soil N_2O production potential; Silt–silt content; Clay–clay content; SOM–soil organic matter; C_{stock}–carbon stock; C/N–carbon to nitrogen ratio; P–available phosphorus; Bases–sum of bases; CEC–cation exchange capacity.

The degree of spatial dependence (DSD) was classified as moderate for all variables (Table 3). DSD is calculated from the ratio between the nugget effect (C_0) and the total variance or sill (C_0+C_1) and it is considered strong for values smaller than 0.25, moderate for values between 0.25 and 0.75, and weak for values higher than 0.75 (CAMBARDELLA et al. 1994). Other studies carried out in mechanically harvested sugarcane areas have found moderate DSD for F_{CO_2} (PANOSSO et al., 2009; BRITO et al., 2010), in addition to several studies conducted on different crops, soils and management systems that have reported DSD for F_{CO_2} varying from weak to strong (LA SCALA et al., 2000a; STOYAN et al., 2000; ISHIZUKA et al., 2005; HERBST et al., 2009).

The ranges (*A*) of the adjusted models for the semivariograms showed values ranging from 4.0 m to 23.7 m for TPV and Sand, respectively (Table 3). The range values provide information regarding the heterogeneity of the spatial distribution related to the variables (TRANGMAR; YOST; UEHARA, 1986). Thus, the highest range value of the spatial variability structures indicates a more homogeneous distribution. The highest range values were observed for the variables Sand (23.7 m), T_s (20.2 m) and Micro (20.2 m), indicating a greater spatial dependence of these attributes in the area and featuring, therefore, a greater homogeneity of these variables compared to the others. On the contrary, the lowest range values were observed for the variables TPV (4.0 m), AFPS (4.9 m), Silt (5.1 m) and pH (5.2 m), which represents a more heterogeneous distribution of these variables in the area.

The adjusted models to the experimental isotropic semivariograms of F_{CO_2}, P_{CO_2}, P_{N_2O}, SMB, T_s, M_s and other soil physical and chemical attributes were used to obtain their estimated values for non-sampled locations by means of the kriging interpolation process, generating maps of spatial patterns (Figures 12, 13, 14 and 15). In general, the spatial variability patterns presented great variations over the grid. However, some similarities may be seen in the spatial distribution of some attributes. The spatial distribution of F_{CO_2} showed similar characteristics to those observed to M_s and Macro; the attributes Micro and C/N presented, in general, a contrary pattern to the that observed to F_{CO_2}, i.e., in regions where the highest values of F_{CO_2} are located, it can be observed, in general, the lowest values of the attributes Micro and C/N. In fact, these variables were related within the same factor in the factor analysis.

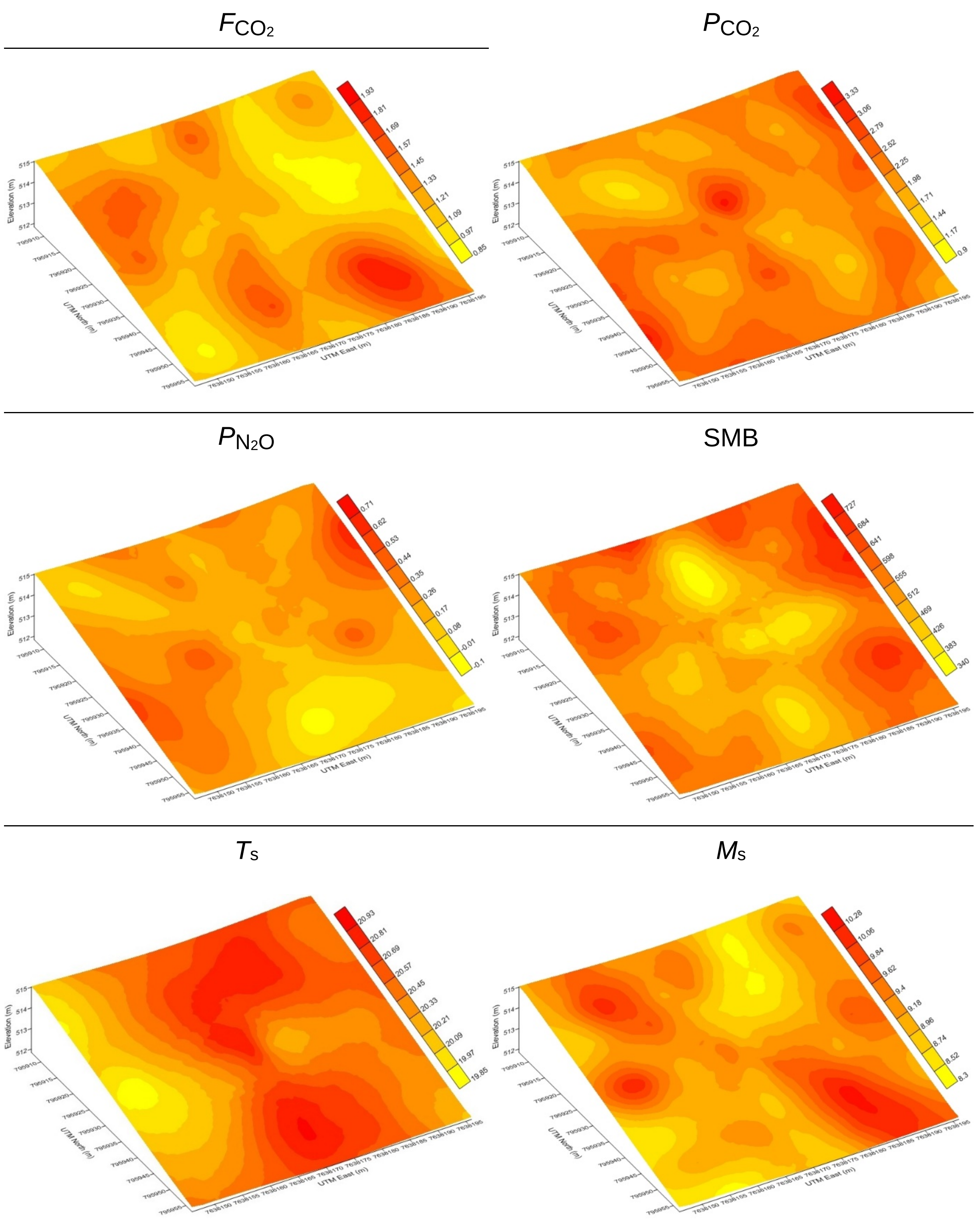

Figure 12. Isotropic maps of spatial pattern based on ordinary kriging comparing the soil CO_2 emission to soil CO_2 and N_2O production potentials and other soil attributes. F_{CO_2}–soil CO_2 emission (µmol CO_2 m^{-2} s^{-1}); P_{CO_2}–soil CO_2 production potential (µg C–CO_2 g^{-1} d^{-1}); P_{N_2O}–soil N_2O production potential (ng N–N_2O g^{-1} d^{-1}); SMB–soil microbial biomass (mg microbial C g^{-1} h^{-1}); T_s–soil temperature (°C); M_s–soil moisture (%).

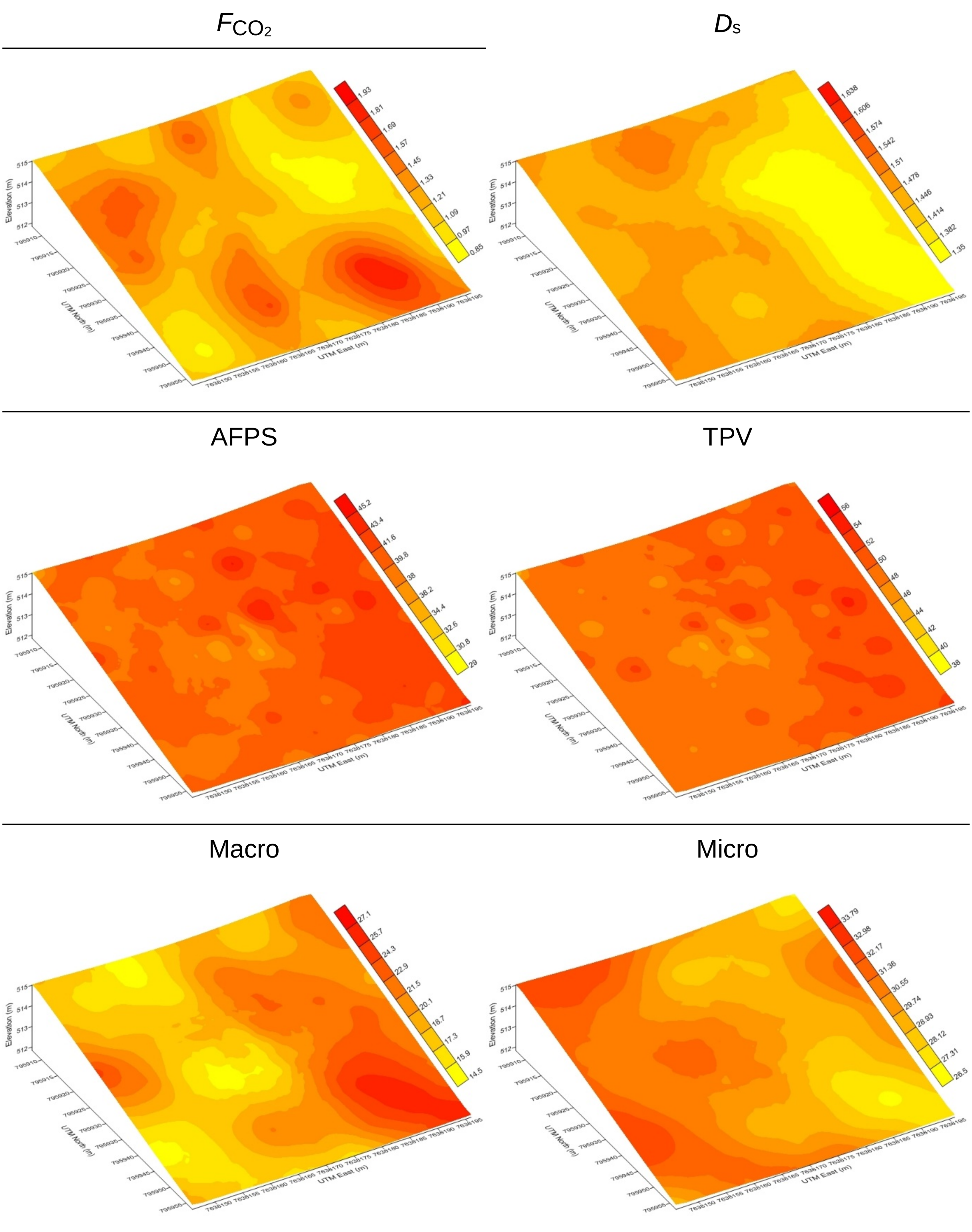

Figure 13. Isotropic maps of spatial pattern based on ordinary kriging comparing the soil CO_2 emission to soil CO_2 and N_2O production potentials and other soil attributes. F_{CO_2}–soil CO_2 emission (µmol CO_2 m^{-2} s^{-1}); D_s–soil bulk density (g cm^{-3}); AFPS–air-filled pore space (%); TPV–total pore volume (%); Macro–macroporosity (%); Micro–microporosity (%).

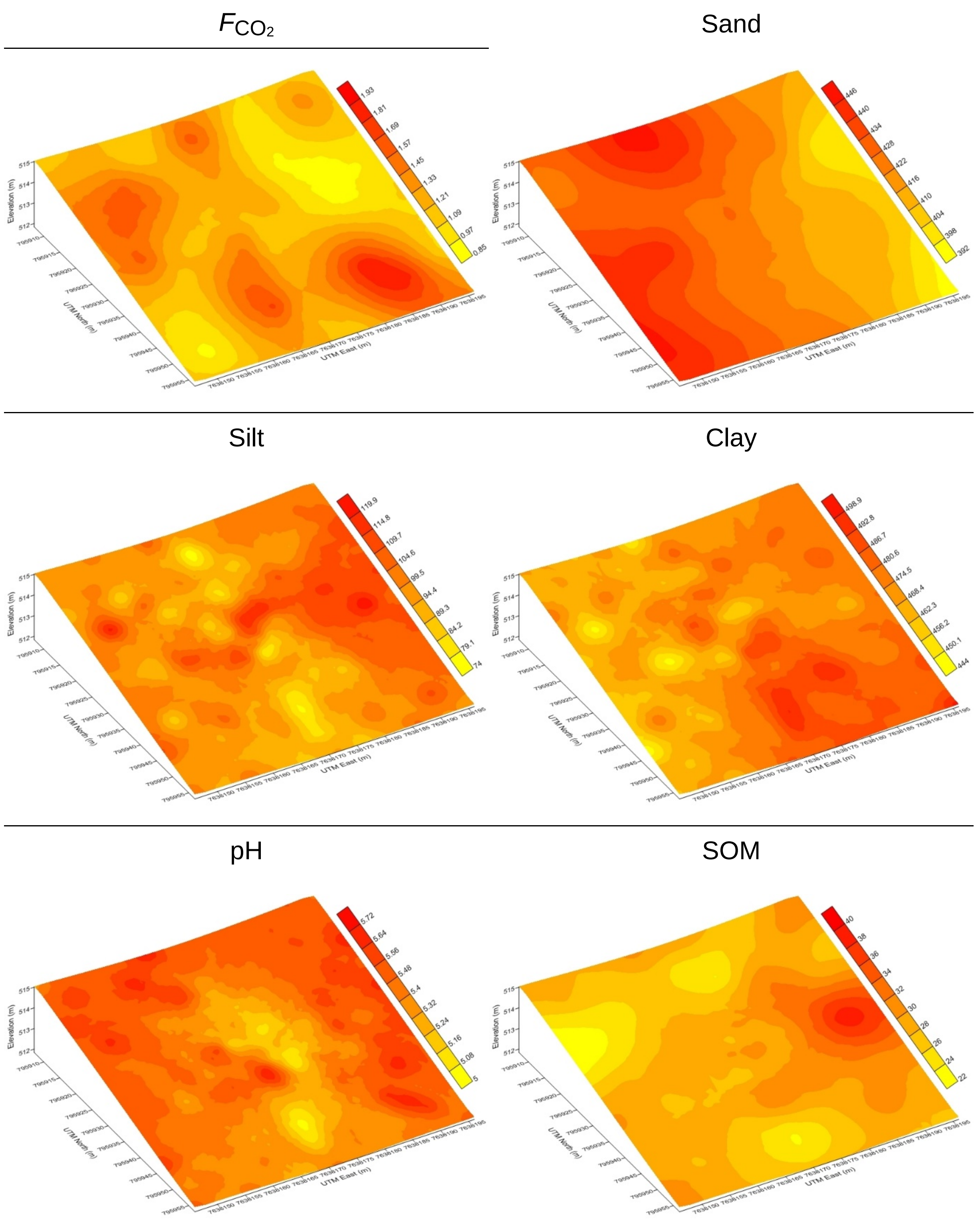

Figure 14. Isotropic maps of spatial pattern based on ordinary kriging comparing the soil CO_2 emission to soil CO_2 and N_2O production potentials and other soil attributes. F_{CO_2}–soil CO_2 emission (µmol CO_2 m^{-2} s^{-1}); Sand–sand content (g kg^{-1}); Silt–silt content (g kg^{-1}); Clay–clay content (g kg^{-1}); SOM–soil organic matter (g dm^{-3}).

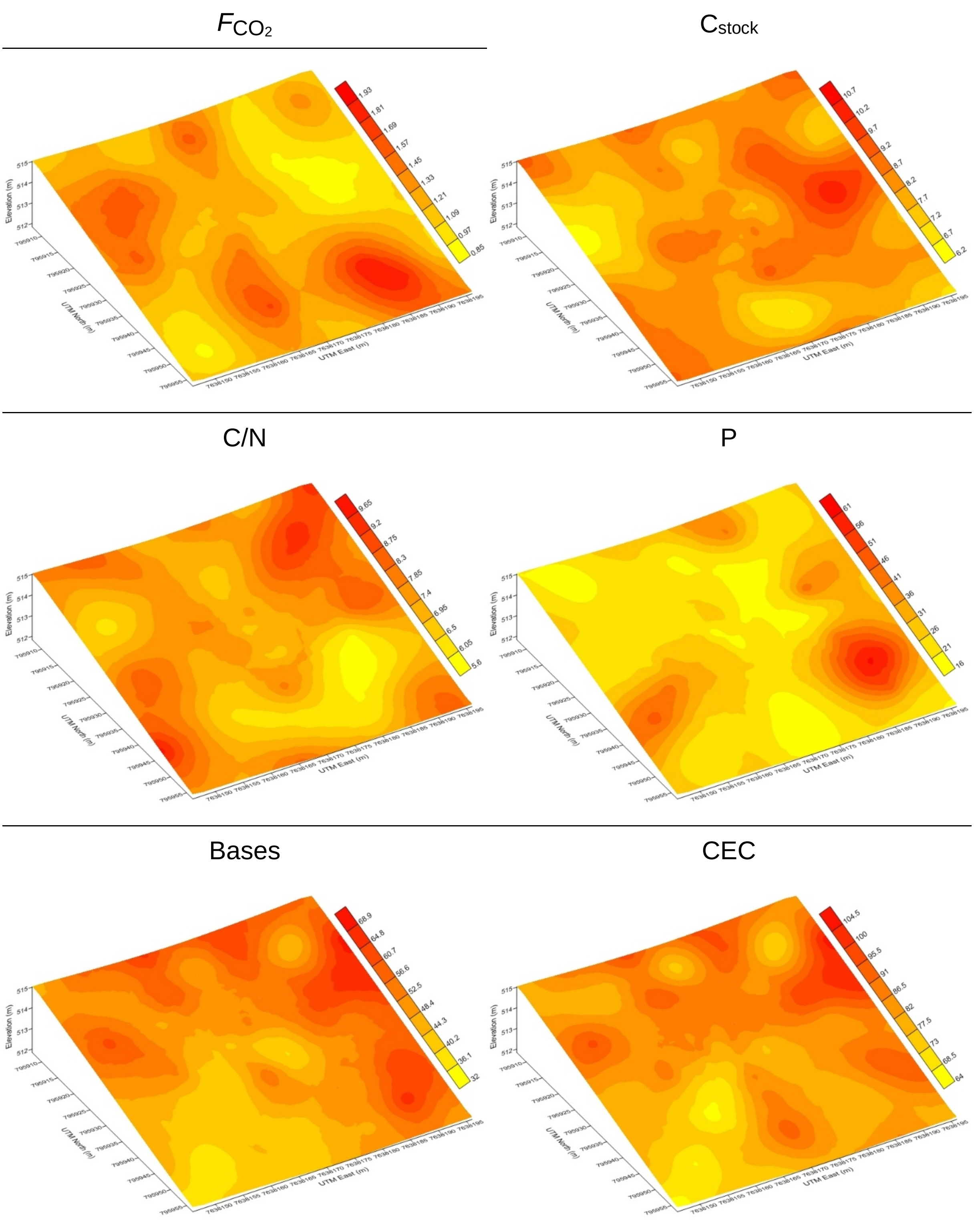

Figure 15. Isotropic maps of spatial pattern based on ordinary kriging comparing the soil CO_2 emission to soil CO_2 and N_2O production potentials and other soil attributes. C_{stock}–carbon stock (Mg ha^{-1}); C/N–carbon to nitrogen ratio; P–available phosphorus (mg dm^{-3}); Bases–sum of bases (mmol$_c$ dm^{-3}); CEC–cation exchange capacity (mmol$_c$ dm^{-3}).

Similarly, the spatial distribution of P_{CO_2} and P_{N_2O} showed similar patterns to the variables SMB, P, Bases and CEC. Thus, in general, as showed in the factor analysis, the spatial pattern of the infield F_{CO_2} was similar to some soil physical attributes; also, the pattern of the spatial distribution of P_{CO_2} and P_{N_2O}, which were obtained under laboratory conditions, was similar to some soil chemical attributes. Therefore, these patterns suggest that the spatial variability of F_{CO_2}, P_{CO_2} and P_{N_2O} is dependent mainly on the spatial variability of soil attributes to which they are related.

When the characterization of the spatial variability structure of soil GHG and soil attributes was determined by adjusting anisotropic models to the experimental semivariograms, it was observed anisotropy only for the gases F_{CO_2} and P_{N_2O} and a few other variables directly related to their production and emission (Table 4). In this case, the anisotropy of the soil physical attributes T_s, M_s, D_s and Macro may be related to the anisotropy of the infield F_{CO_2}. As showed in the previous analyses, soil physical attributes control gas exchange between soil and the atmosphere directly influencing the microbial activity and hence F_{CO_2}. In addition, the anisotropy of SOM, C_{stock} and C/N could be related to the anisotropy of the infield F_{CO_2} as well since the carbon is the main source of CO_2 production in the soil. Also, the bacteria in the soil use organic carbon in the denitrification process; this fact could explain the anisotropy also found for P_{N_2O}.

For all variables that presented anisotropy, the best adjusted model remained the spherical (Table 4), as observed for the isotropic semivariograms (Table 3). The perpendicular directions 0–90° and 45–135° were analyzed, and only the direction 0–90° best fitted to the models of the anisotropic semivariograms (Table 4 and Figures 16 and 17). In this direction, the anisotropy angle or angle of the greater continuity varied depending on the variable analyzed; for F_{CO_2}, P_{N_2O}, T_s, M_s, D_s and Macro, the anisotropy angle was 0°, and for the soil attributes SOM, C_{stock} and C/N, the anisotropy angle was 90° (Table 4). The models of other soil attributes did not fit any of those perpendicular directions and therefore were considered as isotropic.

The anisotropic maps of spatial patterns generated by the kriging interpolation process (Figures 18 and 19) showed great variations over the grid. However, the spatial distribution of F_{CO_2} presented similar characteristics to that observed for M_s as well as the spatial distribution of P_{N_2O} presented certain similarities to those observed for SOM, C_{stock} and C/N. It is important to note that the anisotropy observed by means of geostatistics takes into account only a given scale adjusted to a semivariogram model. On the contrary, by calculating the fractal dimension, the anisotropy can be observed more easily to different scales by using a fractogram, as in the next section.

Table 4. Models and estimated parameters adjusted to experimental isotropic and anisotropic semivariograms obtained for soil CO_2 emission, soil CO_2 and N_2O production potentials, soil microbial biomass, soil temperature, soil moisture and other soil physical and chemical attributes.

Variable	Model	C_0	C_0+C_1	A_1	A_2	SSR	R^2	DSD	a	b	Fa	Aa
F_{CO_2}	Sph	0.04	0.13	19.2	11.6	1.29E−02	0.46	0.33	0.11	0.92	0.60	0
P_{CO_2}	Sph	0.05	0.11	10.3	10.3	4.95E−04	0.67	0.49	0.28	0.88	1.00	*
P_{N_2O}	Sph	0.01	0.03	20.3	12.7	1.29E−03	0.52	0.29	0.08	0.69	0.62	0
SMB	Sph	0.07	0.12	12.0	12.0	8.42E−04	0.60	0.61	35.33	0.95	1.00	*
T_s	Sph	0.07	0.17	22.7	4.7	1.12E−01	0.26	0.41	−0.47	1.02	0.21	0
M_s	Sph	0.25	0.71	11.9	8.8	8.02E−01	0.43	0.35	2.30	0.75	0.74	0
D_s	Sph	0.01	0.01	17.8	0.1	7.56E−05	0.41	0.50	0.36	0.75	0.01	0
AFPS	Sph	8.13	15.21	4.9	4.9	9.67E+00	0.74	0.53	−0.84	1.03	1.00	*
TPV	Sph	8.47	15.85	4.0	4.0	6.12E+00	0.83	0.53	2.63	0.95	1.00	*
Macro	Sph	15.05	35.28	17.7	0.1	1.62E+03	0.35	0.43	6.87	0.65	0.01	0
Micro	Sph	3.24	6.13	20.2	20.2	1.01E+00	0.86	0.53	10.43	0.66	1.00	*
Sand	Sph	24.30	78.86	23.7	23.7	1.68E+02	0.95	0.31	−0.14	0.99	1.00	*
Silt	Sph	174.59	359.20	5.1	5.1	3.52E+03	0.63	0.49	5.9	0.95	1.00	*
Clay	Sph	205.42	390.10	5.7	5.7	1.54E+03	0.83	0.53	26.46	0.94	1.00	*
pH	Sph	0.06	0.10	5.2	5.2	3.57E−04	0.68	0.62	−0.17	1.04	1.00	*
SOM	Sph	1.53	21.16	18.9	12.1	1.90E+03	0.44	0.07	7.48	0.74	0.64	90
C_{stock}	Sph	0.37	1.43	15.1	12.4	1.69E+00	0.82	0.26	2.13	0.74	0.82	90
C/N	Sph	0.01	0.03	15.3	10.3	1.27E−03	0.51	0.13	3.29	0.56	0.67	90
P	Sph	0.05	0.16	15.1	15.1	1.30E−03	0.79	0.33	2.23	0.93	1.00	*
Bases	Sph	0.03	0.06	9.7	9.7	1.30E−05	0.95	0.61	−6.17	1.14	1.00	*
CEC	Sph	46.79	113.69	10.2	10.2	4.48E+02	0.83	0.41	1.57	0.98	1.00	*

F_{CO_2}–soil CO_2 emission; P_{CO_2}–soil CO_2 production potential; P_{N_2O}–soil N_2O production potential; SMB–soil microbial biomass; T_s–soil temperature; M_s–soil moisture; D_s–soil bulk density; AFPS–air-filled pore space; TPV–total pore volume; Macro–macroporosity; Micro–microporosity; Sand–sand content; Silt–silt content; Clay–clay content; SOM–soil organic matter; C_{stock}–carbon stock; C/N–carbon to nitrogen ratio; P–available phosphorus; Bases–sum of bases; CEC–cation exchange capacity; Sph–spherical; C_0–nugget effect; C_0+C_1–total variance or sill; A_1–range major (m); A_2–range minor (m); SSR–sum-square residue; DSD–degree of spatial dependence; a–intercept coefficient of the cross-validation; b–slope coefficient of the cross-validation; Fa–anisotropy factor; Aa–anisotropy angle or angle of the greater continuity; *isotropic model best fitting.

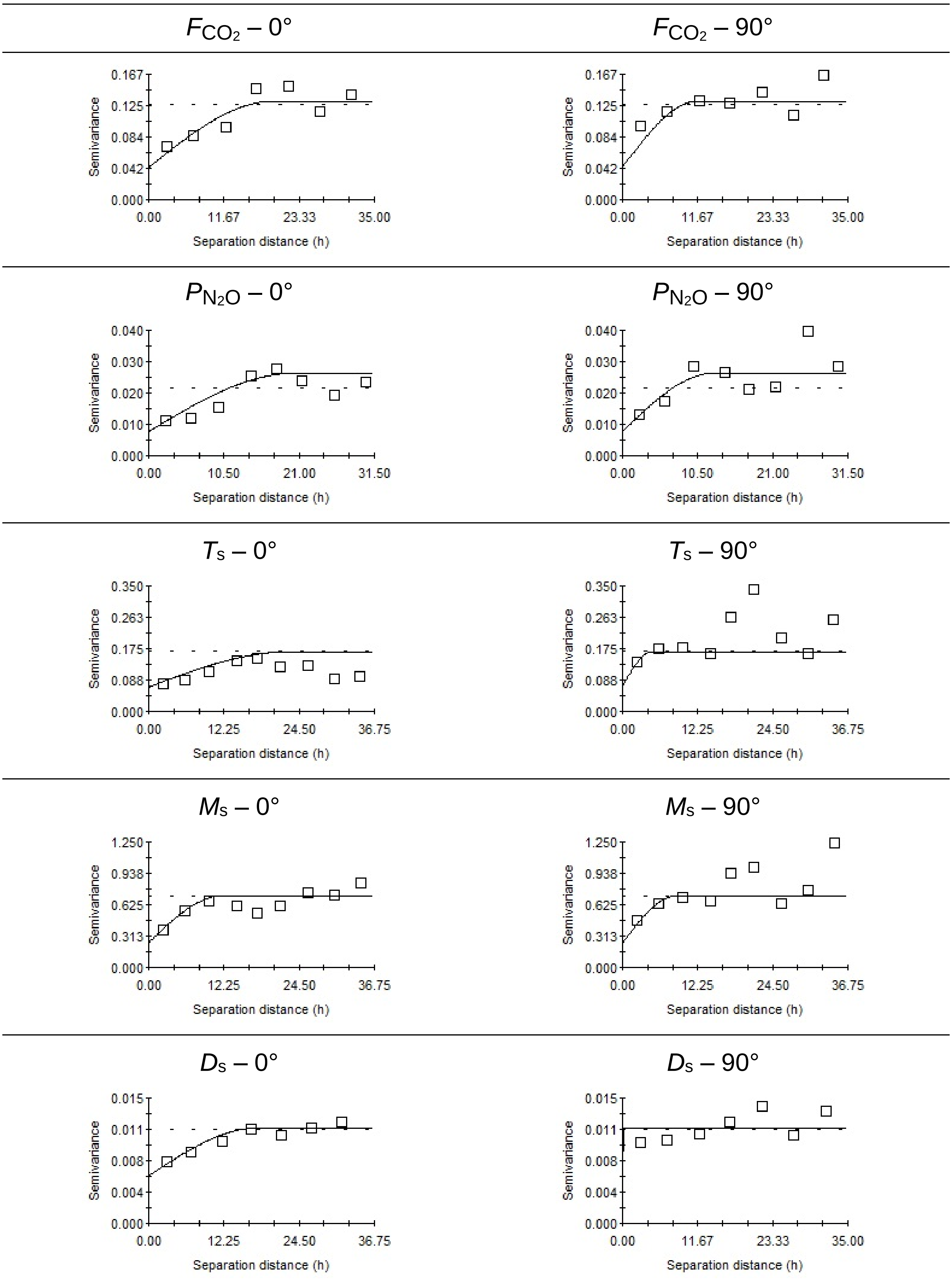

Figure 16. Adjusted anisotropic semivariograms for the soil greenhouse gases and other soil attributes. F_{CO_2}–soil CO_2 emission; P_{N_2O}–soil N_2O production potential; T_s–soil temperature; M_s–soil moisture; D_s–soil bulk density.

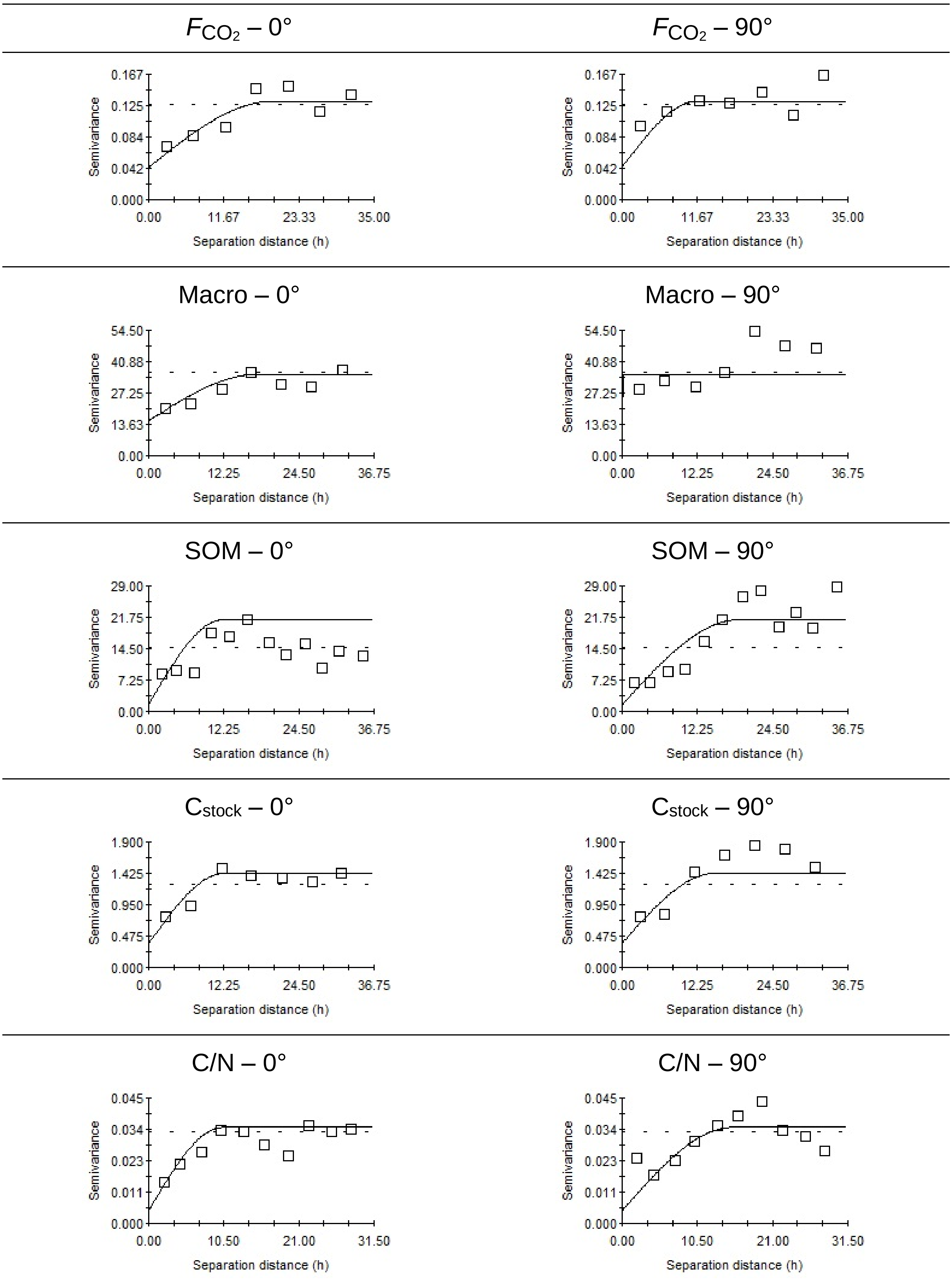

Figure 17. Adjusted anisotropic semivariograms for the soil greenhouse gases and other soil attributes. F_{CO_2}–soil CO_2 emission; Macro–macroporosity; SOM–soil organic matter; C_{stock}–carbon stock; C/N–carbon to nitrogen ratio.

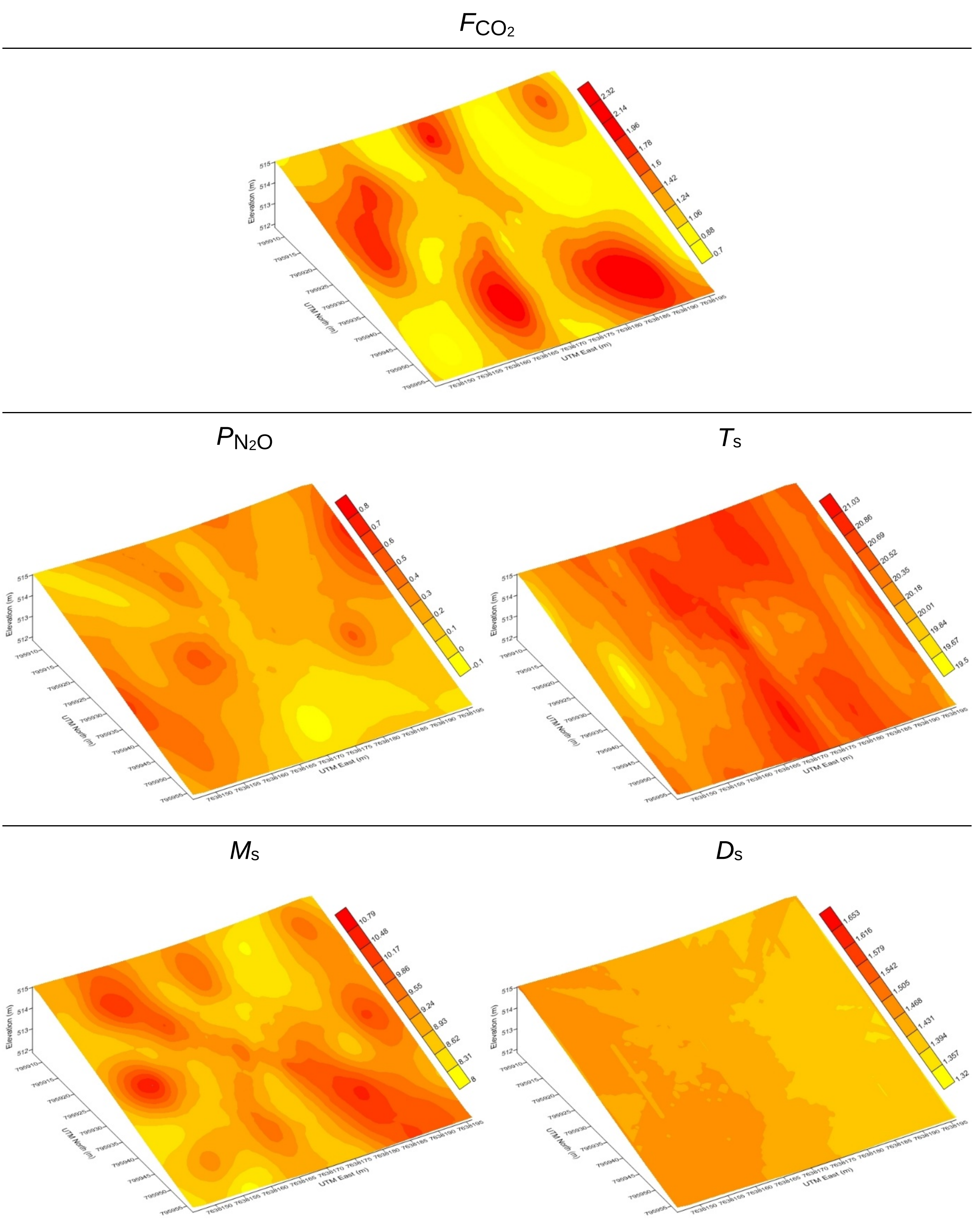

Figure 18. Anisotropic maps of spatial pattern based on ordinary kriging comparing the soil CO_2 emission other soil attributes. F_{CO_2}–soil CO_2 emission (μmol CO_2 m^{-2} s^{-1}); P_{N_2O}–soil N_2O production potential (ng N–N_2O g^{-1} d^{-1}); T_s–soil temperature (°C); M_s–soil moisture (%); D_s–soil bulk density (g cm^{-3}).

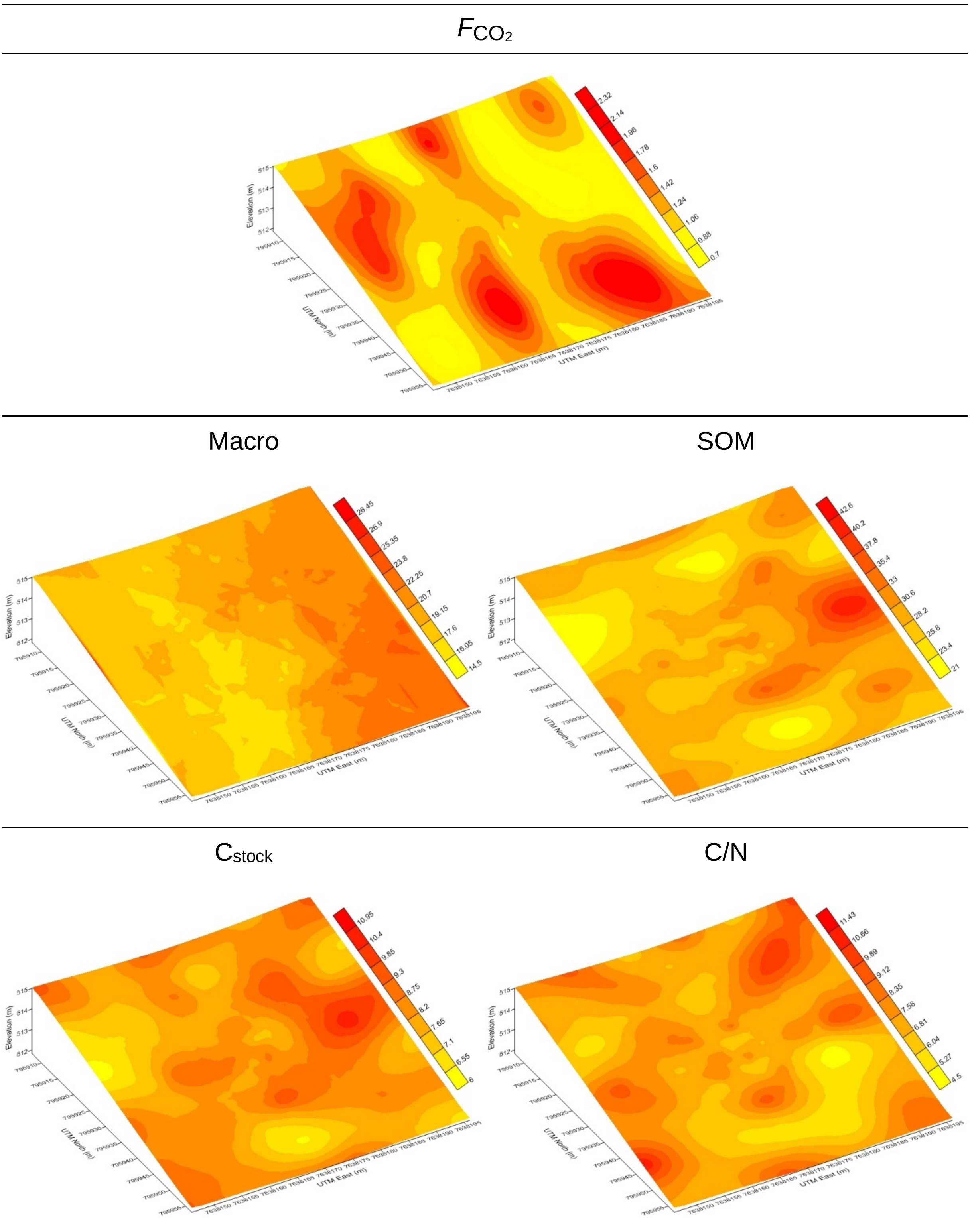

Figure 19. Anisotropic maps of spatial pattern based on ordinary kriging comparing the soil CO_2 emission other soil attributes. F_{CO_2}–soil CO_2 emission (μmol CO_2 m^{-2} s^{-1}); Macro–macroporosity (%); C_{stock}–carbon stock (Mg ha^{-1}); C/N–carbon to nitrogen ratio.

4.5 Fractal dimension and anisotropy of soil greenhouse gas and soil attributes

In order to assess whether the spatial variability patterns of F_{CO_2}, P_{CO_2}, P_{N_2O}, SMB, T_s, M_s and other soil physical and chemical attributes depend on the directions of study, an additional anisotropic characterization of the area was carried out. For the initial characterization of the anisotropy, an analysis of variance was performed with a single factor (the directions 0°, 45°, 90° and 135°), and the significant differences between their means were compared at 5% probability level by Tukey's test (Table 5). For F_{CO_2}, the direction 0° showed an average of 1.05 µmol CO_2 m^{-2} s^{-1}, 45° presented an average of 1.29 µmol CO_2 m^{-2} s^{-1}, 90° an average of 1.21 µmol CO_2 m^{-2} s^{-1} and 135° showed an average of 1.20 µmol CO_2 m^{-2} s^{-1} (Table 5). Despite the lower average value of F_{CO_2} has been observed in the direction 0°, the F test values of the analysis of variance were not significant (P>0.05) for this variable. However, in a study conducted in the same region and in an area of sugarcane under mechanically harvest system, Panosso et al. (2012) observed a value significantly lower (P<0.05) for F_{CO_2} in the direction 0°.

The lowest values of P_{CO_2} and P_{N_2O} were observed in soil samples collected in the direction 45°. For P_{CO_2}, the average of 1.93 µg C–CO_2 g^{-1} d^{-1} found in this direction was significantly different from the directions 0° (2.67 µg C–CO_2 g^{-1} d^{-1}) and 90° (2.49 µg C–CO_2 g^{-1} d^{-1}), but statistically identical to the direction 135° (2.36 µg C–CO_2 g^{-1} d^{-1}); and for P_{N_2O}, the average value of 0.14 ng N–N_2O g^{-1} d^{-1} observed in the direction 45° was significantly different from the directions 90° (0.25 ng N–N_2O g^{-1} d^{-1}) and 135° (0.25 ng N–N_2O g^{-1} d^{-1}) and statistically identical to the direction 0°(0.15 ng N–N_2O g^{-1} d^{-1}) (Table 5). However, some soil physical and chemical attributes showed no significant statistical differences between the studied directions, such as Macro, Micro, Sand, pH, C_{stock}, P and Bases.

Similarly to F_{CO_2}, which showed lower emission in the direction 0°, other soil attributes that are directly related to F_{CO_2} also presented lower or higher values in that direction, most of them statistically significant (P<0.05) (Table 5). The variables SMB, AFPS, TPV, Macro, SOM and P showed the lowest values in this direction. In this case, SOM is the main source of CO_2 production in soils (STOTZKY; NORMAN, 1961; BALL; SCOTT; PARKER, 1999; DOMINY; HAYNES; ANTWERPEN, 2002; KEMMITT et al., 2008; OLIVEIRA et al., 2013; VARGAS et al., 2014) and P is an important limiting factor related to the microbial activity (DUAH-YENTUMI; RONN; CHRISTENSEN, 1998); because they have the lowest values at 0°, these attributes may have influenced the lowest values for SMB and hence the lowest values of F_{CO_2} in this direction.

Table 5. Descriptive statistics of soil CO_2 emission, soil CO_2 and N_2O production potentials, soil microbial biomass, soil temperature, soil moisture, and other soil physical and chemical attributes, for the different directions of study.

Variable	0°		45°		90°		135°	
	Mean	CV	Mean	CV	Mean	CV	Mean	CV
F_{CO_2}*	1.05 a	26.82	1.29 a	29.68	1.21 a	35.17	1.20 a	31.66
P_{CO_2}	2.67 a	27.78	1.93 b	42.81	2.49 a	31.73	2.36 ab	29.59
P_{N_2O}	0.15 b	87.68	0.14 b	97.26	0.25 a	52.69	0.25 a	37.41
SMB	410.10 b	32.05	578.50 a	26.41	465.00 b	35.18	568.10 a	22.57
T_s*	20.89 a	1.37	20.55 b	1.66	20.38 b	1.87	20.48 b	1.68
M_s*	9.00 b	6.70	9.75 a	9.43	9.37 ab	9.81	8.88 b	7.76
D_s	1.52 a	6.90	1.43 b	7.21	1.43 b	8.39	1.43 b	7.87
AFPS	38.81 b	10.46	41.22 ab	8.09	40.67 ab	10.70	41.40 a	9.48
TPV	47.80 b	8.60	50.99 a	7.29	50.03 ab	9.35	50.28 ab	8.17
Macro	17.24 a	32.49	21.11 a	32.83	20.09 a	36.68	19.77 a	31.32
Micro	30.57 a	7.13	29.83 a	9.21	30.62 a	7.91	30.51 a	9.40
Sand	429.80 a	1.70	420.11 a	2.26	425.21 a	2.88	425.11 a	2.13
Silt	88.80 b	24.90	96.90 ab	18.83	105.47 a	15.10	106.92 a	13.34
Clay	481.40 ab	4.92	482.99 a	4.53	469.32 bc	3.35	467.97 c	3.74
pH	5.36 a	6.50	5.46 a	6.92	5.43 a	5.80	5.47 a	5.39
SOM	26.28 b	11.54	28.49 a	12.17	29.55 a	12.94	28.79 a	10.50
C_{stock}	8.20 a	14.40	8.14 a	13.34	8.49 a	15.48	8.26 a	12.06
C/N	6.83 b	18.38	7.40 ab	15.19	7.80 a	18.27	7.40 ab	17.03
P	22.72 a	27.16	23.73 a	33.95	23.45 a	26.66	22.97 a	26.95
Bases	50.35 a	21.65	47.61 a	26.10	49.19 a	22.99	45.26 a	28.20
CEC	87.98 a	10.34	81.32 b	12.02	82.89 ab	10.49	79.01 b	14.77

N = 133; *general mean of all studied days; values followed by the same letters in the same line are not significantly different (P<0.05) by Tukey test; CV–coefficient of variation (%); F_{CO_2}–soil CO_2 emission (μmol CO_2 m^{-2} s^{-1}); P_{CO_2}–soil CO_2 production potential (μg C–CO_2 g^{-1} d^{-1}); P_{N_2O}–soil N_2O production potential (ng N–N_2O g^{-1} d^{-1}); SMB–soil microbial biomass (mg microbial C g^{-1} h^{-1}); T_s–soil temperature (°C); M_s–soil moisture (%); D_s–soil bulk density (g cm^{-3}); AFPS–air-filled pore space (%); TPV–total pore volume (%); Macro–macroporosity (%); Micro–microporosity (%); Sand–sand content (g kg^{-1}); Silt–silt content (g kg^{-1}); Clay–clay content (g kg^{-1}); SOM–soil organic matter (g dm^{-3}); Cstock–carbon stock (Mg ha^{-1}); C/N–carbon to nitrogen ratio; P–available phosphorus (mg dm^{-3}); Bases–sum of bases ($mmol_c$ dm^{-3}); CEC–cation exchange capacity ($mmol_c$ dm^{-3}).

In the same way, the lowest values at 0° of the soil physical attributes AFPS, TPV and Macro, which are related to soil porosity, may have limited the gas exchange between soil and the atmosphere (XU; QI, 2001; EPRON et al., 2006), influencing soil microbial activity and leading to the lowest values of SMB and hence F_{CO_2}. On the other hand, the variables T_s and D_s showed the highest values in the direction 0°; T_s is an important controlling factor of F_{CO_2} (LLOYD; TAYLOR, 1994; EPRON et al., 1999; BURTON; PREGITZER, 2003; EPRON et al., 2006; RYU et al., 2009) and its high value could limit the microbial activity. In fact, the average temperature in the direction 0° (20.89 °C) was significantly higher (P<0.05) compared to the other directions (Table 5). Similarly, higher D_s values are related to lower soil porosity, which could not facilitate soil oxygenation, working against microbial activity and decreasing F_{CO_2}.

Based on the anisotropic experimental semivariograms, we calculated the fractal dimension (D_F) of soil GHG and other soil physical and chemical attributes for the directions 0°, 45°, 90° and 135°. By using D_F values at different scales, we constructed the so-called fractograms (Figures 20, 21 and 22), by which we characterized the complete spatial variability structure (PALMER, 1988; CANTERO et al., 1998). The fractogram allows to interpret the scales at which the spatial variability could be considered as homogeneous ($D_F \geq 3$, i.e., without topological significance) or heterogeneous ($D_F < 3$, i.e., with topological significance) (PALMER, 1988).

The fractogram analysis of F_{CO_2} showed topologically significant D_F values ($D_F < 3$) for almost all scales in the direction 0°; for the directions 45° and 90° only a few scales presented $D_F < 3$; and the direction 135° showed only scales with D_F values without topological significance ($D_F \geq 3$) (Figure 20), indicating no spatial variability structure. It is known that D_F is not a constant function of scale and their spatial variation pattern may not be repeated from one scale to another (PALMER, 1988). Thus, although the results of analysis of variance have evidenced isotropic behavior for F_{CO_2} in the experimental area (Table 5), it is possible to observe an improved spatial variability structure at 0°. Also, the lowest values of D_F were observed in this direction, featuring a greater spatial dependence and indicating that there is anisotropy for F_{CO_2} in the direction 0°, which represents the direction parallel to the sugarcane row. Similarly, in a study conducted in the same region and in a sugarcane area, the lowest D_F values were found in the direction 0° (PANOSSO et al., 2012).

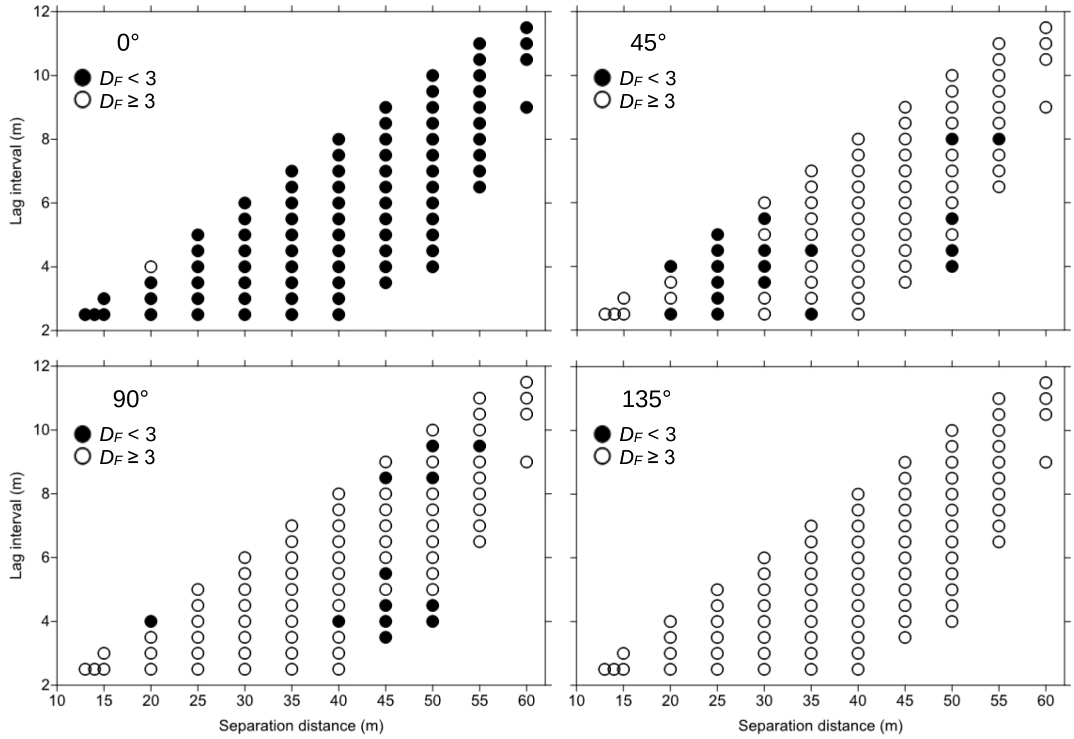

Figure 20. Fractograms of the infield soil CO_2 emission (F_{CO_2}) calculated from anisotropic semivariograms for the directions of 0°, 45°, 90° and 135°, with the fractal dimension for different scales.

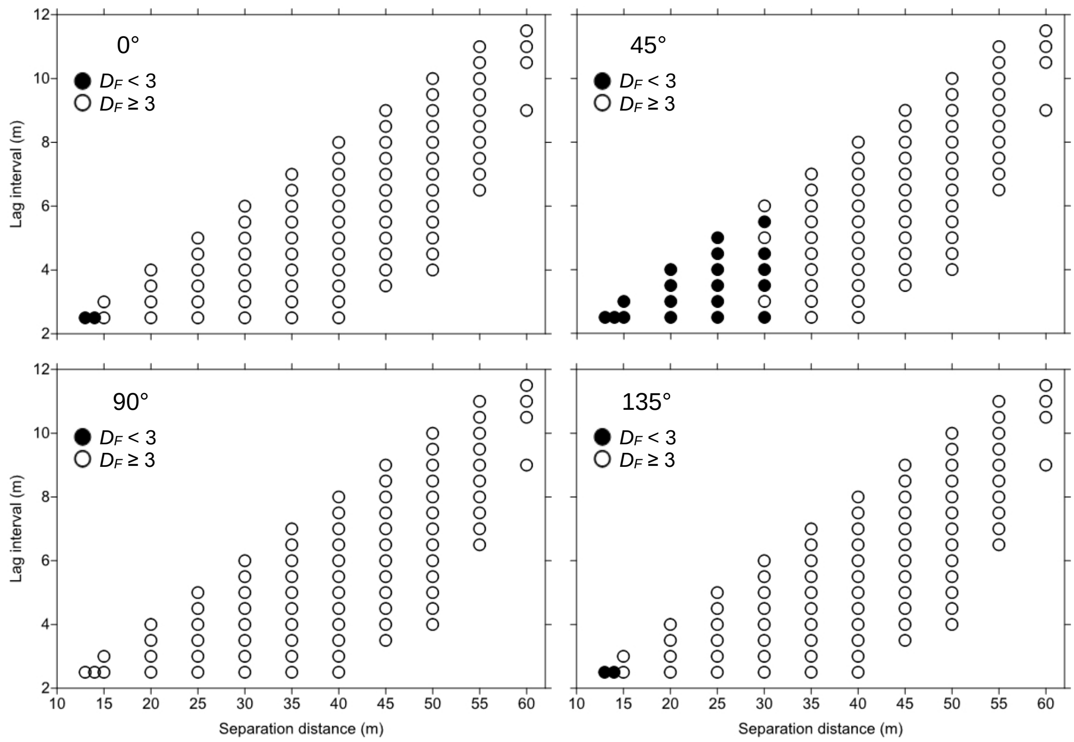

Figure 21. Fractograms of soil CO_2 production potential (P_{CO_2}) calculated from anisotropic semivariograms for the directions of 0°, 45°, 90° and 135°, with the fractal dimension for different scales.

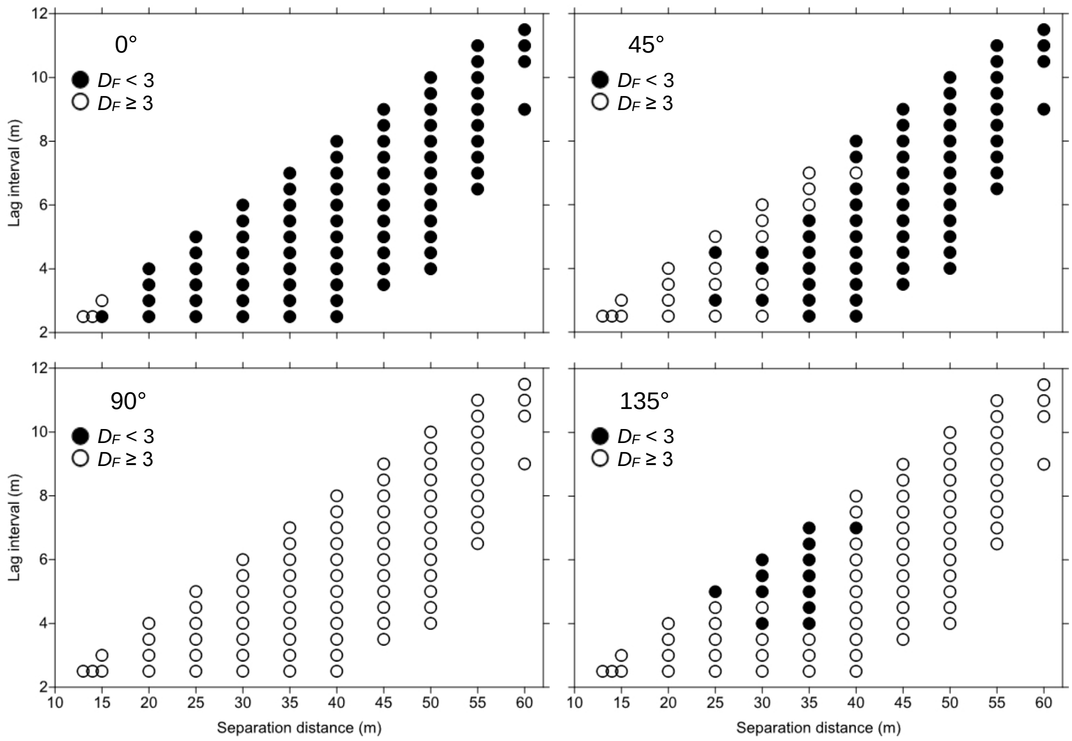

Figure 22. Fractograms of soil N_2O production potential (P_{N_2O}) calculated from anisotropic semivariograms for the directions of 0°, 45°, 90° and 135°, with the fractal dimension for different scales.

In addition, P_{CO_2} showed, in general, D_F values with topological significance only in the direction 45° at small scales up to 30 m (Figure 21). In the other scales and directions, the D_F values were greater than or equal to 3, which represents a lack of spatial dependence. The variograms for P_{N_2O} presented certain similarities in their spatial distribution for the directions 0° and 45° (Figure 22). In fact, this behavior was also observed by the analysis of variance, in which the direction 90° and 135° showed the highest N_2O production values and was significantly different ($P<0.05$) from 0° and 45° (Table 5). Because P_{CO_2} and P_{N_2O} were quantified under laboratory conditions, using disturbed soil samples, soil structure was affected and the effect of soil management was removed, especially in soil physical attributes related to soil porosity. For this reason, it is likely that the anisotropic characterization of these gases may have undergone some interference in their quantification process.

A similar behavior found for the fractograms of F_{CO_2} was also observed in the fractograms of D_s and Macro (Figures 23 and 24). In this case, in general, the D_F values showed topologically significant values in the direction 0°, which means an improved spatial variability structure for most of the scales in this direction; thus, it could suggest the presence of anisotropy for these variables up to 45 m. According to Palmer (1988), the correlation between two attributes at one scale is most likely a result of the relationship between them. This fact may suggest that the spatial variability structure of D_S and Macro are factors that could affect the spatial variability structure of F_{CO_2}.

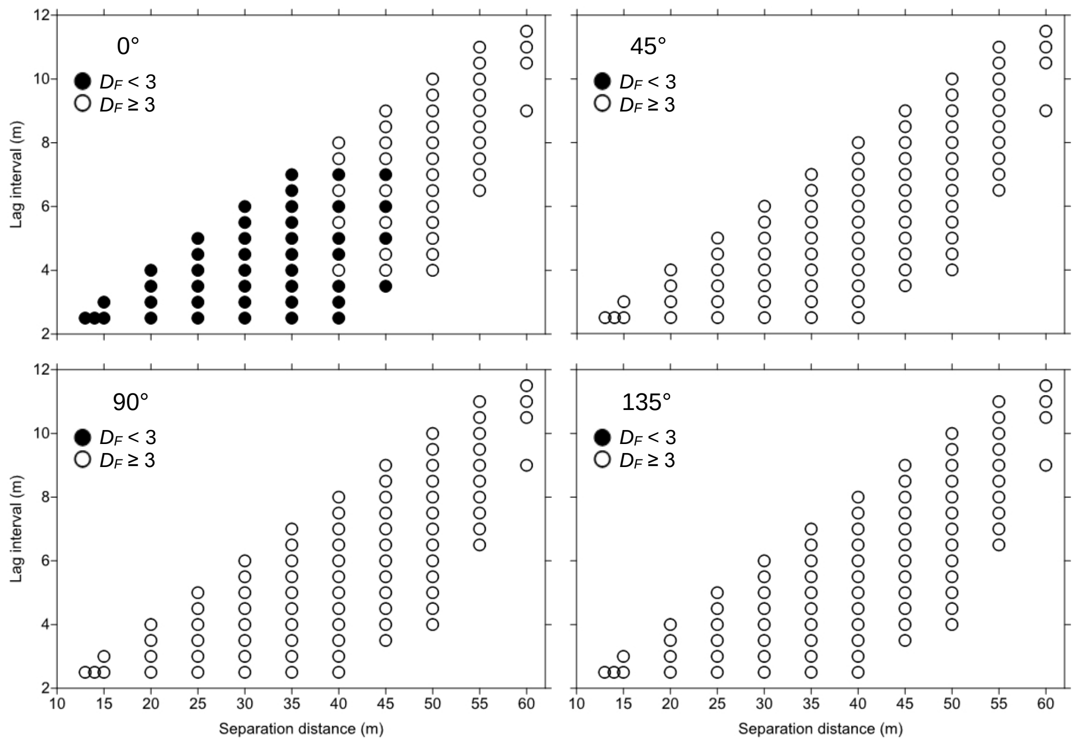

Figure 23. Fractograms of soil bulk density (D_S) calculated from anisotropic semivariograms for the directions of 0°, 45°, 90° and 135°, with the fractal dimension for different scales.

The fractograms constructed for the other soil attributes showed behavior that differed depending on the scale and direction (Appendix), showing no anisotropy as that observed for F_{CO_2}. The spatial variations of D_F observed in this study can be attributed to changes in the heterogeneity of the spatial variability of each soil attribute. Also, those changes are due to modifications in the spatial variability patterns of their controlling factors. Furthermore, for most natural phenomena, many studies have shown that scale, location, or even the orientation of the sampling points in the experimental grid may become unstable estimating D_F (BURROUGH, 1981; KLINKENBERG, 1992; XU; MOORE; GALLANT, 1993; SUN et al., 2006; ABEDINI; SHAGHAGHIAN, 2009).

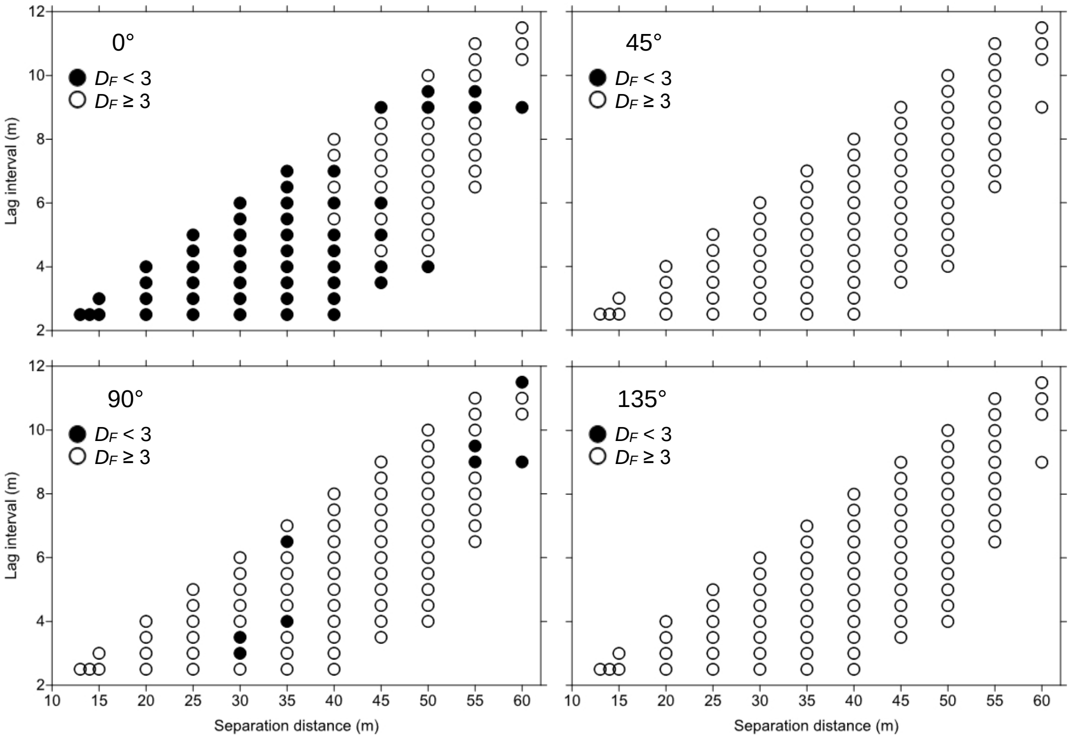

Figure 24. Fractograms of macroporosity (Macro) calculated from anisotropic semivariograms for the directions of 0°, 45°, 90° and 135°, with the fractal dimension for different scales.

5 CONCLUSION

The production and emission of soil greenhouse gas in a mechanically harvested sugarcane area located in southern Brazil, evaluated infield and in laboratory conditions, have been associated with two processes: the production in the soil and its transport to the atmosphere. Under infield conditions, only the process related to the transport of CO_2 was more easily observed, showing the correlation between soil CO_2 emission and soil porosity; under laboratory conditions, soil chemical attributes have a greater importance in the process of production potentials of CO_2 and N_2O. Although presented as independent, these processes are coupled and occur simultaneously in the soil, in addition to provide information about their variability, showing if the infield emissions are due to the gas transport processes or to soil carbon levels and their quality, i.e., the gas production processes.

Furthermore, the spatial dependence of soil CO_2 emission showed similarities to soil physical attributes related to soil porosity, as well as the spatial dependence of soil CO_2 and N_2O production potentials showed similarities to soil chemical attributes. In addition, the anisotropy occurred mainly under infield conditions, mostly for the attributes related to soil porosity since disturbed soils used under laboratory conditions lose their structure and hence the effect of the management found under infield conditions

6 REFERENCES

ABEDINI, M. J.; SHAGHAGHIAN, M. R. Exploring scaling laws in surface topography. **Chaos, Solitons & Fractals**, Oxford, v. 42, n. 4, p. 2373–2383, 2009.

AL-KAYSSI, A. W. Spatial variability of soil temperature under greenhouse conditions. **Renewable Energy**, Oxford, v. 27, n. 3, p. 453–462, 2002.

ALLAIRE, S. E.; LANGE, S. F.; LAFOND, J. A.; PELLETIER, B.; CAMBOURIS, A. N.; DUTILLEUL, P. Multiscale spatial variability of CO_2 emissions and correlations with physico-chemical soil properties. **Geoderma**, Amsterdam, v. 170, n. 1, 251–260, 2012.

AMUNDSON, R. G.; DAVIDSON, E. A. Carbon dioxide and nitrogenous oxide gases in the soil atmosphere. **Journal of Geochemical Exploration**, Amsterdam, v. 38, n. 1–2, p. 13–41, 1990.

ANDERSON, J. P. E.; DOMSCH, K. H. A physiological method for the quantitative measurement of microbial biomass in soils. **Soil Biology and Biochemistry**, Oxford, v. 10, n. 3, 215–221, 1978.

ARAH, J. R. M.; SMITH, K. A.; CRICHTON, I. J.; LI, H. S. Nitrous oxide production and denitrification in Scottish arable soils. **European Journal of Soil Science**, Oxford, v. 42, n. 3, p. 351–367, 1991.

BALL, B. C. Soil structure and greenhouse gas emissions: a synthesis of 20 years of experimentation. **European Journal of Soil Science**, Oxford, v. 64, n. 3, 357–373, 2013.

BALL, B. C.; SMITH, K. A. Gas movement and air-filled porosity. In: SMITH, K. A., MULLINS, C. E. (Eds.). **Soil and environmental analysis:** physical methods. 2. ed. New York: Marcel Dekker, 1991. p. 499–538.

BALL, B. C.; SCOTT, A.; PARKER, J. P. Field N_2O, CO_2 and CH_4 fluxes in relation to tillage, compaction and soil quality in Scotland. **Soil and Tillage Research**, Amsterdam, v. 53, n. 1, p. 29–39, 1999.

BARBIERI, D. M.; MARQUES JÚNIOR, J.; PEREIRA, G. T. Variabilidade espacial de atributos químicos de um argissolo para aplicação de insumos à taxa variável em diferentes formas de relevo. **Engenharia Agrícola**, Jaboticabal, v. 28, n. 4, p. 645–653, 2008.

BARTLETT, K. B.; CRILL, P. M.; SEBACHER, D. I.; HARRISS, R. C.; WILSON, J. O.; MELACK, J. M. Methane flux from the central Amazonian floodplain. **Journal of Geophysical Research: Atmospheres**, Hoboken, v. 93, n. D2, 1571–1582, 1988.

BERNARDI, A. C. C.; RABELLO, L. M.; INAMASU, R. Y.; GREGO, C. R.; ANDRADE, R. G. Variabilidade espacial de parâmetros físico-químicas do solo e biofísicos de superfície em cultivo do sorgo. **Revista Brasileira de Engenharia Agrícola e Ambiental**, Campina Grande, v. 18, n. 6, p. 623–630, 2014

BERNOUX, M.; CARVALHO, M. C. S.; VOLKOFF, B.; CERRI, C. C. Brazil's soil carbon stocks. **Soil Science Society of America Journal**, Madison, v. 66, n. 3, p. 888–896, 2002.

BICALHO, E. S.; PANOSSO, A. R.; TEIXEIRA, D. B.; MIRANDA, J. G. V.; PEREIRA, G. T.; LA SCALA, N. Spatial variability structure of soil CO_2 emission and soil attributes in a sugarcane area. **Agriculture, Ecosystems & Environment**, Amsterdam, v. 189, n. 1, 206–215, 2014.

BLAIR, N. Impact of cultivation and sugar-cane green trash management on carbon fractions and aggregate stability for a Chromic Luvisol in Queensland, Australia. **Soil and Tillage Research**, Amsterdam, v. 55, n. 3–4, p. 183–191, 2000.

BODEGOM, P. M. van; STAMS, A. J. M. Effects of alternative electron acceptors and temperature on methanogenesis in rice paddy soils. **Chemosphere**, Oxford, v. 39, n. 2, p. 167–182, 1999.

BRASIL, Ministério da Ciência e Tecnologia. **Segunda comunicação nacional do Brasil à Convenção-Quadro das Nações Unidas sobre mudança do clima**. Brasília: Ministério da Ciência e Tecnologia, 2010. 520 p.

BRITO, L. F.; MARQUES JÚNIOR, J.; PEREIRA, G. T.; LA SCALA, N. Spatial variability of soil CO_2 emission in different topographic positions. **Bragantia**, Campinas, v. 69, supl., 19–27, 2010.

BRITO, L. F.; MARQUES JÚNIOR, J.; PEREIRA, G. T.; SOUZA, Z. M.; LA SCALA, N. Soil CO_2 emission of sugarcane fields as affected by topography. **Scientia Agricola**, Piracicaba, v. 66, n. 1, p. 77–83, 2009.

BURROUGH, P. A. Fractal dimensions of landscapes and other environmental data. **Nature**, London, v. 294, n. 5838, p. 240–242, 1981.

BURROUGH, P. A. **Principles of geographical information systems for land resources assessment**. Oxford: Clarendon Press, 1986. 193 p.

BURROUGH, P. A.; MCDONNELL, R. A. **Principles of geographical information system**. Oxford: Oxford University Press, 1998, 333 p.

BURTON, A. J.; PREGITZER, K. S. Field measurements of root respiration indicate little to no seasonal temperature acclimation for sugar maple and red pine. **Tree Physiology**, Oxford, v. 23, n. 4, 273–280, 2003.

CABRERA, M. L. Modeling the flush of nitrogen mineralization caused by drying and rewetting soils. **Soil Science Society of America Journal**, Madison, v. 57, n. 1, p. 63–66, 1993.

CAMBARDELLA, C. A.; MOORMAN, T. B.; NOVAK, J. M.; PARKIN, T. B.; KARLEN, D. L.; TURCO, R. F.; KONOPKA, A. E. Field-scale variability of soil properties in central Iowa soils. **Soil Science Society of America Journal**, Madison, v. 58, n. 5, p. 1501–1511, 1994.

CANELLAS, L. P.; BUSATO, J. G.; DOBBSS, L. B.; BALDOTTO, M. A.; RUMJANEK, V. M.; OLIVARES, F. L. Soil organic matter and nutrient pools under long-term non-burning management of sugar cane. **European Journal of Soil Science**, Oxford, v. 61, n. 3, p. 375–383, 2010.

CANELLAS, L. P.; VELLOSO, A. C. X.; MARCIANO, C. R.; RAMALHO, J. F. G. P.; RUMJANEK, V. M.; REZENDE, C. E.; SANTOS, G. A. Propriedades químicas de um Cambissolo cultivado com cana-de-açúcar, com preservação do palhiço e adição de vinhaça por longo tempo. **Revista Brasileira de Ciência do Solo**, Viçosa, v. 27, n. 5, p. 935–944, 2003.

CANTERO, J. J.; LEON, R.; CISNEROS, J. M.; CANTERO, A. Habitat structure and vegetation relationships in central Argentina salt marsh landscapes. **Plant Ecology**, Dordrecht, v. 137, n. 1, p. 79–100, 1998.

CAPECHE, C. L.; MACEDO, J. R.; MELO, A. S.; ANJOS, L. H. C. **Parâmetros técnicos relacionados ao manejo e conservação do solo, água e vegetação:** perguntas e respostas. Rio de Janeiro: Embrapa Solos, 2004. 16 p.

CARDELLINI, C.; CHIODINI, G.; FRONDINI, F. Application of stochastic simulation to CO_2 flux from soil: mapping and quantification of gas release. **Journal of Geophysical Research**, Hoboken, v. 108, n. B9, p. 2425, 2003.

CARMO, J. B.; FILOSO, S.; ZOTELLI, L. C.; SOUSA NETO, E. R.; PITOMBO, L. M.; DUARTE-NETO, P. J.; VARGAS, V. P.; ANDRADE, C. A.; GAVA, G. J. C.; ROSSETTO, R.; CANTARELLA, H.; ELIA NETO, A.; MARTINELLI, L. A. Infield greenhouse gas emissions from sugarcane soils in Brazil: effects from synthetic and organic fertilizer application and crop trash accumulation. **Global Change Biology Bioenergy**, Chichester, v. 5, n. 3, 267–280, 2013.

CERRI, C. E. P.; GALDOS, M. V.; CARVALHO, J. L. N.; FEIGL, B. J.; CERRI, C. C. Quantifying soil carbon stocks and greenhouse gas fluxes in the sugarcane agrosystem: point of view. **Scientia Agricola**, Piracicaba, v. 70, n. 5, 361–368, 2013.

CERRI, C. E. P.; SPAROVEK, G.; BERNOUX, M.; EASTERLING, W. E.; MELILLO, J. M.; CERRI, C. C. Tropical agriculture and global warming: impacts and mitigation options. **Scientia Agricola**, Piracicaba, v. 64, n. 1, p. 83–89, 2007.

CHAN, K.Y. Soil particulate organic carbon under different land use and management. **Soil Use and Management**, Oxford, v. 17, n. 4, p. 217–221, 2001.

CIAIS, P.; SABINE, C.; BALA, G.; BOPP, L.; BROVKIN, V.; CANADELL, J.; CHHABRA, A.; DEFRIES, R.; GALLOWAY, J.; HEIMANN, M.; JONES, C.; LE QUÉRÉ, C.; MYNENI, R. B.; PIAO, S.; THORNTON, P. Carbon and other biogeochemical cycles. In: STOCKER, T. F.; QIN, D.; PLATTNER, G.; TIGNOR, M.; ALLEN, S. K.; BOSCHUNG, J.; NAUELS, A.; XIA, Y.; BEX, V.; MIDGLEY, P. M. (Eds.). **Climate change 2013:** the physical science basis. Cambridge e New York: Cambridge University Press, 2013. p. 465–570.

CONAB, Companhia Nacional de Abastecimento. **Acompanhamento da safra brasileira de cana-de-açúcar, segundo levantamento**. Brasília: Conab, 2015. 33 p.

CONCILIO, A.; CHEN, J. Q.; MA, S.; NORTH, M. Precipitation drives interannual variation in summer soil respiration in a Mediterranean-climate, mixed-conifer forest. **Climatic Change**, Dordrecht, v. 92, n. 1–2, p. 109–122, 2009.

CONEN, F.; DOBBIE, K. E.; SMITH, K. A. Predicting N_2O emissions from agricultural land through related soil parameters. **Global Change Biology**, Oxford, v. 6, n. 4, p. 417–426, 2000.

CORÁ, J. E.; ARAÚJO, A. V.; PEREIRA, G. T.; BERALDO, J. M. G. Variabilidade espacial de atributos do solo para adoção do sistema de agricultura de precisão na cultura de cana-de-açúcar. **Revista Brasileira de Ciência do Solo**, Viçosa, v. 28, n. 6, p. 1013–1021, 2004.

CORRADI, M. M.; PANOSSO, A. R.; MARTINS FILHO, M. V.; LA SCALA, N. Crop residues on short-term CO_2 emissions in sugarcane production areas. **Engenharia Agrícola**, Jaboticabal, v. 33, n. 4, p. 699–708, 2013.

COSTA, F. S.; BAYER, C.; ZANATTA, J. A.; MIELNICZUK, J. Estoque de carbono orgânico no solo e emissões de dióxido de carbono influenciadas por sistemas de manejo no sul do Brasil. **Revista Brasileira de Ciência do Solo**, Viçosa, v. 32, n. 1, p. 323–332, 2008.

DASSELAAR, A. P.; CORRÉ, W. J.; PRIEMÉ, A.; KLEMEDTSSON, Å. K.; WESLIEN, P.; KLEMEDTSSON, L.; STEIN, A.; OENEMA, O. Spatial variability of methane, nitrous oxide, and carbon dioxide emissions from drained grasslands. **Soil Science Society of America Journal**, Madison, v. 62, n. 3, p. 810–817, 1998.

DENMEAD, O. T.; MACDONALD, B. C. T.; BRYANT, G.; NAYLOR, T.; WILSON, S.; GRIFFITH, D. W. T.; WANG, W. J.; SALTER, B.; WHITE, I.; MOODY, P. W. Emissions of methane and nitrous oxide from Australian sugarcane soils. **Agricultural and Forest Meteorology**, Amsterdam, v. 150, n. 6, p. 748–756, 2010.

DOMINY, C. S.; HAYNES, R. J.; ANTWERPEN, R. van. Loss of soil organic matter and related soil properties under long-term sugarcane production on two contrasting soils. **Biology and Fertility of Soils**, Heidelberg, v. 36, n. 5, p. 350–356, 2002.

DONAGEMA, G. K.; CAMPOS, D. V. B.; CALDERANO, S. B.; TEIXEIRA, W. G.; VIANA, J. H. M. **Manual de métodos de análise de solo**. 2. ed. Rio de Janeiro: Embrapa Solos, 2011. 230 p.

DUAH-YENTUMI, S.; RONN, R.; CHRISTENSEN, S. Nutrients limiting microbial growth in a tropical forest soil of Ghana under different management. **Applied Soil Ecology**, Amsterdam, v. 8, n. 1–3, p. 19–24, 1998.

EGHBALL, B.; HERGERT, G. W.; LESOING, G. W.; FERGUSON, R. B. Fractal analysis of spatial and temporal variability. **Geoderma**, Amsterdam, v. 88, n. 3–4, p. 349–362, 1999.

EPRON, D.; BOSC, A.; BONAL, D.; FREYCON, V. Spatial variation of soil respiration across a topographic gradient in a tropical rain forest in French Guiana. **Journal of Tropical Ecology**, Cambridge, v. 22, n. 5, p. 565–574, 2006.

EPRON, D.; FARQUE, L.; LUCOT, E.; BADOT, P. Soil CO_2 efflux in a beech forest: dependence on soil temperature and soil water content. **Annals of Forest Science**, Paris, v. 56, n. 3, p. 221–226, 1999.

EPRON, D.; NOUVELLON, Y.; ROUPSARD, O.; MOUVONDY, W.; MABIALA, A.; SAINT-ANDRÉ, L.; JOFFRE, R.; JOURDAN, C.; BONNEFOND, J.; BERBIGIER, P.; HAMEL, O. Spatial and temporal variations of soil respiration in a *Eucalyptus* plantation in Congo. **Forest Ecology and Management**, Amsterdam, v. 202, n. 1–3, p. 149–160, 2004.

FANG, C.; MONCRIEFF, J. B.; GHOLZ, H. L.; CLARK, K. L. Soil CO_2 efflux and its spatial variation in a Florida slash pine plantation. **Plant and Soil**, Dordrecht, v. 205, n. 2, p. 135–146, 1998.

FELLER, C.; BEARE, M. H. Physical control of soil organic matter dynamics in the tropics. **Geoderma**, Amsterdam, v. 79, n. 1–4, p. 69–116, 1997.

FIERER, N.; SCHIMEL, J. P. A proposed mechanism for the pulse in carbon dioxide production commonly observed following the rapid rewetting of a dry soil. **Soil Science Society of America Journal**, Madison, v. 67, n. 3, p. 798–805, 2003.

FRANKLIN, R. B.; MILLS, A. L. Multi-scale variation in spatial heterogeneity for microbial community structure in an eastern Virginia agricultural field. **FEMS Microbiology Ecology**, Oxford, v. 44, n. 3, p. 335–346, 2003.

FOLLETT, R. F. Soil management concepts and carbon sequestration in cropland soils. **Soil and Tillage Research**, Amsterdam, v. 61, n. 1–2, p. 77–92, 2001.

FUENTES, J. P.; BEZDICEK, D. F.; FLURY, M.; ALBRECHT, S.; SMITH, J. L. Microbial activity affected by lime in a long-term no-till soil. **Soil and Tillage Research**, Amsterdam, v. 88, n. 1–2, p. 123–131, 2006.

GALDOS, M. V.; CERRI, C. C.; CERRI, C. E. P. Soil carbon stocks under burned and unburned sugarcane in Brazil. **Geoderma**, Amsterdam, v. 153, n. 3–4, p. 347–352, 2009.

GONÇALVES, A. C. A.; FOLEGATTI, M. V.; MATA, J. D. V. Análises exploratória e geoestatística da variabilidade de propriedades físicas de um Argissolo Vermelho. **Acta Scientiarum**, Maringá, v. 23, n. 5, p. 1149–1157, 2001.

GRAHAM, M. H.; HAYNES, R. J. Organic matter status and the size, activity and metabolic diversity of the soil microbial community in the row and inter-row of sugarcane under burning and trash retention. **Soil Biology and Biochemistry**, Oxford, v. 38, n. 1, p. 21–31, 2006.

GREGORICH, E. G.; ROCHETTE, P.; HOPKINS, D. W.; MCKIM, U. F.; ST-GEORGES, P. Tillage-induced environmental conditions in soil and substrate limitation determine biogenic gas production. **Soil Biology and Biochemistry**, Oxford, v. 38, n. 9, p. 2614–2628, 2006.

HAIR JUNIOR, J. F.; ANDERSON, R. E.; TATHAM, R. L.; BLACK, W. C. **Análise multivariada de dados**. 5. ed. Porto Alegre: Bookman, 2005. 600 p.

HERBST, M.; PROLINGHEUER, N.; GRAF, A.; HUISMAN, J. A.; WEIHERMÜLLER, L.; VANDERBORGHT, J. Characterization and understanding of bare soil respiration spatial variability at plot scale. **Vadose Zone Journal**, Madison, v. 8, n. 3, p. 762–771, 2009.

HERBST, M.; PROLINGHEUER, N.; GRAF, A.; HUISMAN, J. A.; WEIHERMÜLLER, L.; VANDERBORGHT, J.; VEREECKEN, H. Multivariate conditional stochastic simulation of soil heterotrophic respiration at plot scale. **Geoderma**, Amsterdam, v. 160, n. 1, p. 74–82, 2010.

HUANG, C.; BRADFORD, J. M. Applications of a laser scanner to quantify soil microtopography. **Soil Science Society of America Journal**, Madison, v. 56, n. 1, p. 14–21, 1992.

IAMAGUTI, J. L.; MOITINHO, M. R.; TEIXEIRA, D. B.; BICALHO, E. S.; PANOSSO, A. R.; LA SCALA, N. Preparo do solo e emissão de CO_2, temperatura e umidade do solo em área canavieira. **Revista Brasileira de Engenharia Agrícola e Ambiental**, Campina Grande, v. 19, n. 5, p. 497–504, 2015.

ISAAKS, E. H.; SRIVASTAVA, R. M. **An introduction to applied geostatistics**. New York: Oxford University Press, 1989. 561 p.

ISHIZUKA, S.; ISWANDI, A.; NAKAJIMA, Y.; YONEMURA, S.; SUDO, S.; TSURUTA, H.; MURIYARSO, D. Spatial patterns of greenhouse gas emission in a tropical rainforest in Indonesia. **Nutrient Cycling in Agroecosystems**, Dordrecht, v. 71, n. 1, p. 55–62, 2005.

JASSAL, R. S.; BLACK, T. A.; DREWITT, G. B.; NOVAK, M. D.; GAUMONT-GUAY, D.; NESIC, Z. A model of the production and transport of CO_2 in soil: predicting soil CO_2 concentrations and CO_2 efflux from a forest floor. **Agricultural and Forest Meteorology**, Amsterdam, v. 124, n. 3–4, p. 219–236, 2004.

JEFFERS, J. N. R. **An introduction to system analysis:** with ecological applications. London: Edward Arnold, 1978. 198 p.

JENKINSON, D. S.; HARKNESS, D. D.; VANCE, E. D.; ADAMS, D. E.; HARRISON, A. F. Calculating net primary production and annual input of organic matter to soil from the amount and radiocarbon content of soil organic matter. **Soil Biology and Biochemistry**, Oxford, v. 24, n. 4, p. 295–308, 1992.

JOURNEL, A. G.; HUIJBREGTS, C. J. **Mining geostatistics**. London: Academic Press, 1978. 600 p.

KAISER, H. F. The varimax criterion for analytic rotation in factor analysis. **Psychometrika**, New York, v. 23, n. 3, p. 187–200, 1958.

KANG, S.; KIM, S.; OH, S.; LEE, D. Predicting spatial and temporal patterns of soil temperature based on topography, surface cover and air temperature. **Forest Ecology and Management**, Amsterdam, v. 136, n. 1–3, p. 173–184, 2000.

KARHU, K.; AUFFRET, M. D.; DUNGAIT, J. A. J.; HOPKINS, D. W.; PROSSER, J. I.; SINGH, B. K.; SUBKE, J.; WOOKEY, P. A.; ÅGREN, G. I.; SEBASTIÀ, M.; GOURIVEAU, F.; BERGKVIST, G.; MEIR, P.; NOTTINGHAM, A. T.; SALINAS, N.; HARTLEY, I. P. Temperature sensitivity of soil respiration rates enhanced by microbial community response. **Nature**, London, v. 513, n. 7516, p. 81–84, 2014.

KEMMITT, S. J.; LANYON, C. V.; WAITE, I. S.; WEN, Q.; ADDISCOTT, T. M.; BIRD, N. R. A.; O'DONNELL, A. G.; BROOKES, P. C. Mineralization of native soil organic matter is not regulated by the size, activity or composition of the soil microbial biomass—a new perspective. **Soil Biology and Biochemistry**, Oxford, v. 40, n. 1, p. 61–73, 2008.

KHOMIK, M.; ARAIN, M. A.; MCCAUGHEY, J. H. Temporal and spatial variability of soil respiration in a boreal mixedwood forest. **Agricultural and Forest Meteorology**, Amsterdam, v. 140, n. 1–4, p. 244–256, 2006.

KLINKENBERG, B. Fractals and morphometric measures: is there a relationship? **Geomorphology**, Amsterdam, v. 5, n. 1–2, p. 5–20, 1992.

KONDA, R.; OHTA, S.; ISHIZUKA, S.; ARAI, S.; ANSORI, S.; TANAKA, N.; HARDJONO, A. Spatial structures of N_2O, CO_2, and CH_4 fluxes from *Acacia mangium* plantation soils during a relatively dry season in Indonesia. **Soil Biology and Biochemistry**, Oxford, v. 40, n. 12, p. 3021–3030, 2008.

KOSUGI, Y.; MITANI, T.; ITOH, M.; NOGUCHI, S.; TANI, M.; MATSUO, N.; OHKUBO, S.; NIK, A. R. Spatial and temporal variation in soil respiration in a Southeast Asian tropical rainforest. **Agricultural and Forest Meteorology**, Amsterdam, v. 147, n. 1–2, p. 35–47, 2007.

LA SCALA, N.; BOLONHEZI, D.; PEREIRA, G. T. Short-term soil CO_2 emission after conventional and reduced tillage of a no-till sugar cane area in southern Brazil. **Soil and Tillage Research**, Amsterdam, v. 91, n. 1–2, p. 244–248, 2006.

LA SCALA, N.; PANOSSO, A. R.; PEREIRA, G. T. Modelling short-term temporal changes of bare soil CO_2 emissions in a tropical agrosystem by using meteorological data. **Applied Soil Ecology**, Amsterdam, v. 24, n. 1, p. 113–116, 2003.

LA SCALA, N.; MARQUES JÚNIOR, J.; PEREIRA, G. T.; CORÁ, J. E. Short-term temporal changes in the spatial variability model of CO2 emissions from a Brazilian bare soil. **Soil Biology and Biochemistry**, Oxford, v. 32, n. 10, p. 1459–1462, 2000a.

LA SCALA, N.; MARQUES JÚNIOR, J.; PEREIRA, G. T.; CORÁ, J. E. Carbon dioxide emission related to chemical properties of a tropical bare soil. **Soil Biology and Biochemistry**, Oxford, v. 32, n. 10, p. 1469–1473, 2000b.

LA SCALA, N.; PANOSSO, A. R.; PEREIRA, G. T.; PAZ GONZÁLEZ, A.; MIRANDA, J. G. V. Fractal dimension and anisotropy of soil CO_2 emission in na agricultural field during fallow. **International Agrophysics**, Lublin, v. 23, n. 4, p. 353–358, 2009.

LAL, R. World cropland soils as a source or sink for atmospheric carbon. **Advances in Agronomy**, Madison, v. 71, n. 1, p. 145–191, 2001.

LAL, R., Challenges and opportunities in soil organic matter research. **European Journal of Soil Science**, Oxford, v. 60, n. 2, p. 158–169, 2009.

LAL, R.; FAUSEY, N. R.; ECKERT, D. J. Land use and soil management effects on emissions of radiatively active gases from two soils in Ohio. In: LAL, R.; KIMBLE, J.; LEVINE, E.; STEWART, B. A. (Eds.). **Soil management and greenhouse effect**. Boca Raton: Lewis Publishers, 1995. p. 41–59.

LLOYD, J.; TAYLOR, A. On the temperature dependence of soil respiration. **Functional Ecology**, Oxford, v. 8, n. 3, p. 315–323, 1994.

LUCA, E. F.; FELLER, C.; CERRI, C. C.; BARTHÈS, B.; CHAPLOT, V.; CAMPOS, D. C.; MANECHINI, C. Avaliação de atributos físicos e estoques de carbono e nitrogênio em solos com queima e sem queima de canavial. **Revista Brasileira de Ciência do Solo**, Viçosa, v. 32, n. 2, p. 789–800, 2008.

MANDELBROT, B. B. **Fractals:** form, chance, and dimension. San Francisco: W.H. Freeman, 1977. 365 p.

MARK, D. M.; ARONSON, P. B. Scale-dependent fractal dimensions of topographic surfaces: an empirical investigation, with applications in geomorphology and computer mapping. **Mathematical Geology**, Heidelberg, v. 16, n. 7, p. 671–683, 1984.

MATHERON, G. Principles of geostatistics. **Economic Geology**, Littleton, v. 58, n. 8, p. 1246–1266, 1963.

MIRANDA, J. G. V. **Análisis fractal del microrrelieve del suelo**. 2000. 313 f. Tese (Doutorado em Edafologia) – Faculdade de Ciências, Universidade de A Coruña, A Coruña, Epanha, 2000.

MOITINHO, M. R.; PADOVAN, M. P.; PANOSSO, A. R.; LA SCALA, N. Efeito do preparo do solo e resíduo da colheita de cana-de-açúcar sobre a emissão de CO_2. **Revista Brasileira de Ciência do Solo**, Viçosa, v. 37, n. 6, p. 1720–1728, 2013.

MOITINHO, M. R.; PADOVAN, M. P.; PANOSSO, A. R.; TEIXEIRA, D. B.; FERRAUDO, A. S.; LA SCALA, N. On the spatial and temporal dependence of CO_2 emission on soil properties in sugarcane (*Saccharum* spp.) production. **Soil and Tillage Research**, Amsterdam, v. 148, n. 1, p. 127–132, 2015.

NGAO, J.; EPRON, D.; DELPIERRE, N.; BREDA, N.; GRANIER, A.; LONGDOZ, B. Spatial variability of soil CO_2 efflux linked to soil parameters and ecosystem characteristics in a temperate beech forest. **Agricultural and Forest Meteorology**, Amsterdam, v. 154–155, n. 1, p. 136–146, 2012.

OHASHI, M.; GYOKUSEN, K. Temporal change in spatial variability of soil respiration on a slope of Japanese cedar (*Cryptomeria japonica* D. Don) forest. **Soil Biology and Biochemistry**, Oxford, v. 39, n. 5, p. 1130–1138, 2007.

OLIVEIRA, B. G.; CARVALHO, J. L. N.; CERRI, C. E. P.; CERRI, C. C.; FEIGL, B. J. Soil greenhouse gas fluxes from vinasse application in Brazilian sugarcane areas. **Geoderma**, Amsterdam, v. 200–201, n. 1, p. 77–84, 2013.

OLIVEIRA, V. S.; ROLIM, M. M.; VASCONCELOS, R. F. B.; COSTA, Y. D. J.; PEDROSA, E. M. R. Compactação de um Argissolo Amarelo distrocoeso submetido a diferentes manejos. **Revista Brasileira de Engenharia Agrícola e Ambiental**, Campina Grande, v. 14, n. 9, p. 914–920, 2010.

OYONARTE, C.; REY, A.; RAIMUNDO, J.; MIRALLES, I.; ESCRIBANO, P. The use of soil respiration as an ecological indicator in arid ecosystems of the SE of Spain: spatial variability and controlling factors. **Ecological Indicators**, Amsterdam, v. 14, n. 1, p. 40–49, 2012.

PACHEPSKY, Y.; CRAWFORD, J. W. Fractal analysis. In: HILLEL, D. (Ed.). **Encyclopedia of soils in the environment**. Waltham: Academic Press, 2004. v. 2, p. 85–98.

PALMER, M. W. Fractal geometry: a tool for describing spatial patterns of plant communities. **Vegetatio**, Dordrecht, v. 75, n. 1–2, p. 91–102, 1988.

PANOSSO, A. R.; MARQUES JÚNIOR., J.; PEREIRA, G. T.; LA SCALA, N. Spatial and temporal variability of soil CO_2 emission in a sugarcane area under green and slash-and-burn managements. **Soil and Tillage Research**, Amsterdam, v. 105, n. 2, p. 275–282, 2009.

PANOSSO, A. R.; MARQUES JÚNIOR, J.; MILORI, D. M. B. P.; FERRAUDO, A. S.; BARBIERI, D. M.; PEREIRA, G. T.; LA SCALA, N. Soil CO_2 emission and its relation to soil properties in sugarcane areas under slash-and-burn and green harvest. **Soil and Tillage Research**, Amsterdam, v. 111, n. 2, p. 190–196, 2011.

PANOSSO, A. R.; PERILLO, L. I.; FERRAUDO, A. S.; PEREIRA, G. T.; MIRANDA, J. G. V.; LA SCALA, N. Fractal dimension and anisotropy of soil CO_2 emission in a mechanically harvested sugarcane production area. **Soil and Tillage Research**, Amsterdam, v. 124, n. 1, p. 8–16, 2012.

PERFECT, E.; KAY, B. D. Applications of fractals in soil and tillage research: a review. **Soil and Tillage Research**, Amsterdam, v. 36, n. 1–2, p. 1–20, 1995.

PETERS, V.; CONRAD, R. Sequential reduction processes and initiation of CH_4 production upon flooding of oxic upland soils. **Soil Biology and Biochemistry**, Oxford, v. 28, n. 3, p. 371–382, 1996.

PONNAMPERUMA, F. N. The chemistry of submerged soils. **Advances in Agronomy**, Madison, v. 24, n. 1, p. 29–96, 1972.

RAIJ, B. van. Mecanismos de interação entre solos e nutrientes. In: RAIJ, B. van (Ed.). **Avaliação da fertilidade do solo**. Piracicaba: Instituto da Potassa e Fosfato, 1981. p. 17–31.

RAIJ, B. van; ANDRADE, J. C.; CANTARELLA, H.; QUAGGIO, J. A. **Análise química para avaliação da fertilidade de solos tropicais**. Campinas: Instituto Agronômico, 2001. 284 p.

RAZAFIMBELO, T.; BARTHÈS, B.; LARRÉ-LARROUY, M.; LUCA, E. F.; LAURENT, J.; CERRI, C. C.; FELLER, C. Effect of sugarcane residue management (mulching versus burning) on organic matter in a clayey Oxisol from southern Brazil. **Agriculture, Ecosystems & Environment**, Amsterdam, v. 115, n. 1–4, p. 285–289, 2006.

ROBERTSON, F. A.; THORBURN, P. J. Crop residue effects on soil C and N cycling under sugarcane. In: REES, R. M.; BALL, B. C.; CAMPBELL, C. D.; WATSON, C. A. (Eds.). **Sustainable management of soil organic matter**. Wallingford: CABI Publishing, 2001. p. 112–119.

RYU, S.; CONCILIO, A.; CHEN, J.; NORTH, M.; MA, S. Prescribed burning and mechanical thinning effects on belowground conditions and soil respiration in a mixed-conifer forest, California. **Forest Ecology and Management**, Amsterdam, v. 257, n. 4, p. 1324–1332, 2009.

SARTORI, F.; LAL, R.; EBINGER, M. H.; PARRISH, D. J. Potential soil carbon sequestration and CO_2 offset by dedicated energy crops in the USA. **Critical Reviews in Plant Sciences**, Philadelphia, v. 25, n. 5, p. 441–472, 2006.

SCHNEIDER, S.; SARUKHAN, J.; ADEJUWON, J.; AZAR, C.; BAETHGEN, W.; HOPE, C.; MOSS, R.; LEARY, N.; RICHELS, R.; YPERSELE, J. van. Overview of impacts, adaptation, and vulnerability to climate change. In: MCCARTHY, J. J.; CANZIANI, O. F.; LEARY, N. A.; DOKKEN, D. J.; WHITE, K. S. (Eds.). **Climate change 2001:** impacts, adaptation, and vulnerability. Cambridge e New York: Cambridge University Press, 2001. p. 75–104.

SCHWENDENMANN, L.; VELDKAMP, E.; BRENES, T.; O'BRIEN, J. J.; MACKENSEN, J. Spatial and temporal variation in soil CO_2 efflux in an old-growth neotropical rain forest, La Selva, Costa Rica. **Biogeochemistry**, Dordrecht, v. 64, n. 1, p. 111–128, 2003.

SIGNOR, D.; CERRI, C. E. P. Nitrous oxide emissions in agricultural soils: a review. **Pesquisa Agropecuária Tropical**, Goiânia, v. 43, n. 3, p. 322–338, 2013.

SIGNOR, D.; PISSIONI, L. L. M.; CERRI, C. E. P. Emissões de gases de efeito estufa pela deposição de palha de cana-de-açúcar sobre o solo. **Bragantia**, Campinas, v. 73, n. 2, p. 113–122, 2014.

SILVA-OLAYA, A. M.; CERRI, C. E. P.; LA SCALA, N.; DIAS, C. T. S.; CERRI, C. C. Carbon dioxide emissions under different soil tillage systems in mechanically harvested sugarcane. **Environmental Research Letters**, Bristol, v. 8, n. 1, p. 015014, 2013.

SILVEIRA, P. M.; STONE, L. F. Sistemas de preparo do solo e rotação de culturas na produtividade de milho, soja e trigo. **Revista Brasileira de Engenharia Agrícola e Ambiental**, Campina Grande, v. 7, n. 2, p. 240–244, 2003.

SIX, J.; ELLIOTT, E. T.; PAUSTIAN, K. Aggregate and soil organic matter dynamics under conventional and no-tillage systems. **Soil Science Society of America Journal**, Madison, v. 63, n. 5, p. 1350–1358, 1999.

SIX, J.; FREY, S. D.; THIET, R. K.; BATTEN, K. M. Bacterial and fungal contributions to carbon sequestration in agroecosystems. **Soil Science Society of America Journal**, Madison, v. 70, n. 2, p. 555–569, 2006.

SNEATH, P. H. A.; SOKAL, R. R. **Numerical taxonomy:** the principles and practice of numerical classification. San Francisco: W. H. Freeman, 1973. 573 p.

SOUZA, Z. M.; MARQUES JÚNIOR, J.; PEREIRA, G. T. Variabilidade espacial da estabilidade de agregados e matéria orgânica em solos de relevos diferentes. **Pesquisa Agropecuária Brasileira**, Brasília, v. 39, n. 5, p. 491–499, 2004.

SOUZA, Z. M.; PRADO, R. M.; PAIXÃO, A. C. S.; CESARIN, L. G. Sistemas de colheita e manejo da palhada de cana-de-açúcar. **Pesquisa Agropecuária Brasileira**, Brasília, v. 40, n. 3, p. 271–278, 2005.

SPOKAS, K. A. Impact of biochar field aging on laboratory greenhouse gas production potentials. **Global Change Biology Bioenergy**, Chichester, v. 5, n. 2, p. 165–176, 2013.

SPOKAS, K. A.; REICOSKY, D. C. Impacts of sixteen different biochars on soil greenhouse gas production. **Annals of Environmental Science**, v. 3, n. 1, p. 179–193, 2009.

STOTZKY, G.; NORMAN, A. G. Factors limiting microbial activities in soil. **Archiv für Mikrobiologie**, Heidelberg, v. 40, n. 4, p. 341–369, 1961.

STOYAN, H.; DE-POLLI, H.; BÖHM, S.; ROBERTSON, G. P.; PAUL, E. A. Spatial heterogeneity of soil respiration and related properties at the plant scale. **Plant and Soil**, Dordrecht, v. 222, n. 1, p. 203–214, 2000.

SUN, W.; XU, G.; GONG, P.; LIANG, S. Fractal analysis of remotely sensed images: a review of methods and applications. **International Journal of Remote Sensing**, Essex, v. 27, n. 22, p. 4963–4990, 2006.

TAVARES, R. L. M.; FARHATE, C. V. V.; SOUZA, Z. M.; LA SCALA, N.; TORRES, J. L. R.; CAMPOS, M. C. C. Emission of CO_2 and soil microbial activity in sugarcane management systems. **African Journal of Agricultural Research**, Lagos, v. 10, n. 9, p. 975–982, 2015.

TEDESCHI, V.; REY, A.; MANCA, G.; VALENTINI, R.; JARVIS, P. L.; BORGHETTI, M. Soil respiration in a Mediterranean oak forest at different developmental stages after coppicing. **Global Change Biology**, Oxford, v. 12, n. 1, p. 110–121, 2006.

TEIXEIRA, D. B.; PANOSSO, A. R.; CERRI, C. E. P.; PEREIRA, G. T.; LA SCALA, N. Soil CO_2 emission estimated by different interpolation techniques. **Plant and Soil**, Dordrecht, v. 345, n. 1, p. 187–194, 2011.

TEIXEIRA, L. G.; CORRADI, M. M.; FUKUDA, A.; PANOSSO, A. R.; REICOSKY, D.; LOPES, A.; LA SCALA, N. Soil and crop residue CO_2–C emission under tillage systems in sugarcane-producing areas of southern Brazil. **Scientia Agricola**, Piracicaba, v. 70, n. 5, p. 327–335, 2013a.

TEIXEIRA, D. B.; BICALHO, E. S.; PANOSSO, A. R.; CERRI, C. E. P.; PEREIRA, G. T.; LA SCALA, N. Spatial variability of soil CO_2 emission in a sugarcane area characterized by secondary information. **Scientia Agricola**, Piracicaba, v. 70, n. 3, p. 195–203, 2013b.

THORBURN, P. J.; MEIER, E. A.; COLLINS, K.; ROBERTSON, F. A. Changes in soil carbon sequestration, fractionation and soil fertility in response to sugarcane residue retention are site-specific. **Soil and Tillage Research**, Amsterdam, v. 120, n. 1, p. 99–111, 2012.

THORNTHWAITE, C. W. An approach toward a rational classification of climate. **The Geographical Review**, Hoboken, v. 38, n. 1, p. 55–94, 1948.

TOMINAGA, T. T.; CÁSSARO, F. A. M.; BACCHI, O. O. S.; REICHARDT, K.; OLIVEIRA, J. C. M.; TIMM, L. C. Variability of soil water content and bulk density in a sugarcane field. **Australian Journal of Soil Research**, Clayton, v. 40, n. 4, p. 604–614, 2002.

TRANGMAR, B. B.; YOST, R. S.; UEHARA, G. Application of geostatistics to spatial studies of soil properties. **Advances in Agronomy**, Madison, v. 38, n. 1, p. 45–94, 1986.

TSAI, S. M.; BARAIBAR, A. V. L.; ROMANI, V. L. M. Efeitos de fatores físicos e químicos sobre os microrganismos do solo umidade e aeração. In: CARDOSO, E. J. B. N.; TSAI, S. M.; NEVES, M. C. P. (Eds.). **Microbiologia do solo**. Campinas: Sociedade Brasileira de Ciência do Solo, 1992. p. 60–89.

USOWICZ, B.; LIPIEC, J. Spatial distribution of soil penetration resistance as affected by soil compaction: the fractal approach. **Ecological Complexity**, Amsterdam, v. 6, n. 3, p. 263–271, 2009.

USSIRI, D. A. N.; LAL, R. Long-term tillage effects on soil carbon storage and carbon dioxide emissions in continuous corn cropping system from an alfisol in Ohio. **Soil and Tillage Research**, Amsterdam, v. 104, n. 1, p. 39–47, 2009.

VARGAS, L. K.; SCHOLLES, D. Biomassa microbiana e produção de C–CO_2 e N mineral de um Podzólico Vermelho-Escuro submetido a diferentes sistemas de manejo. **Revista Brasileira de Ciência do Solo**, Viçosa, v. 24, n. 1, p. 35–42, 2000.

VARGAS, V. P.; CANTARELLA, H.; MARTINS, A. A.; SOARES, J. R.; CARMO, J. B.; ANDRADE, C. A. Sugarcane crop residue increases N_2O and CO_2 emissions under high soil moisture conditions. **Sugar Tech**, New Delhi, v. 16, n. 2, p. 174–179, 2014.

VAUCLIN, M.; VIEIRA, S. R.; VACHAUD, G.; NIELSEN, D. R. The use of cokriging with limited field soil observations. **Soil Science Society of America Journal**, Madison, v. 47, n. 2, p. 175–184, 1983.

VELDKAMP, E. Organic carbon turnover in three tropical soils under pasture after deforestation. **Soil Science Society of America Journal**, Madison, v. 58, n. 1, p. 175–180, 1994.

VESTERDAL, L.; SCHMIDT, I. K.; CALLESEN, I.; NILSSON, L. O.; GUNDERSEN, P. Carbon and nitrogen in forest floor and mineral soil under six common European tree species. **Forest Ecology and Management**, Amsterdam, v. 255, n. 1, p. 35–48, 2008.

VIDAL VÁZQUEZ, E.; MIRANDA, J. G. V.; PAZ GONZÁLEZ, A. Characterizing anisotropy and heterogeneity of soil surface microtopography using fractal models. **Ecological Modelling**, Amsterdam, v. 182, n. 3–4, p. 337–353, 2005.

VIDAL VÁZQUEZ, E.; VIEIRA, S. R.; DE MARIA, I. C.; PAZ GONZÁLEZ, A. Fractal dimension and geostatistical parameters for soil microrelief as a function of cumulative precipitation. **Scientia Agricola**, Piracicaba, v. 67, n. 1, p. 78–83, 2010.

WANG, G. X.; GERTNER, G.; SINGH, V.; SHINKAREVA, S.; PARYSOW, P.; ANDERSON, A. Spatial and temporal prediction and uncertainty of soil loss using the revised universal soil loss equation: a case study of the rainfall–runoff erosivity *R* factor. **Ecological Modelling**, Amsterdam, v. 153, n. 1–2, p. 143–155, 2002.

WASSMAN, R.; LANTIN, R. S.; NEUE, H. **Methane emissions from major rice ecosystems in Asia**. Dordrecht: Kluwer Academic Publishers, 2000. 394 p.

XU, M.; QI, Y. Soil-surface CO_2 efflux and its spatial and temporal variations in a young ponderosa pine plantation in northern California. **Global Change Biology**, Oxford, v. 7, n. 1, p. 667–677, 2001.

XU, T.; MOORE, I. D.; GALLANT, J. C. Fractals, fractal dimensions and landscapes – a review. **Geomorphology**, Amsterdam, v. 8, n. 4, p. 245–262, 1993.

APPENDIX

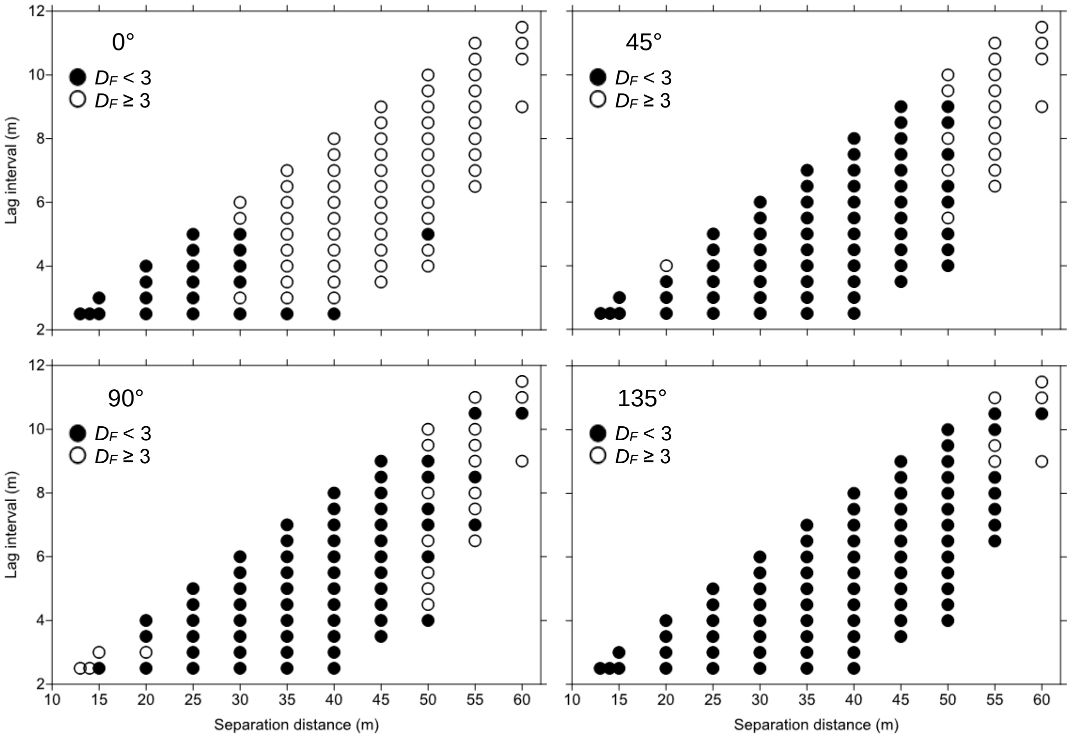

Figure A1. Fractograms of soil microbial biomass (SMB) calculated from anisotropic semivariograms for the directions of 0°, 45°, 90° and 135°, with the fractal dimension for different scales.

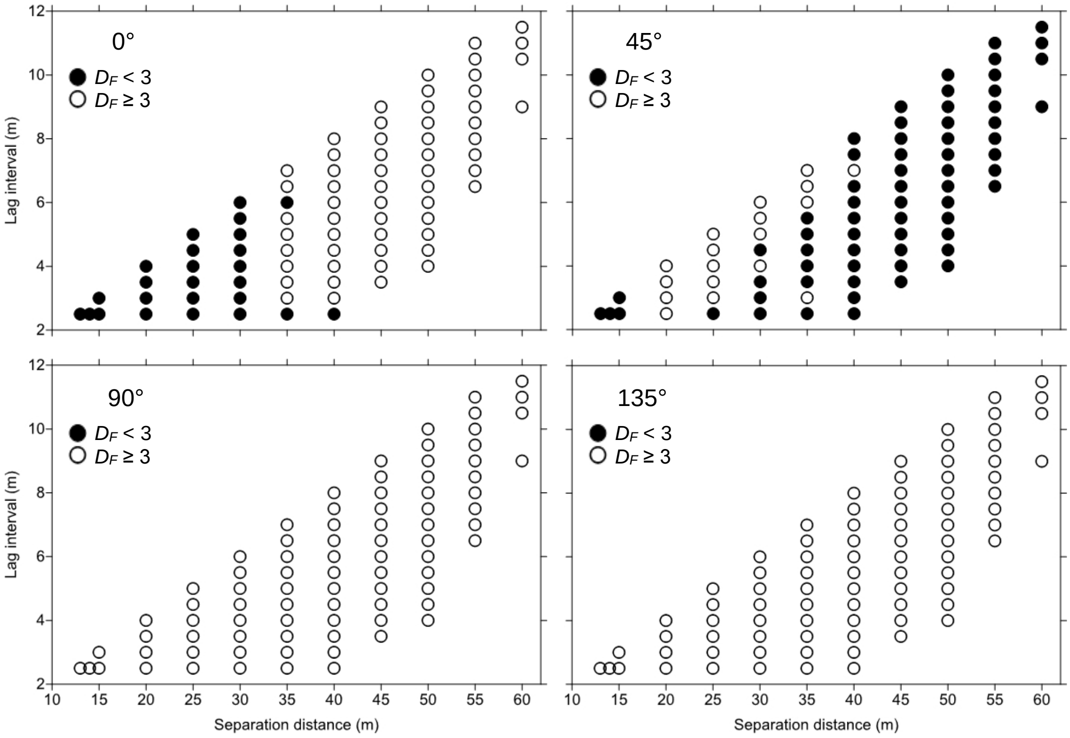

Figure A2. Fractograms of soil temperature (T_S) calculated from anisotropic semivariograms for the directions of 0°, 45°, 90° and 135°, with the fractal dimension for different scales.

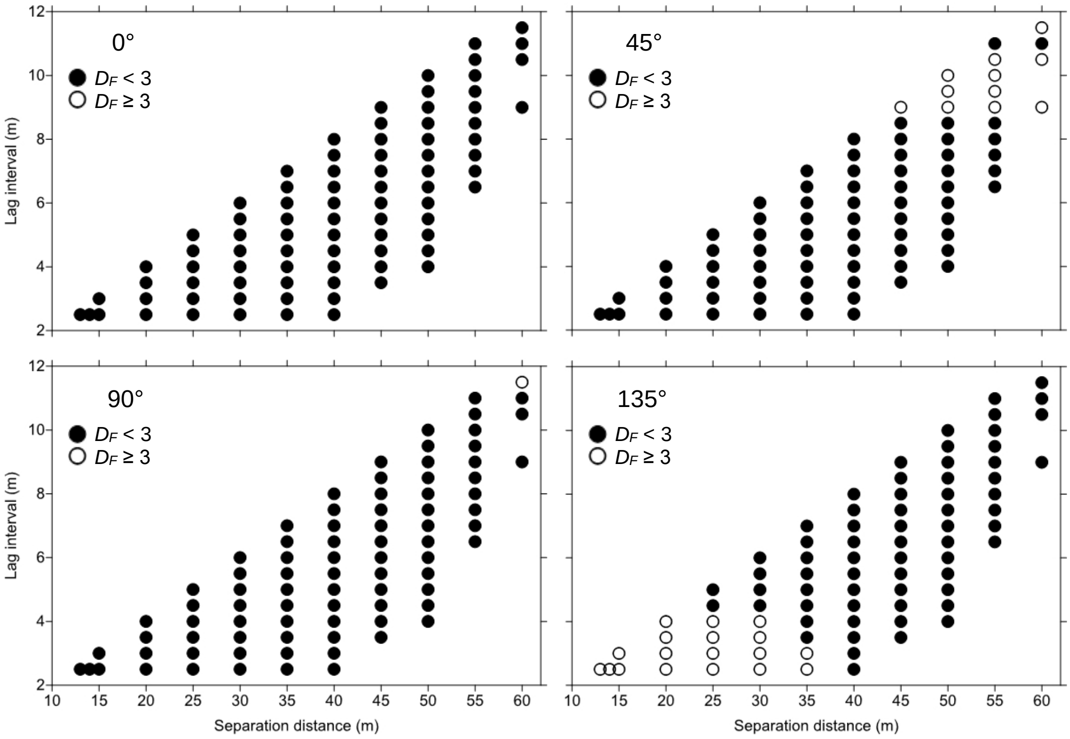

Figure A3. Fractograms of soil moisture (M_S) calculated from anisotropic semivariograms for the directions of 0°, 45°, 90° and 135°, with the fractal dimension for different scales.

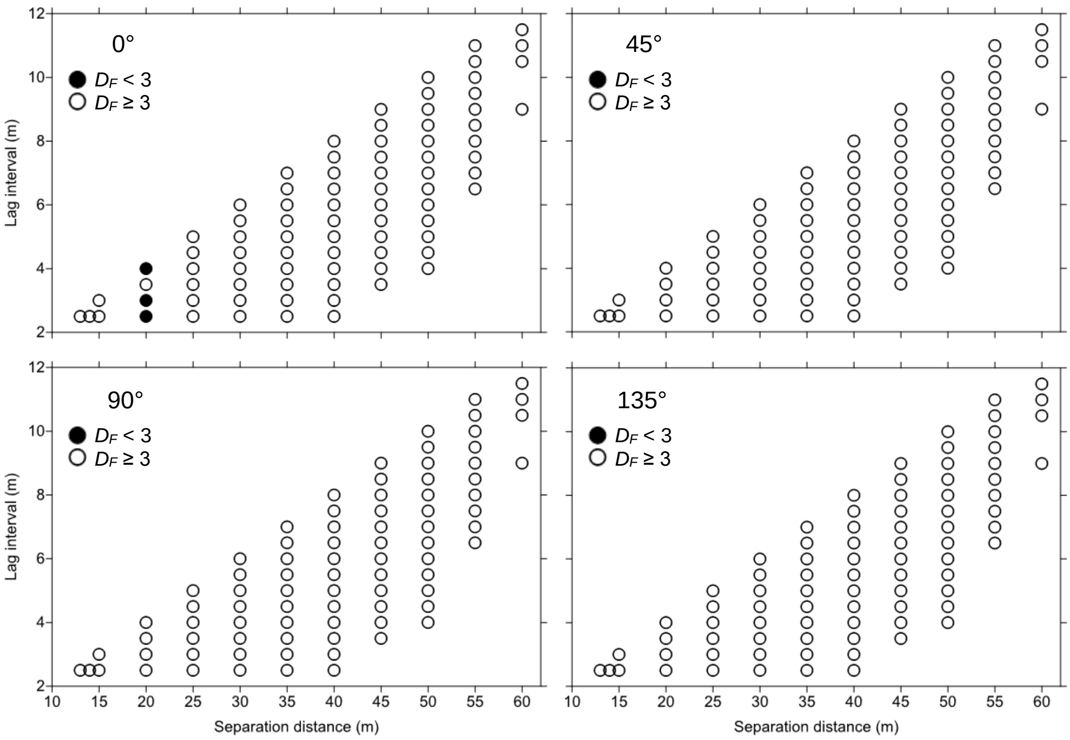

Figure A4. Fractograms of air-filled pore space (AFPS) calculated from anisotropic semivariograms for the directions of 0°, 45°, 90° and 135°, with the fractal dimension for different scales.

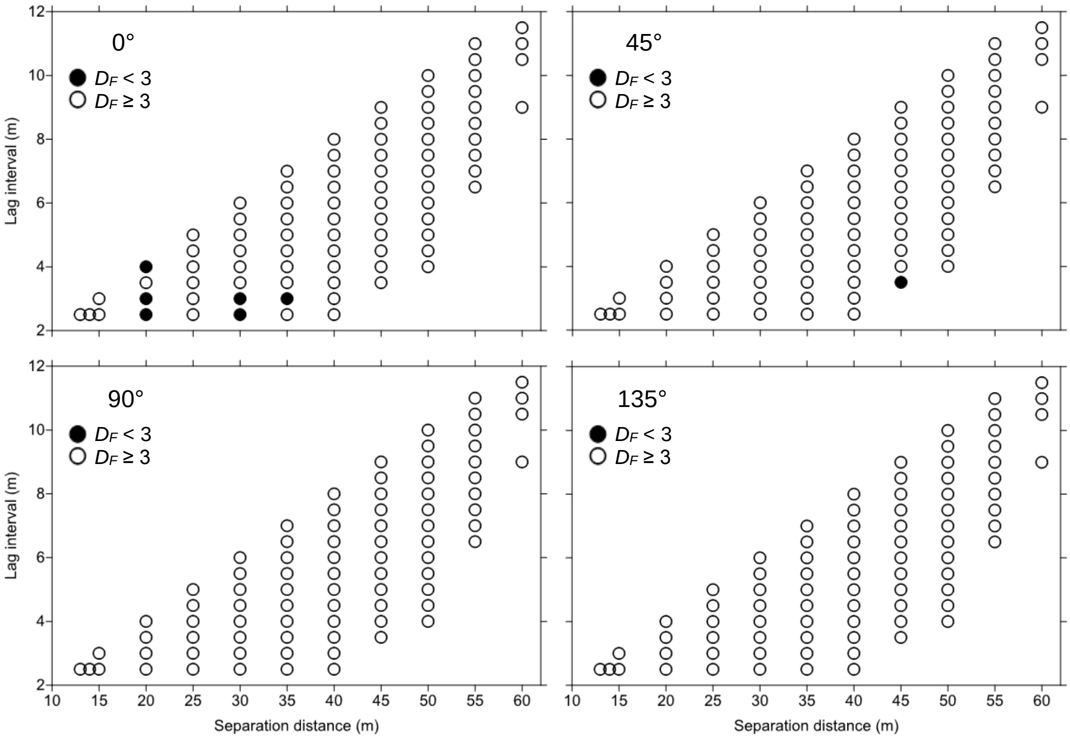

Figure A5. Fractograms of total pore volume (TPV) calculated from anisotropic semivariograms for the directions of 0°, 45°, 90° and 135°, with the fractal dimension for different scales.

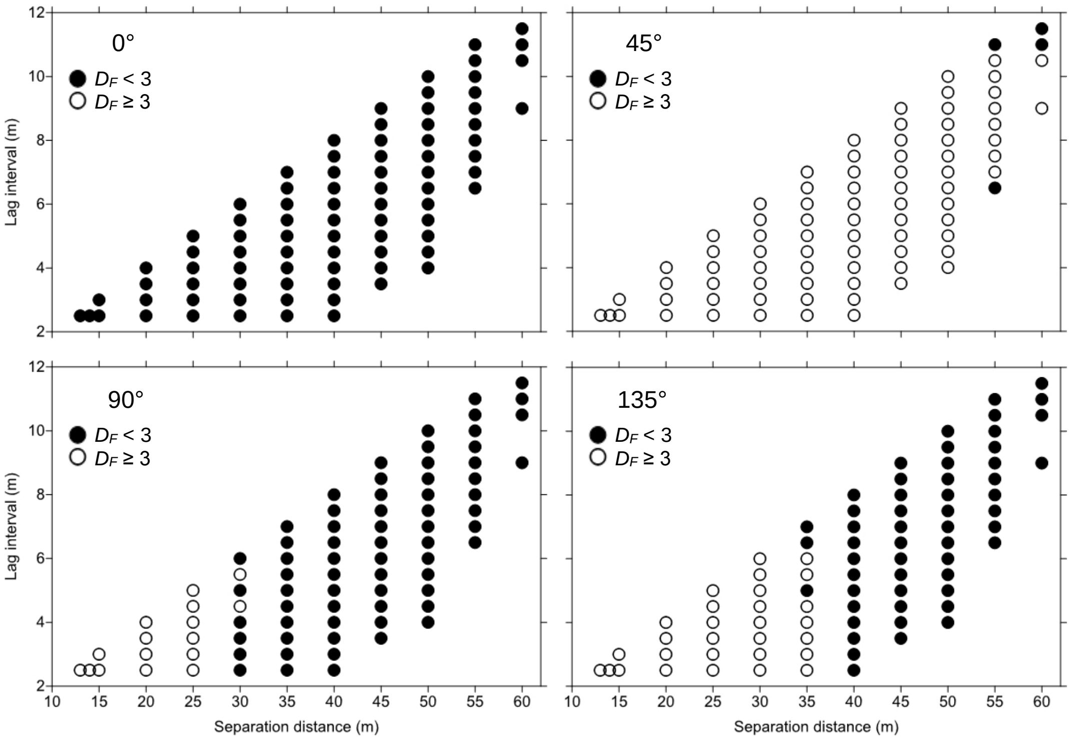

Figure A6. Fractograms of microporosity (Micro) calculated from anisotropic semivariograms for the directions of 0°, 45°, 90° and 135°, with the fractal dimension for different scales.

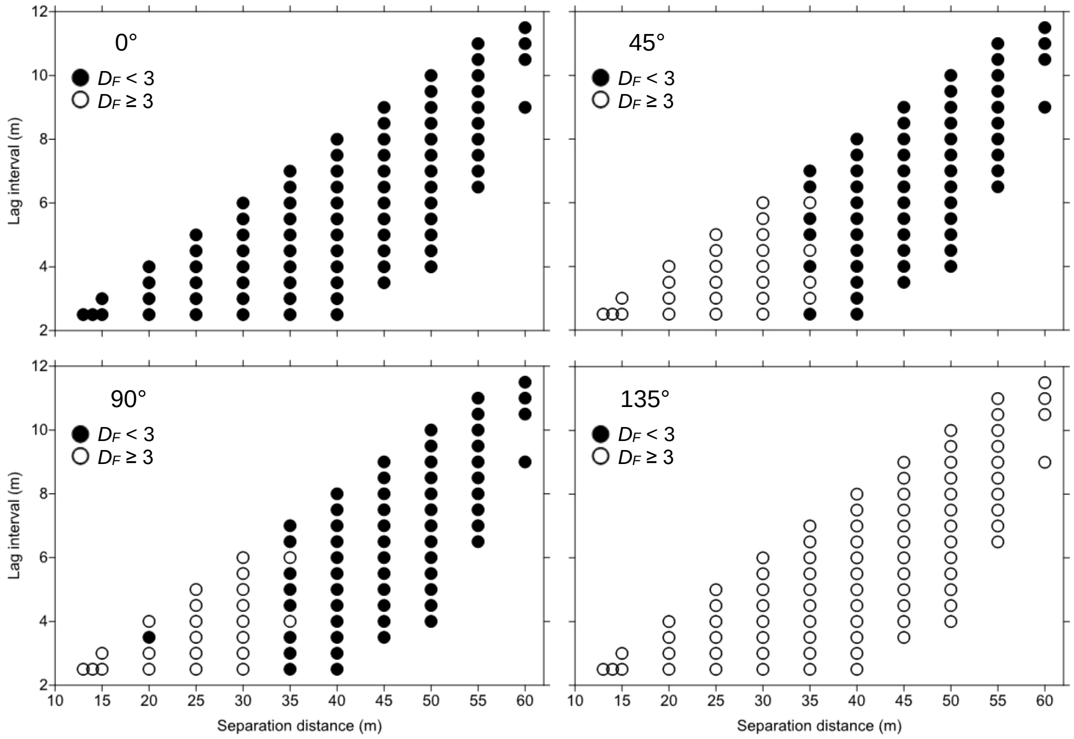

Figure A7. Fractograms of sand content (Sand) calculated from anisotropic semivariograms for the directions of 0°, 45°, 90° and 135°, with the fractal dimension for different scales.

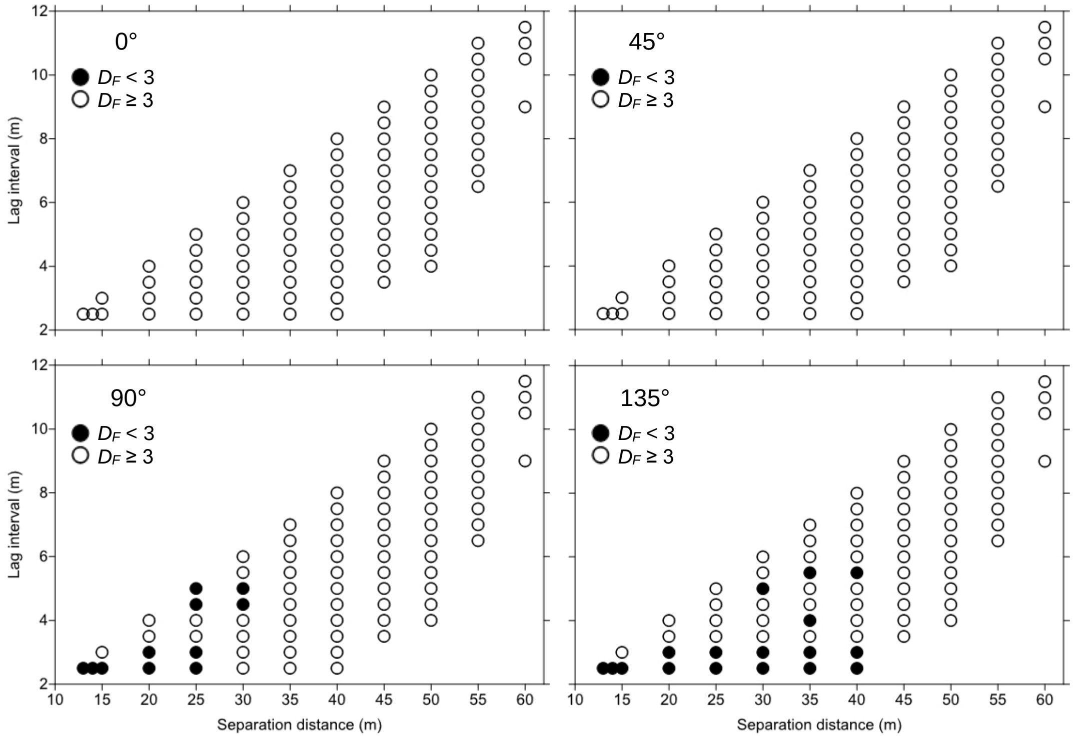

Figure A8. Fractograms of silt content (Silt) calculated from anisotropic semivariograms for the directions of 0°, 45°, 90° and 135°, with the fractal dimension for different scales.

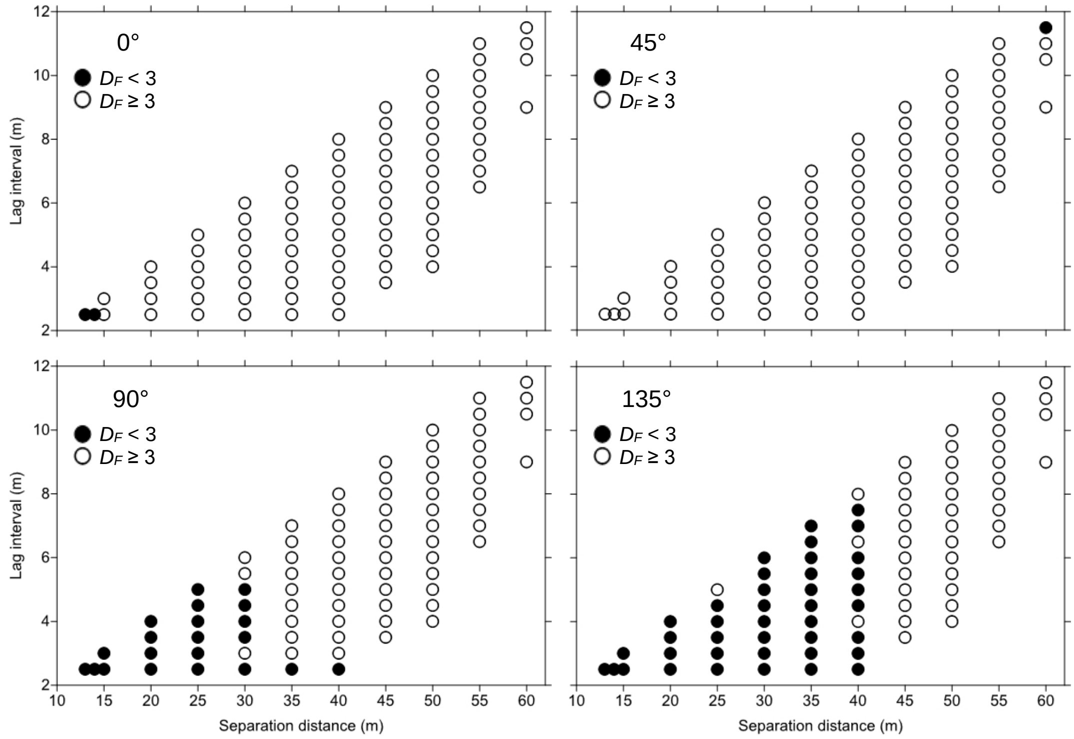

Figure A9. Fractograms of clay content (Clay) calculated from anisotropic semivariograms for the directions of 0°, 45°, 90° and 135°, with the fractal dimension for different scales.

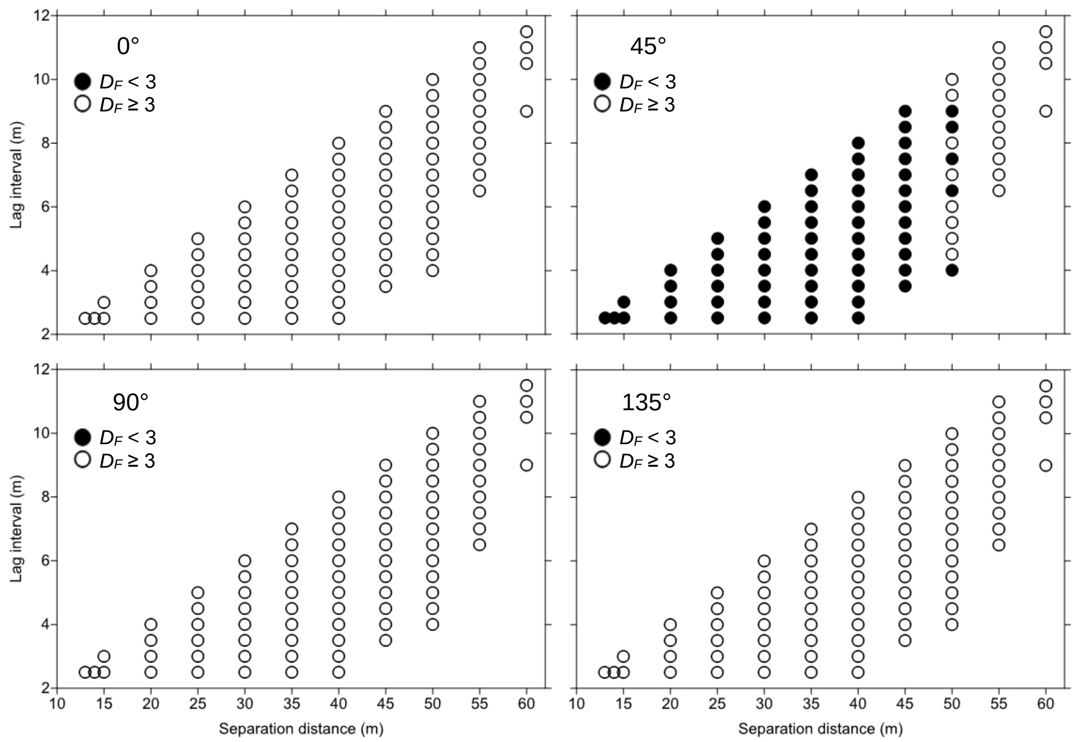

Figure A10. Fractograms of soil pH calculated from anisotropic semivariograms for the directions of 0°, 45°, 90° and 135°, with the fractal dimension for different scales.

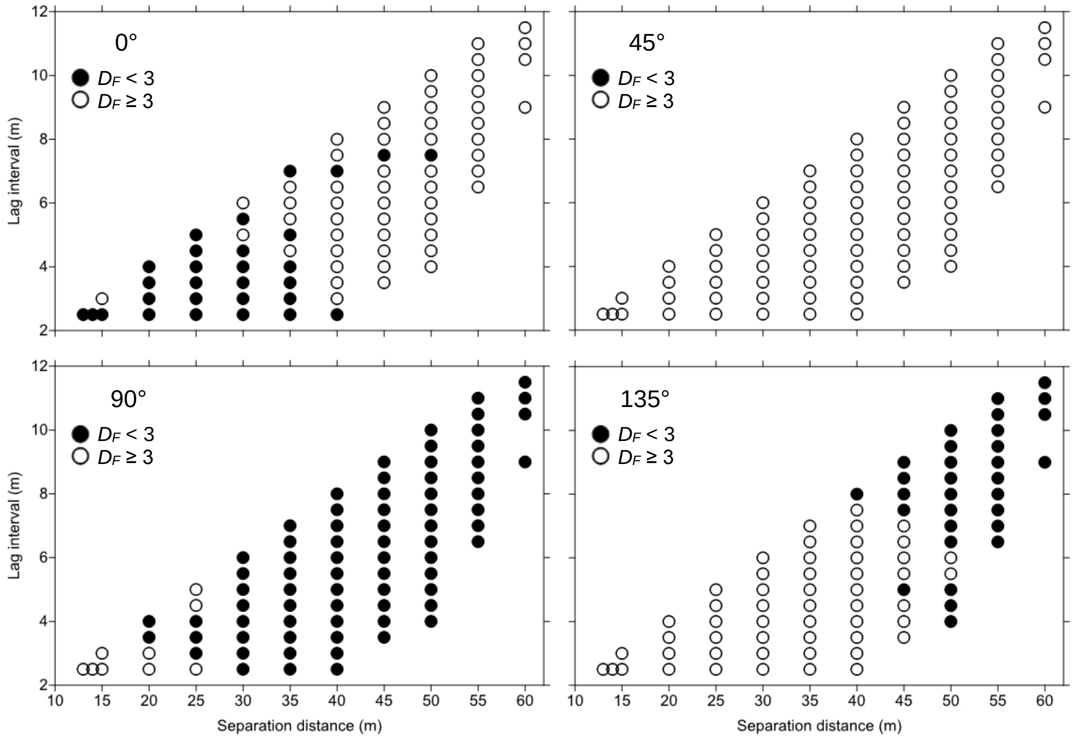

Figure A11. Fractograms of soil organic matter (SOM) calculated from anisotropic semivariograms for the directions of 0°, 45°, 90° and 135°, with the fractal dimension for different scales.

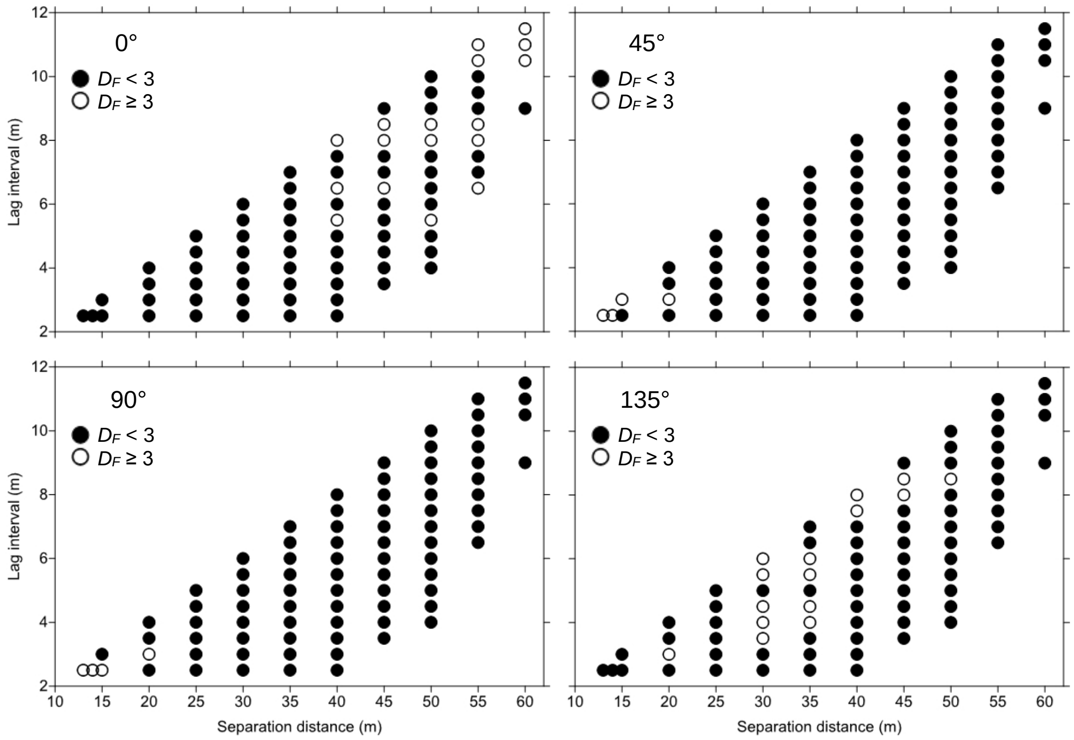

Figure A12. Fractograms of carbon stock (C_{stock}) calculated from anisotropic semivariograms for the directions of 0°, 45°, 90° and 135°, with the fractal dimension for different scales.

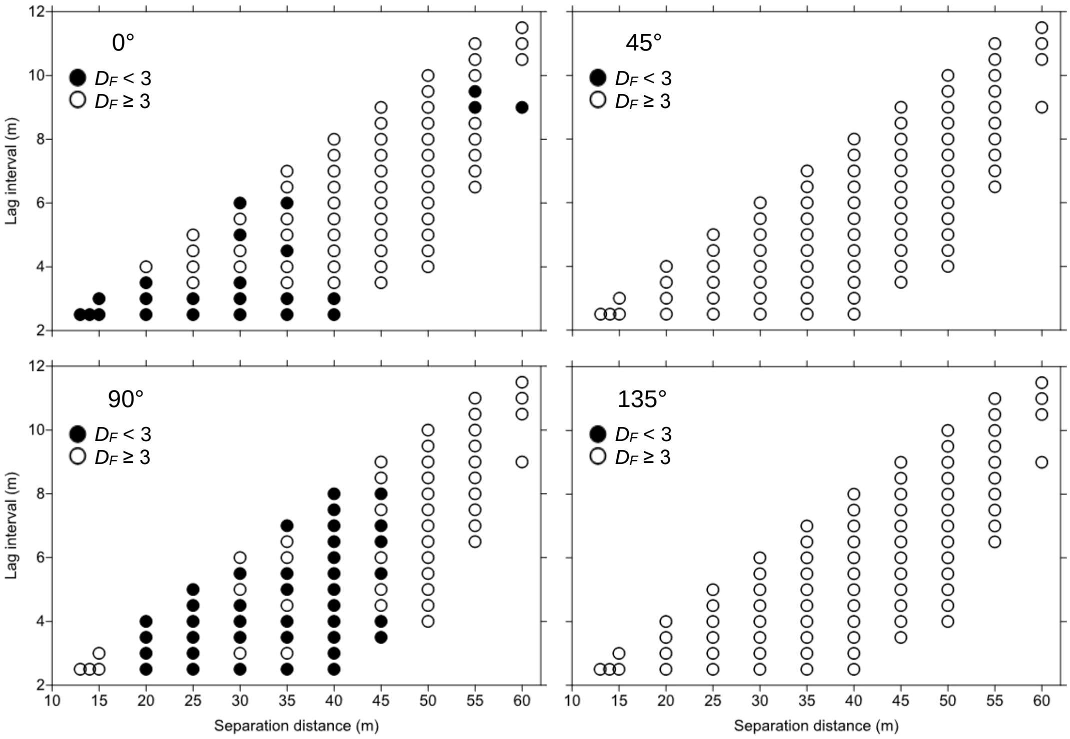

Figure A13. Fractograms of the carbon to nitrogen ratio (C/N) calculated from anisotropic semivariograms for the directions of 0°, 45°, 90° and 135°, with the fractal dimension for different scales.

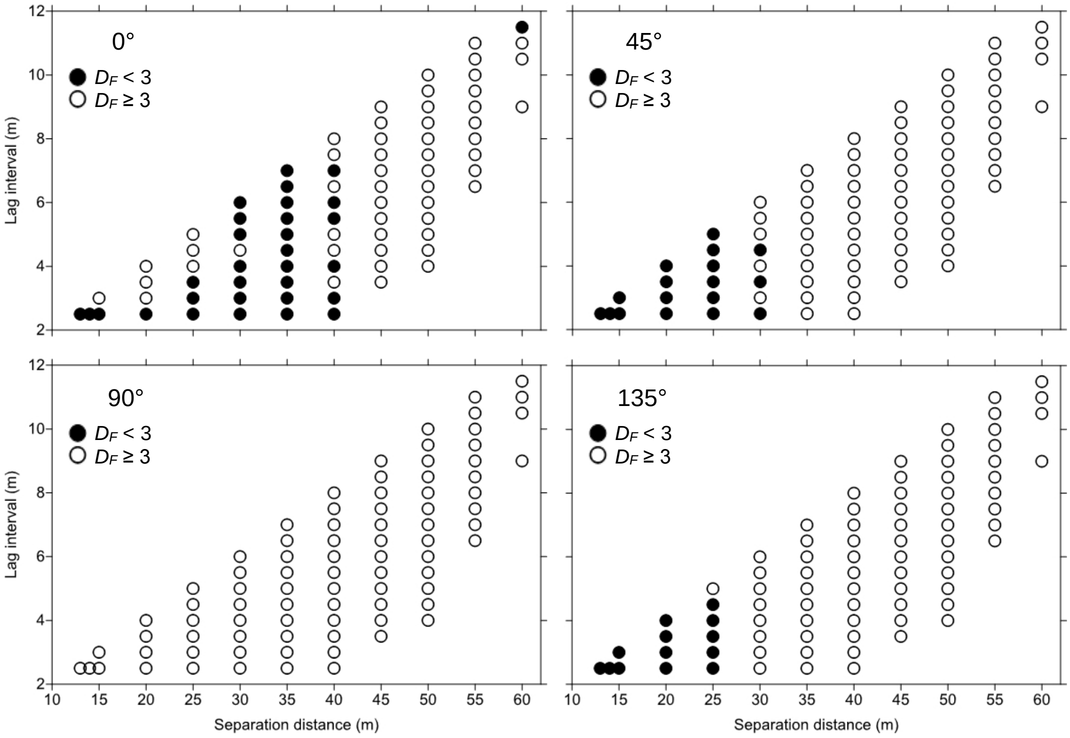

Figure A14. Fractograms of available phosphorus (P) calculated from anisotropic semivariograms for the directions of 0°, 45°, 90° and 135°, with the fractal dimension for different scales.

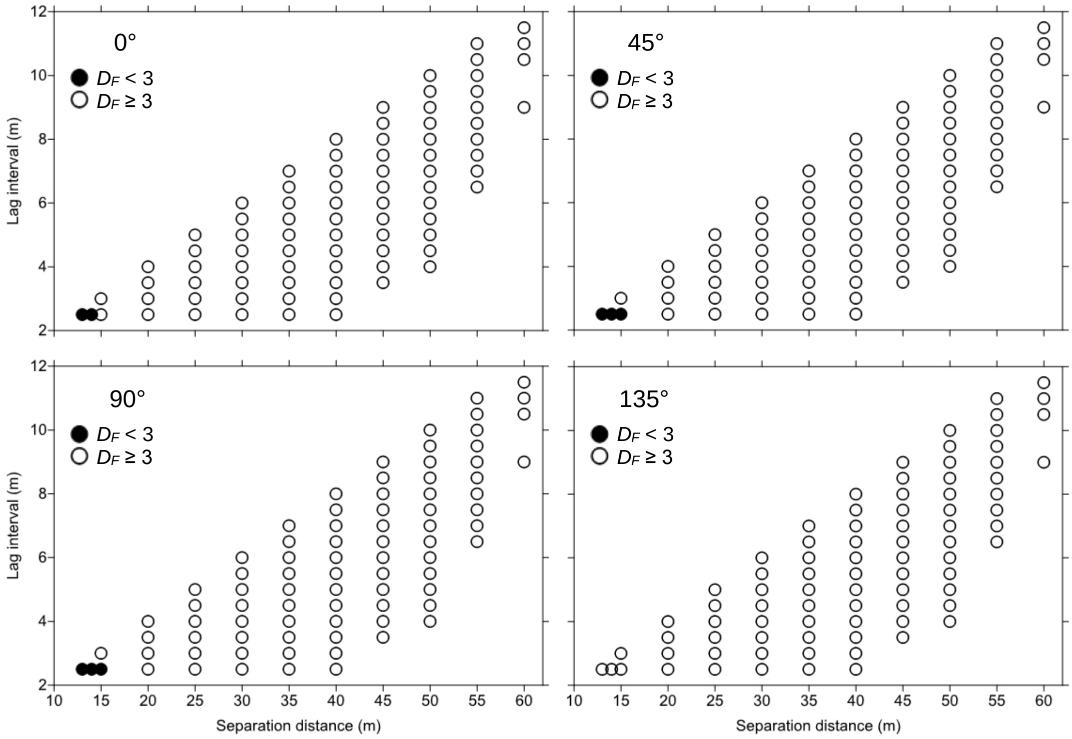

Figure A15. Fractograms of sum of bases (Bases) calculated from anisotropic semivariograms for the directions of 0°, 45°, 90° and 135°, with the fractal dimension for different scales.

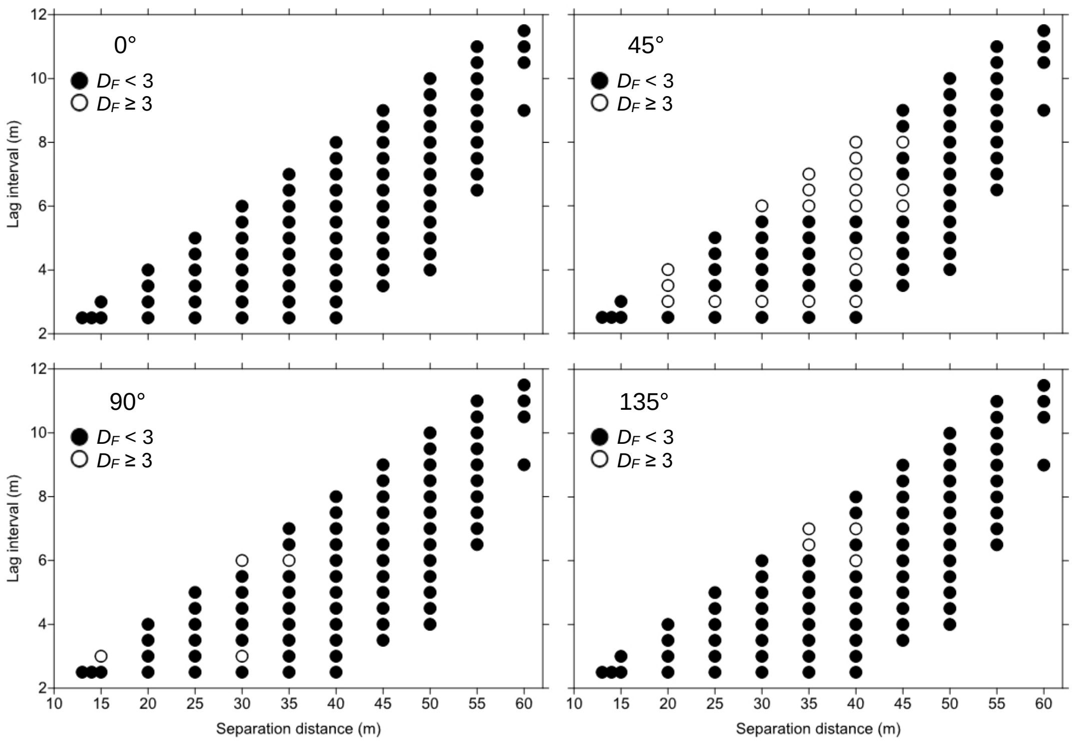

Figure A16. Fractograms of cation exchange capacity (CEC) calculated from anisotropic semivariograms for the directions of 0°, 45°, 90° and 135°, with the fractal dimension for different scales.